Appendix A
The Harmonic Oscillator

Properties of the harmonic oscillator arise so often throughout this book that it seemed best to treat the mathematics involved in a separate Appendix.

A.1 Simple Harmonic Oscillator

The harmonic oscillator equation dates to the time of Newton and Hooke. It follows by combining Newton's Law of motion ($F = Ma$, where F is the force on a mass M and a is its acceleration) and Hooke's Law (which states that the restoring force from a compressed or extended spring is proportional to the displacement from equilibrium and in the opposite direction: thus, $F_{\text{Spring}} = -Kx$, where K is the spring constant) (Fig. A.1). Taking $x = 0$ as the equilibrium position and letting the force from the spring act on the mass:

$$M\frac{d^2x}{dt^2} + Kx = 0. \tag{A.1}$$

Dividing by the mass and defining $\omega_0^2 = K/M$, the equation becomes

$$\frac{d^2x}{dt^2} + \omega_0^2 x = 0. \tag{A.2}$$

As may be seen by direct substitution, this equation has simple solutions of the form

$$x = x_0 \sin \omega_0 t \text{ or } x_0 = \cos \omega_0 t, \tag{A.3}$$

The original version of this chapter was revised: Pages 329, 330, 335, and 347 were corrected. The correction to this chapter is available at https://doi.org/10.1007/978-3-319-92796-1_8

© Springer Nature Switzerland AG 2018

W. R. Bennett, Jr., *The Science of Musical Sound*,
https://doi.org/10.1007/978-3-319-92796-1

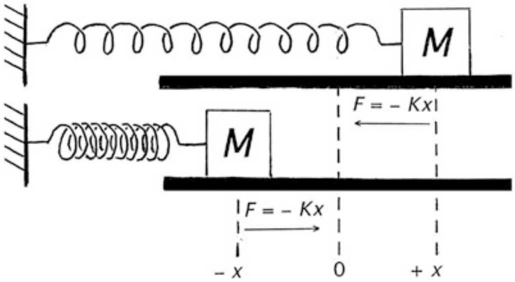

Fig. A.1 Frictionless harmonic oscillator showing the spring in compressed and extended positions

where t is the time and x_0 is the maximum amplitude of the oscillation. The angular resonance frequency ω_0 is related to the cyclical resonance frequency F_0 and period $T(= 1/F_0)$ of the oscillator by $\omega_0 = 2\pi F_0 = 2\pi/T$ where

$$\omega_0 = \sqrt{K/M}. \tag{A.4}$$

A.2 Energy

Without dissipation, the total energy in the oscillator at any instant in time is constant and given by

$$\text{Energy} = \frac{1}{2}(Mv^2 + Kx^2), \tag{A.5}$$

where the first term is the kinetic energy of the moving mass ($v = dx/dt$) and the second term is the potential energy stored in the spring. The energy oscillates back and forth between those two forms during alternate half periods. At the turning points, where the velocity of the mass is zero, the energy is stored in the spring. At x $= 0$, where the velocity is maximum, the energy is all kinetic. If $x = x_0 \sin \omega t$, then $v = dx/dt = \omega x_0 \cos \omega t$ and

$$\begin{aligned} \text{Energy} &= \frac{1}{2}[M(\omega_0 x_0 \cos \omega_0 t)^2 + K(x_0 \sin \omega_0 t)^2] \\ &= \frac{1}{2}K{x_0}^2(\sin^2 \omega_0 t + \cos^2 \omega_0 t) = \frac{K{x_0}^2}{2}, \end{aligned} \tag{A.6}$$

where again $\omega_0 = K/M$ and $(\sin^2 \omega_0 t + \cos^2 \omega_0 t) = 1$. Regardless of its kinetic energy the particle is trapped in a potential well of the type shown in Fig. A.2. Since the restoring force from the spring is

$$F \equiv -\frac{dU}{dx} = -Kx, \text{ the potential is } U(x) = \frac{M\omega_0^2 x^2}{2}, \tag{A.7}$$

where x is defined with respect to the equilibrium position of the oscillator and $U = 0$ at $x = 0$.

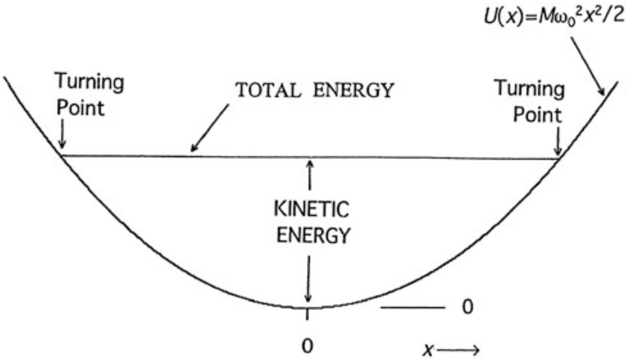

Fig. A.2 Potential well for the simple harmonic oscillator. In this model the particle is bound, regardless of its kinetic energy

A.3 The Damped Simple Harmonic Oscillator

In any real system there will be a "damping" force due to friction that at low velocities takes the form

$$F_{\text{Damping}} = -\Gamma \frac{dx}{dt}, \tag{A.8}$$

where Γ is a damping constant characteristic of the system. The total force acting on the mass M now becomes $F = Ma = -\Gamma dx/dt - Kx$. Hence, the equation of motion becomes

$$M\frac{d^2x}{dt^2}\Gamma\frac{dx}{dt} + Kx = 0. \tag{A.9}$$

Dividing through by the mass and moving everything to the left side puts the equation for the damped simple harmonic oscillator in the more convenient form,

$$\frac{d^x}{dt^2} + \gamma\frac{dx}{dt} + \omega_0^2 x = 0 \tag{A.10}$$

where we have defined $\gamma = \Gamma/M$ as the damping constant per unit mass. Exact solutions to this equation may be obtained in the following straightforward manner. Substituting a trial solution, $x = e^{\mu t}$, gives a quadratic equation

$$\mu^2 + \gamma\mu + \omega_0^2 = 0, \tag{A.11}$$

that has $\mu_\pm$ roots of the form

$$\mu_\pm = -\frac{\gamma}{2} \pm i\omega_0\sqrt{1-\left(\frac{\gamma}{2\omega_0}\right)^2} \tag{A.12}$$

where $i^2 \equiv -1$. The solutions without a driving term are of the form $x = Ae^{\mu+t} + Be^{\mu-t}$, where A and B are complex constants determined by the initial conditions (i.e., the displacement from equilibrium and the velocity at $t = 0$).

For $(\gamma/2\omega_0)^2 < 1$, which is typical of resonant systems, the roots have an imaginary component that leads to free oscillation at a frequency

$$\omega \approx \omega_0 - \frac{\gamma^2}{8\omega_0} + \text{Order}\left\{\omega_0\left(\frac{\gamma}{4\omega_0}\right)^2\right\} \tag{A.13}$$

that is damped at the amplitude decay rate γ. For $\gamma_{\text{Crit}} = 2\omega 0$, no oscillation occurs, the damping is fastest and is said to be "Critical." For $(\gamma/2\omega_0)^2 << 1$, one solution is

$$x(t) \approx x_0 e^{-\gamma t/2} \sin\omega_0 t, \tag{A.14}$$

which corresponds to giving the mass an initial velocity kick at x = 0 and t = 0. In this case the total energy in the oscillator decays with time as

$$\text{Total Energy} \propto |x(t)^2| \propto e^{\gamma t}. \tag{A.15}$$

Note that the energy decay rate is a factor of 2 faster than the amplitude decay rate simply because the energy in this classical motion problem is proportional to the square of the amplitude.

A.4 Resonance or Cavity Width and Quality Factor (Q)

Because the amplitude of the damped oscillator decays with time, the spectrum of its motion is spread out in frequency about $\omega 0$. Regardless of the initial conditions chosen, we know that the total energy decays as shown in Eq. (A.15). Since $x(t)$ is of the form $\exp(-\gamma t/2 + i\omega 0t)$, the Fourier transform of the amplitude is of the general form,

$$|x| \propto \int_0^\infty x(t)e^{-i\omega t}dt \propto \frac{1}{|\gamma/2 + i(\omega-\omega_0)|}. \tag{A.16}$$

Hence, the spectral distribution of energy in the resonant mode will be of the form

$$|x_\omega|^2 \propto \frac{1}{|1+\left(\frac{\omega-\omega_0}{\gamma/2}\right)^2|}, \tag{A.17}$$

which is sometimes called a “Lorentzian” function of the frequency and, provided $(\omega-\omega0)2 >> (\gamma/2)2$, is symmetric about the angular resonant frequency $\omega0$ with full cavity width at half-maximum energy response given by $\Delta\omega = \gamma 2\pi \Delta F$. The quantity

$$\Delta F_{\rm cav} = \frac{\gamma}{2\pi} = \frac{f}{\pi}\frac{c}{4L} \tag{A.18}$$

is sometimes called the cavity resonance width. In general, for standing-wave resonances in a long cavity such as an organ pipe, $\gamma = f(c/2L)$ where c is the running wave velocity, L is the cavity length, and f is the round trip fractional energy loss. For example, for a closed-pipe model of the first formant (F_1) of the vocal tract,

$$\Delta F_{\rm cav} = F_1\frac{f}{\pi}. \tag{A.19}$$

The *Quality Factor*, or Q of a resonance, is defined traditionally by the relation

$$Q = 2\pi\frac{\text{Energy Stored}}{\text{Energy Lost per Cycle}} = \omega_0\frac{\text{Energy Stored}}{\text{Rate of Energy Loss}}, \tag{A.20}$$

where the rate of energy loss is $\gamma \times$ (Energy Stored). Noting that $\gamma = \Delta\omega$, an alternative expression for the Quality Factor is

$$Q = \frac{\omega_0}{\Delta\omega} = \frac{F_0}{\Delta F}, \tag{A.21}$$

where F_0 is the cyclical resonance frequency and ΔF is the full cyclical width at half-maximum energy response, both measured in Hz.

A.5 Driven Damped Oscillation

When a sinusoidal or cosinusoidal driving term of the type

$$E(t) = E\ \cos\omega t \tag{A.22}$$

is added to the damped oscillator, the equation becomes

$$\frac{d^2x}{dt^2} + \gamma \frac{dx}{dt} + \omega_0^2 x = E(t) \tag{A.23}$$

where $E(t)$ on the right-hand side represents the driving force per unit mass. This equation has the closed-form solution

$$x = \frac{E}{D} \sin(\omega t + \Phi), \tag{A.24}$$

where the denominator D is given by

$$D = \sqrt{(\omega^2 - \omega_0^2)^2 + \left(\frac{\gamma\omega}{M}\right)^2} \tag{A.25}$$

and the phase angle is

$$\Phi = \cos^{-} 1 \left(\frac{\gamma}{MD}\right) \text{ radians.} \tag{A.26}$$

The introduction of damping causes the oscillator to lag in phase from the driving term. Without damping, $|x| \to \infty$ as $\omega \to \omega_0$.

A.6 Electric Circuit Equivalent of the Damped Driven Oscillator

The equation for the damped, driven oscillator has an exact equivalent in the series *LCR* (inductance-capacitance-resistance) circuit shown in Fig. A.3. Written in terms of the charge q on the condenser C, the equation for the voltage drop around the loop becomes

$$L\frac{d^2q}{dt^2} + R\frac{dq}{dt} + \frac{q}{C} = E(t), \tag{A.27}$$

where the current $i = dq/dt$, and we have made use of the basic relations for *ac* voltage drops across the circuit elements: $V_L = Ldi/dt = Ld^2q/dt^2$ (Henry's Law), $V_R = Ri = Rdq/dt$ (Ohm's Law), and $V_C = q/C$ (Faraday's Law). By comparison with the original equation for the oscillator, we find the equivalent relationships in Table A.1.

One may determine the steady-state behavior of a linear resonant circuit using complex ac circuit analysis. In this analysis, one usually assumes that the transient solution has died down to a steady complex current of constant amplitude and phase running through the various resistive and reactive elements of the circuit and that

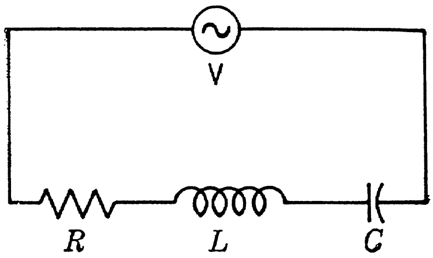

Fig. A.3 Series resonant LCR circuit driven by a sinusoidal EMF (electro-motive force)

Table A.1 Electrical and mechanical equivalent parameters

AC circuit	Mechanical oscillator
Charge, $q \Rightarrow x$	Amplitude
Current, $i \Rightarrow v$	Velocity
Inductance, $L \Rightarrow M$	Mass
Resistance, $R \Rightarrow \gamma$	Damping constant
Capacitance, $C \Rightarrow 1/K$	1/(Spring constant)
EMF, $E(t) \Rightarrow F(t)/M = E(t)$	Driving force

AC circuit mechanical oscillator

the real part of the resultant voltage drops correspond to values one would measure. Thus, if the current running through a circuit loop is of the form[1]

$$i = i_0 e^{j\omega t} = i_0(\cos\omega t + j\sin\omega t), \tag{A.28}$$

the voltage drops across the elements L (inductance), R (resistance), and C (capacitance) may be written as

$$V_L = L\frac{di}{dt} = i(j\omega L),\ \ V_R = iR,\ \text{and}\ V_C = \frac{q}{C} = \frac{1}{C}\int^t i_0 e^{j\omega t}dt = i\left(\frac{-j}{\omega C}\right). \tag{A.29}$$

Note that in the expression for VC we have made use of the fact that the charge on the capacitance is the integral of the current over time; i.e., the current feeding the capacitance is $i = dq/dt$, where q is the time-dependent charge on the capacitance.

In applying this convention, one makes use of Kirchoff's Laws: (1) The sum of the voltage drops around a closed loop equals the sum of the Emfs ("electromotive forces"), which is a statement of the conservation of energy; (2) The sum of the currents at any junction must be zero, which is a statement of the conservation of charge. Using the methods and notation of complex steady-state ac circuit analysis just discussed, the loop equation for the circuit in Fig. A.3 may be written

[1]The relation $e^{i\theta} = \cos\theta + i\sin\theta$ where $i^2 = -1$ is known as Euler's formula and may be derived from the infinite series for e^x and those for $\cos\theta$ and $\sin\theta$ by letting $x = i\theta$. This type of ac circuit analysis was invented by Campbell, a research engineer at the A.T. & T Company in 1911, who referred to it as "Cisoidal Oscillations"—an abbreviation for "cos i sin" Campbell (1911).

$$E = i\left[R + j\left(\omega L - \frac{1}{\omega C}\right)\right]. \tag{A.30}$$

The magnitude of the current is

$$|i| = \frac{E}{\sqrt{R^2 + \left(\omega L - \frac{1}{\omega C}\right)^2}} \tag{A.31}$$

and it lags the driving voltage in phase by ϕ where

$$\tan^{-} 1\phi = -\frac{\omega L - \frac{1}{\omega C}}{R} \approx \frac{(\omega^2 - \omega_0^2)}{\omega L/R} \approx \frac{(\omega_0 - \omega)}{\Delta\omega/2}. \tag{A.32}$$

Here, the final approximation holds near resonance where ω is close to ω_0.

The power loss in the resistor is

$$P_R = |i|^2 R = \frac{E^2/R}{1 + \frac{(\omega^2 - \omega_0^2)}{(\omega L/R)^2}} \tag{A.33}$$

and is of resonant Lorentzian shape with full width at half maximum given by

$$\Delta\omega \approx R/L \approx 2\pi\Delta F. \tag{A.34}$$

The Q or "Quality Factor" of the circuit is then

$$Q = \omega_0/\Delta\omega \approx \omega_0 L/R. \tag{A.35}$$

These properties are summarized in Fig. A.4.

A.7 A Different Approach

Normally, one uses ac circuit analysis to determine steady-state currents in the presence of applied Emfs. However, useful results are obtained even when $E = 0$ in Fig. A.3. In that case, we can use the loop equation to determine the (complex) frequency, an approach that gives the transient behavior of the circuit. Hence, if the Emf is zero in Fig. A.3, we get

$$i\left[R + j\left(\omega L - \frac{1}{\omega C}\right)\right] = 0. \tag{A.36}$$

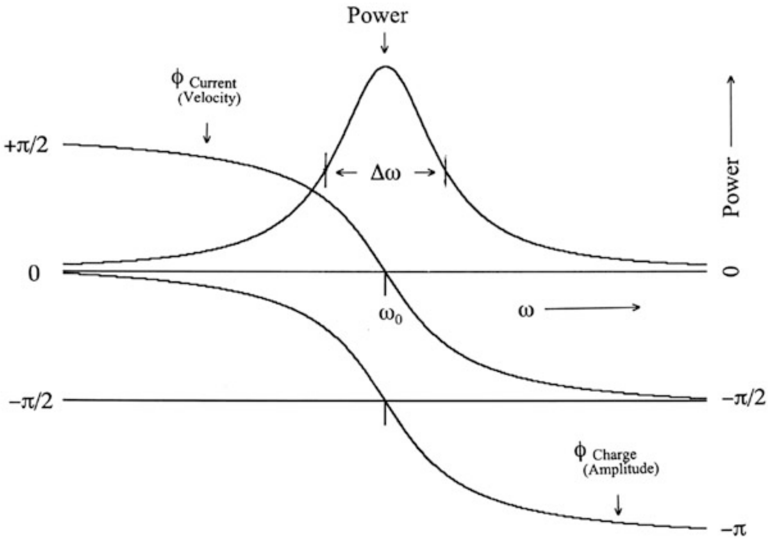

Fig. A.4 Power resonance and phase shifts in the series LCR circuit, related to the properties of the driven, damped mechanical oscillator

Assuming that $i \neq 0$ (i.e., that there is some initial charge or current flowing in the circuit), the large square bracket must equal zero and we obtain a quadratic equation in ω:

$$\omega^2 - j\omega\frac{R}{L} - \frac{1}{LC} = 0, \tag{A.37}$$

whose roots are

$$\omega = j\frac{R}{2L} \pm \omega_0\sqrt{1 - \left(\frac{R}{2\omega_0 L}\right)^2}. \tag{A.38}$$

If we substitute this expression back into Euler's formula, we get

$$e^{j\omega t} = e^{\frac{R}{2L}t} e^{\pm j\omega_0\sqrt{1-\left(\frac{R}{2\omega_0 L}\right)^2}\,t}, \tag{A.39}$$

where the first exponential describes damping of the current and the second exponential gives the oscillatory solution through use of Euler's formula with a real frequency

$$\omega = \pm\omega_0\sqrt{1 - \left(\frac{R}{2\omega_0 L}\right)^2}. \tag{A.40}$$

Hence, the "steady-state "solution can actually give us the transient behavior of the circuit. (Note that the sign on the real part of the frequency merely alters the phase of the oscillation.) The damped oscillatory solution is, of course, the same one we got earlier for the behavior of the damped mechanical oscillator using a trial solution of the type $e^{\mu}t$. The present approach provides a less tedious way to analyze coupled circuits, if you are comfortable with ac circuit analysis.

A.8 Coupled Oscillations, Wolf Tones and the Una Corda Piano Mode

The double-strung pianos dating from the early work of Bartolomeo Cristofori provide an interesting example of mode coupling with unusual potential for musical expression. The physical processes involved were discussed qualitatively in Chap. 4. We would like to show here that it is easy to derive the important quantitative properties of the coupled system from an electric circuit model. As implied by the term "double-strung," each note on the piano has two strings tuned closely to the same pitch, each of which can be represented as a damped harmonic oscillator. We will only consider the fundamental resonances of the strings here, although the present method could easily be extended to include harmonics of each fundamental frequency. In the piano, the motion of the two strings is coupled through their attachment to the bridge, which in turn transfers energy to the soundboard. We will represent this situation by the pair of coupled circuits shown in Fig. A.5. For simplicity, we will assume that the corresponding circuit elements are identical and that each oscillator is initially tuned approximately to the same frequency given by $\omega_0^2 = 1/LC$. (One might represent a string resonance and the other an air resonance in a violin.)

The coupled circuits in Fig. 4.5 result in two loop equations:

$$i_1 \left[R + j \left(\omega L - \frac{1}{\omega C} \right) \right] - i_2 R = 0 \tag{A.41}$$

and

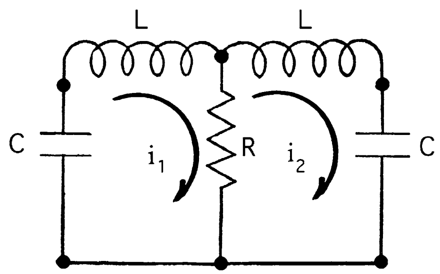

Fig. A.5 Coupled circuit model for one note on a double-strung piano. The two current magnitudes may be different

$$-i_1R + i_2\left[Rj\left(\omega L - \frac{1}{\omega C}\right)\right] = 0. \tag{A.42}$$

Solving both of these equations for i_1/i_2, we obtain

$$\frac{i_1}{i_2} = \frac{R}{R + j\left(\omega L - \frac{1}{\omega C}\right)} = \frac{R + j\left(\omega L - \frac{1}{\omega C}\right)}{R} \tag{A.43}$$

Hence, we get an equation involving the complex frequency,

$$\left(\omega L - \frac{1}{\omega C}\right)\left(\omega L - \frac{1}{\omega C} - 2jR\right) = 0, \tag{A.44}$$

which has two distinct solutions for ω^2 yielding roots for ω,

$$\omega = \pm\omega_0 \text{ and } \omega = j\frac{R}{L} \pm \omega_0\sqrt{1 - \left(\frac{R}{\omega_0 L}\right)^2}. \tag{A.45}$$

The first mode has no loss and oscillates at the resonant frequency, ω_0. The second, lossy mode has the real component of its frequency shifted downward in magnitude to

$$\omega = \omega_0\sqrt{1 - \left(\frac{R}{\omega_0 L}\right)^2} \tag{A.46}$$

and an amplitude decay rate of R/L, which is twice as large as that for either LCR loop by itself. Note that the Q of each resonant circuit is $\omega_0 L/R \gg 1$. Hence, the second term in the square root provides a small, real correction to the resonant frequency, although the shift is larger than in either single isolated LCR loop alone.

The two coupled modes of oscillation may be interpreted in terms of the coupled circuits shown in Fig. A.6. Here, the same current magnitude i flows in both loops, but in different directions for the two different normal modes. The even-symmetric mode on the left is the high-loss mode (with decay rate of R/L) since the two currents flowing through the resistance are in phase. It corresponds to the normal position of the hammer on the piano in which both strings are struck simultaneously. Striking both strings in the normal hammer position is equivalent to depositing the same charge on each capacitor at $t = 0$. The odd-symmetry mode at the right is the low-loss mode and would correspond to a case in the piano where both undamped strings were hit simultaneously with hammers moving in opposite directions. In the circuit, opposite charges would have to be placed suddenly on the two capacitors at $t = 0$. For the odd-symmetric case (the right side of Fig. A.6), the mode has no loss at all because the two equal currents flowing through the resistor are 180°out of phase. In the piano, that mode corresponds to periodic pulses from the two strings

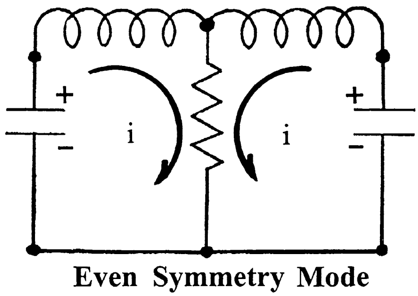

Fig. A.6 The even-symmetric (left) and odd-symmetric (right) modes of the coupled circuit (the current magnitudes are all equal)

arriving at the bridge out of phase. A similar situation arises in the case of "Wolf Tones" on bowed stringed instruments. (See Chap. 5.)

However, pure excitation of the odd-symmetry mode would not occur in a normal piano because only the right-hand string is struck (in the double-strung piano) by the hammer with the una corda pedal depressed. (The hammer is shifted to the right so as to hit only one string, with both strings undamped.) Hence, to simulate the actual una corda case, we need to take the difference between equal amounts of the two normal coupled-circuit modes. Thus, initially,

$$i_{\text{UnaCorda}} = i_{\text{EvenSymmetric}} - i_{\text{OddSymmetric}}. \tag{A.47}$$

This combination localizes the current on the right side of the coupled circuit when the hammer hits, after which the even-symmetric component rapidly dies out leaving only the long-lived odd-symmetric mode still oscillating. Because the odd-symmetric mode has the least loss (no loss at all for the idealized circuit in Fig. A.6), the excitation would always tend to settle down in the odd-symmetry mode with frequency ω_0. The apparent pitch goes up slightly as the high-loss mode dies out. In reality there is some loss in the vibrating strings themselves due to air resistance. That could easily be included in the electric circuit model by adding a small resistance in series with each coil in the separate current loops. A reactive component could also be added in series with the load resistance R representing loss to the soundboard. Because equal currents flow in the two loops in the odd-symmetric mode, the crescendo effect described in Chap. 4 after the string is struck (produced by damping one string in the una corda mode after the sound decays) would be limited to about $20Log_{10}2 \approx 6$ dB, or about the amount observed experimentally.

A.9 Harmonics and Subharmonics

As discussed throughout this book, most musical instruments produce waveforms that are at least quasi-periodic and contain harmonics. These harmonics often result from some nonlinearity in the oscillatory system, for example, the vibrating reed in a woodwind, or the vibrating lips of the brass instrumentalist. In general, by "nonlinearity" we mean that the output amplitude from the system does not rise in simple direct proportion to the amplitude of the input signal as it would if the system were perfectly linear (i.e., if the output simply varied as the first power of the input). Instead, the output amplitude may depend on various powers of the input amplitude. As a general rule, if we feed a sinusoidal signal into such a system, signals at different frequencies that are harmonically related to the fundamental (i.e., are given by integer multiples of the original frequency) will appear in the output. Further, these harmonics are generally phase-locked to the fundamental frequency. This can be understood in terms of basic trigonometry relations. For example, if you square a sinewave, you will get a signal varying as the second harmonic of the input signal which is in phase with the fundamental; if you cube the signal, the third harmonic is produced; and so on. More strikingly, if you feed two signals with different frequencies into the system, the output may contain extraneous signals at the sum and difference frequencies of the two original frequencies.[2] All of these effects can be simply explained (albeit, tediously in some instances) through application of the basic trigonometry identities such as those treated in high school.

Under some conditions, the output may even contain subharmonics of the input frequency; i.e., frequencies that are lower than the input driving frequency. Understanding how to produce subharmonics used to be a mysterious art. To quote one of the pioneers who first demonstrated their existence in electromechanical systems, "Most authors pass over this question in silence, as they take it for granted that the occurrence of subharmonics is an impossibility." (Pedersen 1934)[3]

It is useful to treat the simple mechanical oscillator model of Fig. A.1 with the inclusion of nonlinear terms in the spring constant. As we will show, this model can produce both harmonics and subharmonics, not to mention rectification.

---

[2]To see how these extraneous frequencies come about, just consider the trigonometric identity, $2\sin(A)\cos(B) = \sin(A+B)+\sin(A-B)$. Let $A = 2\pi F_0 t$ and $B = 2\pi F t$ be the higher frequency resonance. Multiplying the two waves together yields "sidebands" at $F = F_0$. If $F = NF_0$, where $N = 1, 2, 3, 4$, etc., "sidebands" spaced by F_0 will occur throughout the entire spectrum, even if there is no strong acoustic wave at F_0.

[3]"Hi-Fi" enthusiasts will want to note that Pedersen got interested in this subject because his Jensen high-fidelity loudspeaker was producing both first and second subharmonics of sinusoidal tones.

A.10 The Nonlinear Oscillator

In general, one expects the oscillator equation will become nonlinear at large enough amplitudes. For example, when x is sufficiently negative the spring will compress, the coils will touch and a large repulsive force will occur. At large positive values of x, the spring constant will begin to decrease and the restoring force will saturate. Assuming that the restoring force from the spring is a continuous function of x with continuous derivatives, it can be expanded in a power series of the form

$$F = -[K_1 x + K_2 x^2 + K_3 x^3 + \dots] \tag{A.48}$$

where x is the departure from equilibrium position at $x = 0$. K_1 is just the normal spring constant and may be expressed in terms of ω_0. Then, the driven oscillator equation may be rewritten

$$\frac{d^2x}{dt^2} + \gamma \frac{dx}{dt} + \omega_0^2 \left[x + \frac{x^2}{X_q} + \frac{x^3}{X_c} \right] = E \sin \omega t \tag{A.49}$$

where γ is the damping term from friction per unit mass and the coefficients X_q and X_c have been defined to have dimensions of length and length-squared and describe the amounts of quadratic and cubic nonlinearity. We will ignore terms higher than cubic in x. Here, E is the driving acceleration per unit mass at frequency ω that would be supplied by the Bernoulli effect in the real case. The quadratic term will yield both even harmonics and subharmonics, as well as rectification; the cubic term provides odd harmonics; and with both terms present, additional sum and difference terms arise. The term on the right-hand side of the equation represents the driving force per unit mass. It could be sinusoidal at the normal resonant frequency ω_0. To investigate subharmonic production, it is useful to replace the driving frequency by $2\omega_0$. Then the subharmonic appears at ω_0. Stable solutions to nonlinear equations have very specific phase relationships that are determined by the parameters of the system. Closed-form solutions to this type of nonlinear equation have been investigated in the past, but are extraordinarily tedious to derive and usually only hold for very small driving terms.[4] However, it is relatively easy to solve the equation numerically with a computer.

[4] Lord Rayleigh (1877) investigated low-amplitude solutions to nonlinear differential equations of this type in closed form. Also see, Hartley (1939), Hussey and Wrathall (1936) and Pedersen (1934) for approaches to the closed-form solution of similar nonlinear equations.

A.11 Potential Wells for the Nonlinear Oscillator

As shown in Fig. A.2, the potential well for the ideal linear oscillator has even symmetry about the equilibrium point (x = 0) and can trap the mass regardless of its kinetic energy. The situation changes drastically when we add a quadratic nonlinearity.

The potential curve shown at the left in Fig. A.7 is for an oscillator containing both linear and quadratic terms. Here, the restoring force is of the form,

$$F \equiv -\frac{dU}{dx} = -K_1 x - K_2 x^2, \text{ hence } U(x) = \omega_0^2 \left[\frac{x^2}{2} + \frac{x^3}{3X_q} \right], \tag{A.50}$$

where again $U \equiv 0$ at $x = 0$, but we have written U as the potential per unit mass. As can be seen from the figure, the quadratic force term reduces the potential barrier on one side of equilibrium, while increasing it on the other. The result is that the mass can now escape from the well at the left if it acquires enough kinetic energy from the driving force to reach the top of the potential bump.[5] (The top of the bump occurs at x = −Xq and is of magnitude $\Delta U = \omega_0^2 X_q^2/6$.) Consequently, the oscillator with only the addition of a quadratic force term tends to be unstable, except at very low driving amplitudes where the kinetic energy per unit mass is kept less than $\omega_0^2 X_q^2/6$. With a large enough damping constant, the loss of energy inhibits the escape of the mass over the potential bump. However, if γ is made very large, the harmonic (and subharmonic motion) is damped out as well.

Finally, the potential well on the right in Fig. A.7 includes the effect of both quadratic and cubic force terms. Here,

$$F \equiv -\frac{dU}{dx} = -K_1 x - K_2 x^2 - K_3 x^3 \text{ and } U(x) = \omega_0^2 \left[\frac{x^2}{2} + \frac{x^3}{3X_q} + \frac{x^4}{4X_c^2} \right]. \tag{A.51}$$

The cubic term in the spring constant introduces a stabilizing term to the potential. Hence, with the cubic force term present, stable solutions are obtained at very much larger driving amplitudes than with the quadratic term alone. Surprisingly, with the cubic term present, finite solutions exist at resonance for large driving amplitudes even without the presence of damping. However, in that case, the oscillator never settles down to a steady-state solution.

[5] This same phenomenon occurs in the dissociation of diatomic molecules.

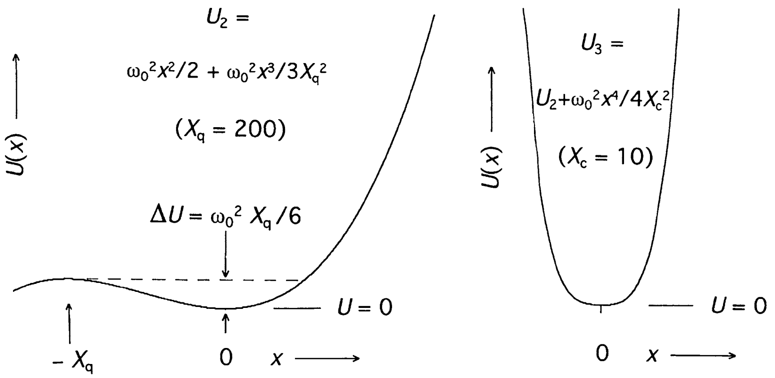

Fig. A.7 Potential wells for nonlinear oscillators containing quadratic (left) and both quadratic and cubic forces (right)

A.12 Numerical Solutions to the Non-linear Oscillator Equation

The driven oscillator equation with nonlinear terms is exceedingly tedious to solve in closed form. However, numerical solutions with a computer are straightforward using a computational method previously developed by the author (Bennett 1976, p. 200). Here, the main trick is to minimize numerical errors that tend to build up in successive integration intervals. That objective may be accomplished by expanding the acceleration in a Taylor series in the time and integrating that series term-by-term over an interval, t, that is small compared to the period of the driving oscillation.

First, we rewrite the basic equation with the acceleration on the left-hand side. For example, the equation for the driven, damped oscillator with quadratic and cubic nonlinear terms given above can be rewritten

$$a = \frac{d^2x}{dt^2} = E \sin \omega t - \gamma \frac{dx}{dt} - \omega_0^2 \left[x + \frac{x^2}{X_q} + \frac{x^3}{X_c} \right]. \tag{A.52}$$

Note that we now have an explicit closed-form expression for the acceleration that can be differentiated as many times as we want to obtain the coefficients in the Taylor series. Thus, after the small time interval t, the new values for the acceleration, velocity, and position will be given by

$$a' = a + bt + c\frac{t^2}{2!} + d\frac{t^3}{3!} + Order(t^4) = \frac{dv}{dt} \tag{A.53}$$

$$v' = v + at + b\frac{t^2}{2!} + c\frac{t^3}{3!} + d\frac{t^4}{4!} + Order(t^5) = \frac{dx}{dt} \tag{A.54}$$

$$x' = x + vt + a\frac{t^2}{2!} + b\frac{t^3}{3!} + c\frac{t^4}{4!} + d\frac{t^5}{5!} + Order(t^6) \tag{A.55}$$

where we have integrated the successive equations term-by-term and have included constants of integration (the values of the quantities x, v, and a at $t = 0$) in each case. The errors in a' are now of order t^4 and those for the new position of the particle x' are of order t^6. Hence, by making t sufficiently small, we can make the results as precise as we wish.

Putting these expressions into a reiterative computer loop where at each successive step one sets the initial values of a, v, and x to be the values computed for a', v', x' at the end of the last interval t yields x as a function of time to high accuracy. One could, of course, add more and more terms to the Taylor series for a, but terminating the series as shown above is more than adequate for the present examples.

The equations for a, v, and x are especially adaptable to inclusion in a computer program loop of the type used in BASIC or FORTRAN. One can simplify the numerical equations further by adopting a time scale in which the time increment t is defined to be unity. In that case the important program steps for solving the nonlinear oscillator may be written as follows. First, we define some constants dependent on the parameters of the oscillator.

Driving frequency	Resonant frequency
W = ω	W0 = ω_0
W2 = W $*$ W	W02 = W0*W0
W3 = W $*$ W2	
Damping constant per unit mass	
G = γ	

In terms of these computer variables, the equation for the acceleration becomes

$$AE * SIN(W * T)G * VW02 * (XX * X/XqX * X * X/Xc)dV/dT. \tag{A.56}$$

For example, choosing the oscillator period to be 60 time units (or $\omega_0 = 2\pi/60$), means that a step size of $t = 1$ leads to an error $\approx$ 5 parts in 10^10 in the calculation of x over one increment. One typically wants to do the calculation over a time interval $T_{\max} \approx 5$ oscillator periods for the transient solution to settle down to a steady-state solution.

The initial conditions on position and velocity are:

$X = V = 0$

The reiterative loop equations then take the form in BASIC:[6]

[6]Or in FORTRAN, DO T = 0,Tmax,1 followed by END DO instead of NEXT T.

```
FOR T = 0  TO  T max 'with implied steps of T = 1
 S1 = SIN (W * T ) 'W = Driving Frequency. S1 and C1
are defined to avoid
 C1 = COS(W * T ) 'recalculating the SIN and COS within
each iteration
 A = E*S1–G*V–W02*(X+X*X/Xq+X*X*X/Xc)
 B = W*E*C1–G*A–W02*(V+2*X*V/Xq+3*X*X*V/Xc)
 C = –W2*E*S1–G*B–W02*(A+2*(X*A+V*V)/Xq+3*(2*X*V*V
      +X*X*A)/Xc)
 D = –W3*E*C1–G*C–W02*(B+2*(V*A+X*B+2*V*A)/Xq)
 D = D–W02*3*(2*V*V*V+4*X*V*A+2*X*V*A+X*X*B)/Xc
 X = X+V+A/2+B/6+C/24+D/120       'Use V to find X before
changing V
 V = V + A + B / 2 + C / 6 + D / 24
 REM Plot or Print results here NEXT  T
```

Note that $A = dV/dt$, $B = dA/dt$, $C = dB/dt$, $D = dC/dt$ and that the time scale was defined so that $t = 1$ in the Taylor expansion for A and step size in the loop on T.

A.13 Examples of Nonlinear Oscillator Solutions

Solutions of the nonlinear equation containing both quadratic and cubic force terms are shown in Fig. A.8, where it was assumed that $Xq = Xc = 10$ and the driving frequency was tuned to the normal resonance frequency, ω_0. A damping constant $\gamma = 0.5\omega0$ was chosen for this illustration.

Time increases from $t = 0$ at the left of each trace in Fig. A.8 and the full transient response of the oscillator for the mass starting from rest at $x = 0$ is shown for increasing values of the driving amplitude, E. The driving term is shown in dotted lines and the oscillator response is in solid curves. For $E = 0.01$ (the lowest curve), the response is nearly sinusoidal. However, as the driving amplitude increases, various even and odd harmonics develop in the waveform. The behavior of the oscillator becomes very complex when the excursion of the mass reaches the critical region where $x \approx X_q = X_c = 10$. For the conditions assumed, that point occurs at $E \approx 0.1$. Although the different Fourier amplitudes are continuous in their dependence on E, there are discontinuities in slope that appear when new harmonics cross threshold. Many of these discontinuities result in a reversal of the direction of the dependence of a given harmonic on excitation level. As a result, small changes in E can produce large changes in the spectral distribution. Even harmonics are present that also oscillate with increasing excitation level, but decrease in relative importance above $E \approx 0.05$. The cubic characteristic dominates at large excitation levels where one sees a series of peaks in the different odd

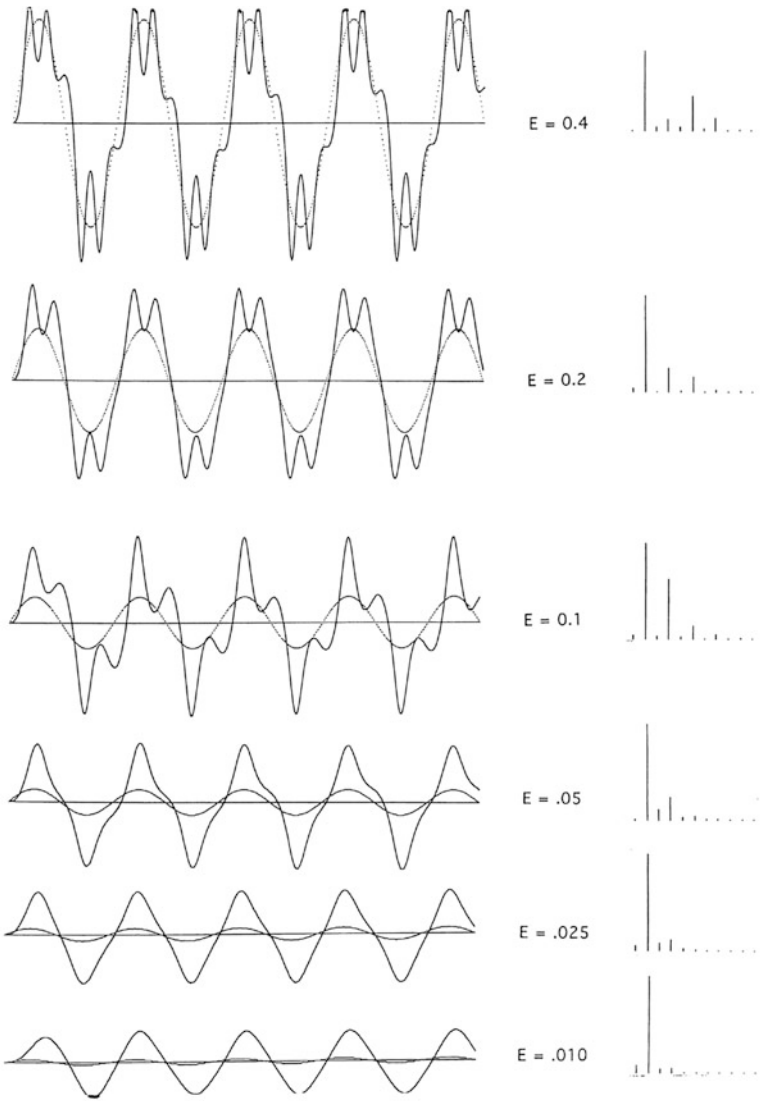

Fig. A.8 Solutions to the nonlinear oscillator equation when driven at the normal oscillator resonance frequency with $\gamma = 0.5\omega_0$, and $Xq = Xc = 10$. E increases from bottom to top. The driving wave (amplitude E) is shown dotted. A histogram of the relative spectral amplitudes is shown at the right in each case, normalized to the response at the driving frequency (the first term represents the response at DC) harmonics. The waveform amplitude saturates above $E \approx 0.5$, although more and more ripples occur with increasing excitation. That behavior is characteristic of many reed and brass instrument, not to mention the human voice. Above the saturation level, the sensation of further loudness arises primarily due to the increase in harmonic content rather than output power.

The relative harmonic amplitudes for $N = 0, 1, 2, 3, \ldots, 10$ normalized to the fundamental component ($N = 1$) are shown at the right in Fig. A.8 as a histogram, as determined by Fourier analysis. ($N = 0$ corresponds to a DC rectification term.) Rectification, harmonics, and even subharmonics are an automatic consequence of the nonlinearities assumed. Although subharmonics are not shown in the Fourier spectrum of Fig. A.8, their production in the case of a strong quadratic nonlinear term is discussed in the chapter on the human voice.

A.14 Dynamic Chaos

At very high values of the driving force E, the nonlinear oscillator begins to exhibit characteristics of chaos in its motion. As an extreme example, consider the case where there is no damping force at all in the presence of large quadratic and cubic terms in the spring constant with high values of a periodic driving force. Here, even though the solutions are still bound and have strong spectral components at the driving frequency and its higher harmonics, the solutions are not periodic (i.e., they don't repeat themselves from one period to the next). Hence, the oscillator motion becomes unpredictable in detail from one cycle of the driving frequency to the next. An example of this behavior is shown in Fig. A.9. It is not clear that this regime of the nonlinear mechanical oscillator has any direct relevance to the behavior of the real human voice or other musical instruments. But some laryngologists have suggested that dynamic chaos may be present in vibrations of the vocal fold in the

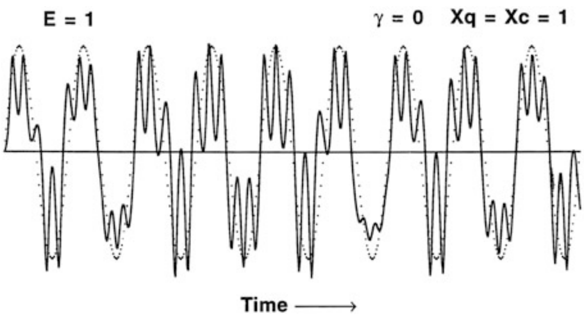

Fig. A.9 Example of chaotic behavior of the nonlinear oscillator. Here, the damping has been eliminated altogether ($\gamma = 0$) and the oscillator is driven at a very high excitation level (E = 1). As before, the driving term is at the normal resonance frequency and indicated by dotted lines. Note that the waveform does not repeat itself precisely from one period to the next singing voice. (See Sataloff et al. 1998 and Hawkshaw et al. 2001.) However at the present time, these suggestions seem largely to be speculation drawn by analogy to other biomechanical systems where chaos has actually been observed.

A.15 Subharmonic Solutions

There is some indication that subharmonics may be present in some musical instruments. For example, the subtones produced by violinist Mari Kimura through use of very large bowing pressure were interpreted by her as subharmonics. (See Chap. 5.) Similarly, the extremely low frequencies produced by the Gyütö monks and the Tuva throat singers might also be due to subharmonic generation. (See Chap. 6 on the singing voice (Fig. A.10).)

Figure A.11 shows a subharmonic solution to the nonlinear oscillator when it only contains a quadratic nonlinear term in the spring constant. As discussed above, the oscillator is highly unstable under these conditions. A very weak potential well exists to trap the mass and the driving force has to be exceedingly small (or the

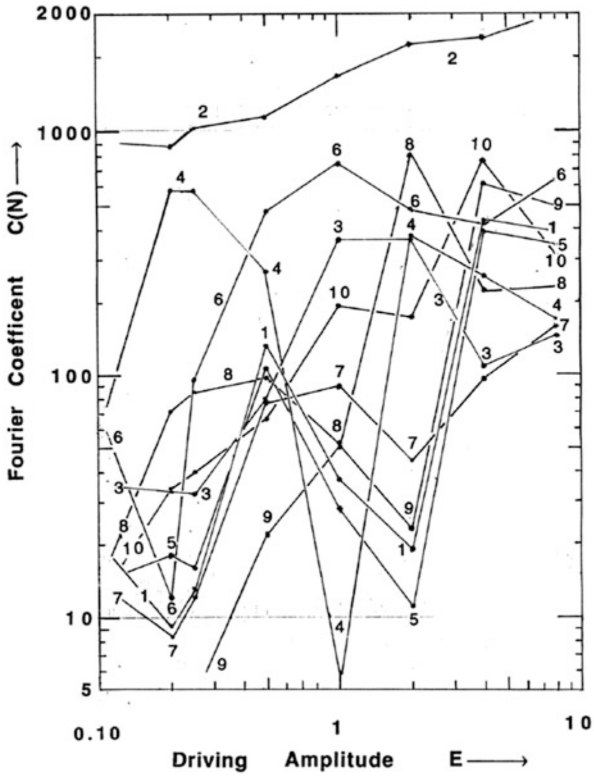

Fig. A.10 Variation of Fourier coefficients for nonlinear oscillator solutions of the type in Fig. A.9. As a function of driving amplitude

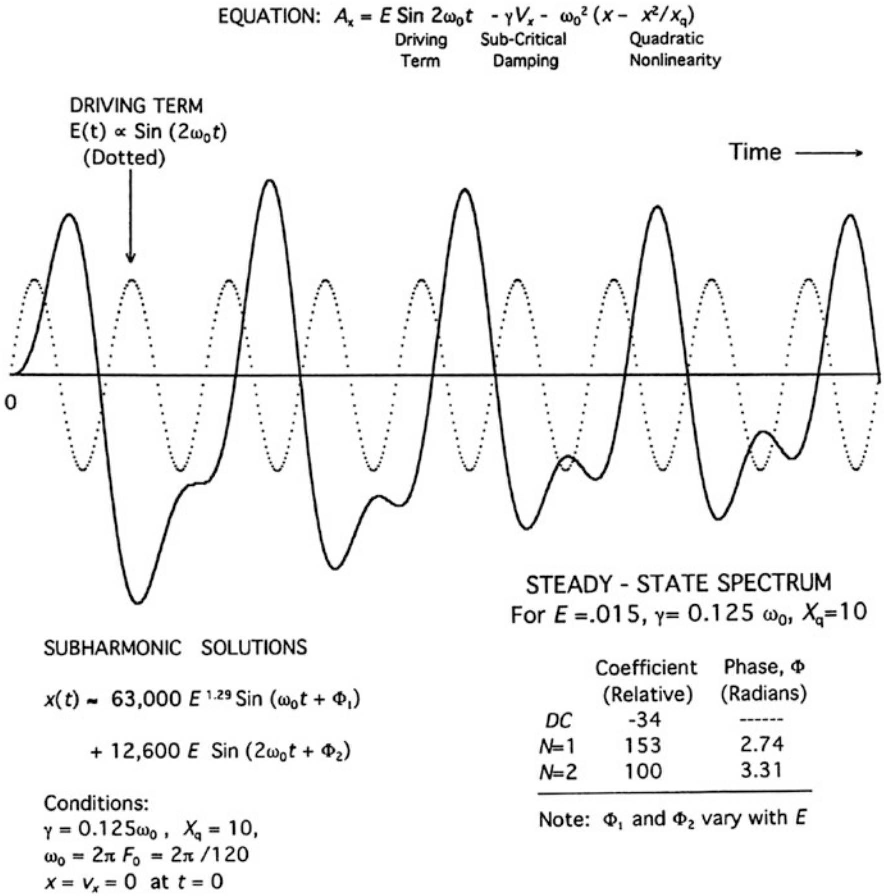

Fig. A.11 Subharmonic solution to the forced nonlinear oscillator containing a quadratic term in the spring constant

damping very high) to prevent the oscillator from flying apart, which will happen if $|x| \geq X_q$.

To illustrate a subharmonic solution, it is useful to assume that the driving acceleration is applied at twice the resonant frequency of the normal linear oscillator. Hence, we will assume

$$E(t) = E \sin(2\omega_0 t) \tag{A.57}$$

as indicated by the dotted lines in Fig. A.11. The subharmonic then occurs at ω_0. The damping constant γ for the solution in the figure was chosen to be much smaller than the value ($2\omega 0$) for critical damping in order to enhance production of the suboctave harmonic. (Although adding a large damping term would increase the stability of the oscillator, it would suppress the subharmonic component.) The solution shown includes the transient response when the driving force is initially turned on with the particle at rest at $x = 0$. The oscillator amplitude (solid curve) decays into the steady-state solution at the extreme right of the figure, where the fact that it is periodic in half the driving frequency is easily seen by eye. The first two Fourier coefficients and their phases are shown in Fig. A.11, where $C(1)$ is the subharmonic amplitude and $C(2)$ is the amplitude of the response at $2\omega_0$.

The phases of the two components (Φ_1, Φ_2) in Fig. A.11 vary in a complex manner with the driving amplitude. As previously noted, the oscillator with a quadratic nonlinearity acts as a rectifier. That is, a significant DC ("Direct Current") offset occurs in the solutions. With the human voice, the latter might correspond to a net average opening of the glottis which increases with driving amplitude. As discussed above, the presence of a cubic force term results in a stable potential well. A cubic (or at least an odd-symmetric force term) is also to be expected with most mechanical oscillators on a physical basis. As the spring in the mechanical oscillator compresses, the coils will eventually touch each other, creating a strong repulsive force back toward the equilibrium position ($x = 0$). An analogous situation occurs in the larynx when the glottis completely closes. At the other extreme, a large opening of the glottis would result in increased contact with other tissue in the larynx and provide a similar repulsive force back toward equilibrium. Hence, there is justification for an odd-symmetric force at large amplitudes and a cubic term is the simplest one to incorporate. However, the presence of the cubic term produces odd harmonics and reduces the subharmonic content.

A.16 The Relaxation Oscillator

A relaxation oscillator was used in the Dudley VODER discussed in the chapter on speech synthesis and a mechanical analog to the relaxation oscillator occurs in the grab-slip phenomenon in bowed strings discussed in the chapter on bowed strings. A very simple version is shown in Fig. A.12.

In Fig. A.12, a battery or other DC ("Direct Current") voltage supply at the left charges the capacitor C by means of a current $i = dq/dt$ flowing through the resistor R. Ignoring the neon tube at the right of the circuit for the moment, the charge q flowing to the capacitor would obey the equation,

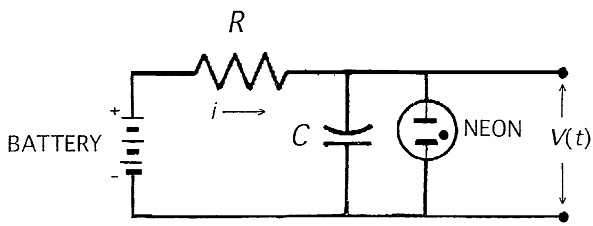

Fig. A.12 A simple relaxation oscillator circuit

$$E = R\frac{dq}{dt} + \frac{q}{C}, \tag{A.58}$$

where E is the battery voltage (or "electromotive force"). Dividing the equation by R and using the integrating factor $e^{(t/RC)}$, it is seen that the voltage across the capacitor is

$$V(t) = \frac{q(t)}{C} = E\left[1 - e^{t/RC}\right], \tag{A.59}$$

where we have assumed that there was no initial charge on the capacitor before connecting the battery. Expanding the exponent,

$$V(t) = E\frac{t}{RC} + \text{ Order}\left(\frac{t}{RC}\right)^2. \tag{A.60}$$

Hence, for $t \ll RC$, the voltage $V(t)$ rises linearly with time.

It is a characteristic of neon bulbs that once the voltage reaches a threshold value called the "ignition voltage," a value somewhat above the ionization potential of the neon atom ($\approx$ 21.6 V) but dependent on the pressure and electrode geometry, a discharge occurs through the gas. The discharge current persists until the voltage drops below the "extinction voltage," a value somewhat below the first excited state of the atom ($\approx$ 11.5 V), but again modified by the geometry and pressure. Hence, the capacitor, C, will be repeatedly charged up through the resistor R and then discharged through the neon bulb. The period for this process will be in the order of RC (a time constant characteristic of the circuit), but will be modified by the magnitude of the power supply voltage.

If the discharge through the neon bulb occurred instantaneously, the output voltage $V(t)$ in the limit that t«RC would approach an ideal sawtooth waveform, which has harmonic amplitudes that decrease as $1/n$, where n is the harmonic number; i.e., the power spectrum falls off as $1/n^2$. For example, if the RC time constant were adjusted so that the fundamental frequency of the oscillator were 120 Hz (typical of the vocal cord resonance in an adult male and the source frequency used in the Dudley VODER and VOCODER), the power spectrum of the oscillator would be distributed as shown by the solid line in Fig. A.13. In practice, the discharge time is not zero and is limited by drift mobilities of ions and electrons and other collision processes in the neon tube to values somewhat less than a millisecond (but also modified by pressure and tube geometry). The finite discharge time can reduce the harmonic output of the relaxation oscillator significantly, as shown by the histogram in Fig. A.13. The histogram was computed by Fourier analysis for an assumed discharge time of 2/3 of a millisecond. The minima at the harmonics for N = 13 and 26 correspond to multiples of the ratio of the oscillator period to the discharge time ($\approx$13:1).

The limitations of the simple oscillator in Fig. A.12 may be overcome by using more complex circuitry such as that shown in Fig. A.14. For example, the capacitor

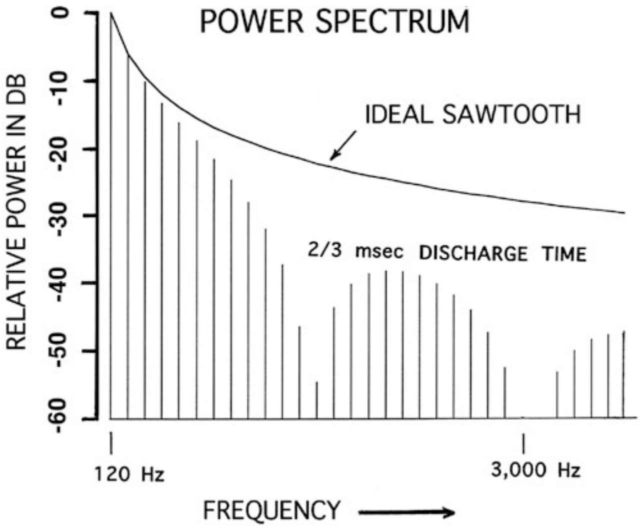

Fig. A.13 Power spectrum for a relaxation oscillator with finite discharge time compared with the spectrum from an ideal sawtooth waveform. The histogram was computed from the square of the Fourier coefficient amplitudes for the waveform

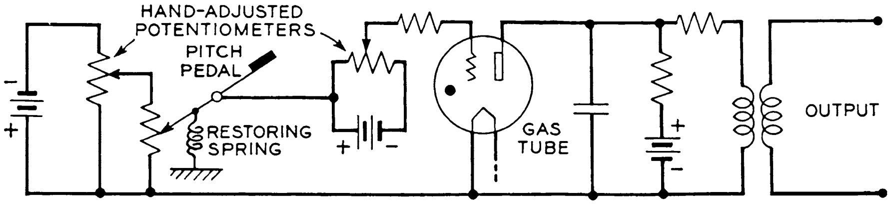

Fig. A.14 Relaxation oscillator used in the Dudley VODER (a manually operated synthetic speaker) first exhibited at the 1939 San Francisco Exhibition and New York World's Fair. Reproduced from Dudley (1939) by permission of Lucent Bell Laboratories, Jean Dudley Tintle and Richard Dudley. The spectrum produced by this circuit closely matched that for the Ideal Sawtooth shown in Fig. A.13

could be charged by a constant current generator to provide greater linearity during the charging cycle and the discharge of the capacitance could be achieved through a triggered, high- mutual-conductance tube or avalanche diode. Dudley's oscillator was actually the inverse of the circuit shown in Fig. A.12. He used a gas triode with a control grid and filament to charge the capacitance (in ≈ 0.3 ms). The capacitance was then allowed to discharge by itself with roughly a 0.8-ms time constant. The period of his oscillator (nominally $\approx$ 10 ms) was varied by biasing the control grid on the gas tube. Because the discharge pulse occupied a small fraction of the period, the power spectrum was very close to that for the ideal sawtooth shown in

Fig. A.13.[7] (Contemporary VOCODERS such as the MAM Model VF-11 use linear sawtooth generators that do not depend on gas discharge tubes.)

A.17 The Helmholtz Resonator

A number of acoustical problems can be analyzed in terms of Helmholtz Resonators. The diagram in Fig. A.15 is useful in deriving the resonant frequency of such a volume resonator.

We first want to calculate the change in pressure in the large volume that occurs when the gas (not necessarily just air) contained in the small cylinder is pushed into the sphere of initial volume V_0. Since a small volume of gas is added and we are ultimately going to consider changes in which that volume of gas goes in and out of the sphere, it is appropriate to think of the process as one in which there is no net heat flow in or out of the system. For such an "adiabatic" process involving an ideal gas, it is shown in thermodynamic texts that[8]

$$PV^{\gamma} = \text{ constant, with } \gamma = C_p/C_V, \tag{A.61}$$

where P is the pressure of gas occupying volume V and γ is the ratio of specific heats for the gas at constant pressure C_P and constant volume C_V. The ratio γ varies appreciably depending on the molecular complexity of the gas. (See Table A.2.)

Now suppose a piston of area A is pushed through the cylinder of length L in Fig. A.14 forcing the gas from the small volume

$$\Delta V = A \times L \tag{A.62}$$

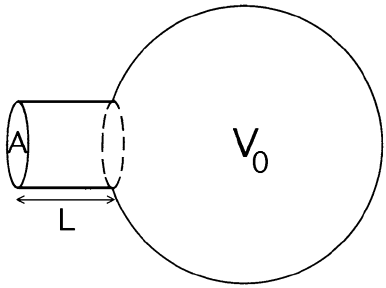

Fig. A.15 Schematic diagram of a Helmholtz oscillator of volume V_0

[7]See Dudley 1939; Figs, 7, 10, and 11.

[8]See, e.g., Zemansky (1951, Section 6.7.)

Table A.2 Values of γ for different common gases near room temperature

Gas	Wet air	Helium	Argon	Hydrogen	Nitrogen	Carbon dioxide	Methane
γ	1.37	1.67	1.67	1.40	1.40	1.29	1.30

Source: Zemansky (1951, pp. 129, 130). Zemansky notes that a method for measuring γ was devised by Rüchhardt in 1929 in which the mass of air in the Helmholtz cylinder was replaced by a small metal ball fitting snugly in the tube and measuring the oscillation frequency when the apparatus was oriented with the tube in the vertical direction

into the sphere. Differentiating Eq. (A.60) yields

$$\Delta P V^{\gamma} \gamma P V^{\gamma-1} \Delta V = 0, \tag{A.63}$$

where ΔP is the change from the initial pressure P in the sphere due to the change in gas volume ΔV. Rearranging that equation,

$$\Delta P = \gamma P \Delta V / V. \tag{A.64}$$

Hence, the change in pressure in the sphere is

$$\Delta P = \frac{\gamma P A L}{V_0} \tag{A.65}$$

which results in a force pushing back on the hypothetical piston per unit length of the cylinder (i.e., the effective "spring constant" K for the system) given by

$$K = \frac{\gamma P A^2}{V_0}. \tag{A.66}$$

One thus has a situation where a pressure fluctuation pushing in on the cylinder of gas with mass $\rho A L$ activates harmonic oscillation. Comparing these results with the basic harmonic oscillator equations [Eq. (A.1) through Eq. (A.4)], the oscillation frequency at resonance is seen to be

$$\omega_0 = 2\pi f_0 = \sqrt{\frac{\gamma P A^2}{V_0}} / \sqrt{\rho A L} = \sqrt{\frac{\gamma P A}{\rho L V_0}}. \tag{A.67}$$

The resonant frequency can be rewritten in terms of the velocity of sound c in the gas as

$$f_0 = \frac{c}{2\pi} \sqrt{\frac{A}{L V_0}} \text{ where } c = \sqrt{\frac{\gamma P}{\rho}} \tag{A.68}$$

Appendix B
Vibrating Strings and Membranes

B.1 The Wave Equation for the Vibrating String

Just as with the harmonic oscillator described in Appendix A, the differential equation describing the motion of a vibrating string can be derived by a simple application of Newton's law of motion, $\mathbf{F} = m\mathbf{a}$. Here, it is especially important to realize that both the force $\mathbf{F}$ and the acceleration $\mathbf{a}$ are vectors (i.e., have direction as well as magnitude).

Consider the element of string under tension T between positions x and $x + \Delta x$ along the horizontal axis as shown in Fig. B.1. We assume that the magnitude of the tension is constant throughout the length of the string and that the deflection $y(x)$ in the vertical direction is small. By small, we mean specifically that the angle θ that the curve makes with respect to the x-axis is small enough so that

$$\sin\theta = \tan\theta = \frac{\partial y}{\partial x} \tag{B.1}$$

at each point on the curve. The net force on the string in the vertical (y) direction is then given by the difference in y components (each of form $T\sin\theta$) of the tension between x and $x + \Delta x$. Defining μ to be the mass per unit length and using approximation B.1, the net vertical component of Newton's equation acting on the differential string element Δx with mass $\Delta m = \mu\Delta x$ becomes

$$F_y \approx T\left[\left(\frac{\partial y}{\partial x}\right)_{x+\Delta x} - \left(\frac{\partial y}{\partial x}\right)_x\right] = \Delta m a_y = \mu\Delta x\frac{\partial^2 y}{\partial t^2}. \tag{B.2}$$

(The horizontal components of force cancel within the present approximation.)

The original version of this chapter was revised: Pages 359, 366, 367, and 369 were corrected. The correction to this chapter is available at https://doi.org/10.1007/978-3-319-92796-1_8

© Springer Nature Switzerland AG 2018

W. R. Bennett, Jr., *The Science of Musical Sound*,
https://doi.org/10.1007/978-3-319-92796-1

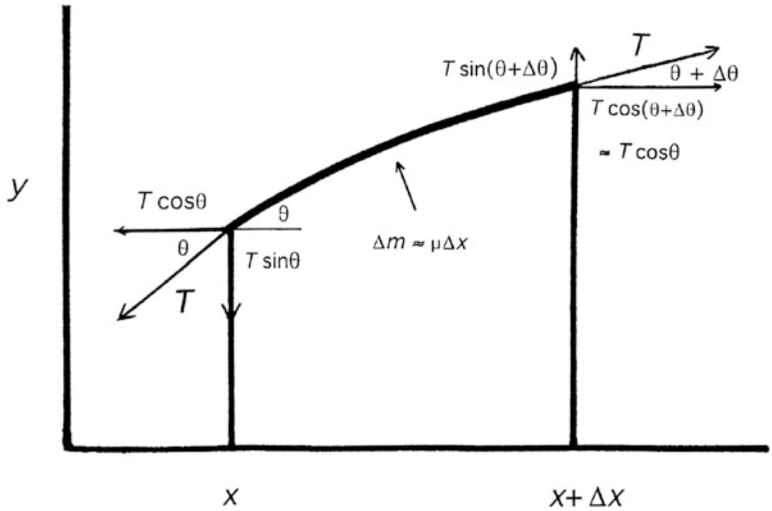

Fig. B.1 Forces on a differential element of a vibrating string

Next, we expand the function y/x in a Taylor series about the point x, noting[1]

$$\left(\frac{\partial y}{\partial x}\right)_{x+\Delta x} = \left(\frac{\partial y}{\partial x}\right)_x + \frac{\partial}{\partial x}\left(\frac{\partial y}{\partial x}\right)_x \Delta x^1 + \text{Order}(\Delta x^2). \tag{B.3}$$

Substituting Eq. (B.3) into the left side of Eq. (B.2) gives

$$F_y \approx T\frac{\partial}{\partial x}\left(\frac{\partial y}{\partial x}\right)_x \Delta x^1 + \text{Order}(\Delta x^2). \tag{B.4}$$

Substituting Eq. (B.4) into Eq. (B.2) and taking the limit as $\Delta x \to 0$ yields

$$T\frac{\partial^2 y}{\partial x^2} = \mu\frac{\partial^2 y}{\partial t^2} \tag{B.5}$$

which is the same as the wave equation,

$$\frac{\partial^2 y}{\partial x^2} = \frac{1}{c^2}\frac{\partial^2 y}{\partial t^2} \tag{B.6}$$

[1]The Taylor series permits evaluating any well-behaved function f(x) at a point displaced to $x + \Delta x$ by the infinite series

$f(x + \Delta x) = f(x) + \left(\frac{\partial y}{\partial x}\right)_x \Delta x^1 + \frac{1}{2}\left(\frac{\partial^2 y}{\partial x^2}\right)_x \Delta x^2 + \frac{1}{3!}\left(\frac{\partial^3 y}{\partial x^3}\right)_x \Delta x^3 + \ldots$ Here, we simply let $f(x) = \partial y/\partial x$.

given in Chap. 1, provided the velocity of the wave is

$$c = \sqrt{\frac{T}{\mu}} \tag{B.7}$$

Note that μ is in units of mass per unit length.

B.2 General Solution of the Wave Equation

Equation (B.6) is linear and can be solved by separating the space- and time-dependent variables through a substitution of the type

$$y(x, t) = X(x)T(t) \tag{B.8}$$

where $X(x)$ is only a function of x and $T(t)$ is only a function of t. Substituting this definition into Eq. (B.6) and dividing by $y(x, t)$ yields

$$\frac{1}{X(x)}\frac{\partial^2 X(x)}{\partial x^2} = \frac{1}{c^2 T(t)}\frac{\partial^2 T(t)}{\partial t^2} \equiv -k^2 = \text{constant}. \tag{B.9}$$

That is, the only way the left side of the equation (which depends only on x) could equal the right side (which depends only on t) for all values of x and t is to have both sides equal to the same constant, chosen here to be $-k^2$ to insure that it is a negative value. (If we had chosen a positive constant at this point the solutions would not be oscillatory.) Equation (B.9) implies two separate differential equations,

$$\frac{\partial^2 X(x)}{\partial x^2} + k^2 X(x) = 0 \text{ and } \frac{\partial^2 T(t)}{\partial t^2} + k^2 c^2 T(t) = 0. \tag{B.10}$$

These equations are both of the Harmonic Oscillator type discussed in Appendix A and have solutions of the form

$$X(x) \propto \sin kx \text{ and } T(t) \cos \omega t \text{ or } T(t) \propto \sin \omega t \tag{B.11}$$

provided $k^2 c^2 = \omega^2$. (The solution $X(x) \propto \cos kx$, although perfectly valid, would not satisfy the boundary conditions on x in the present problem.) The requirement that $X(x) = 0$ at both $x = 0$ and $x = L$ in Eq. (C.11) is satisfied by

$$k_n = n\pi/L \text{ where } n = 1, 2, 3, \ldots, \text{ hence, } \omega_n = k_n c = n\pi c/L. \tag{B.12}$$

The cyclical resonant frequencies are then given by $F_n = \omega n/2\pi = nc/2L$ as we showed in Chap. 1 by two different methods. Note that the spatial boundary conditions in Eq. (B.12) are what actually determine the resonant frequencies of the string. Again, because the wave equation is linear, any linear combination of solutions of the type described by Eq. (B.11) is a solution to Eq. (B.6). The most general solution is of the form originally given by Daniel Bernoulli,

$$y(x,t) = \sum_{n=1}^{\infty} A_n \sin(n\pi x/L)\cos(2\pi n F_0 t) \text{ or } \sum_{n=1}^{\infty} A_n \sin(n\pi x/L)\sin(2\pi n F_0 t). \tag{B.13}$$

The form on the left containing $\cos(2\pi n F_0 t)$ is most useful when the shape of the string is known at $t = 0$ (as in the case of the plucked string). The second form containing $\sin(2\pi n F_0 t)$ is most useful when the initial conditions involve the velocity at some point on the string, because there one needs to evaluate $\partial y/\partial t \propto \cos(2\pi n F_0 t)$ at $t = 0$ (as for a string struck by a piano hammer, or bowed on a violin).[2]

B.3 The Plucked String

Here, the first form of the solution given in Eq. (B.13) is the most useful. At $t = 0$, the string is distorted into a triangular shape of the type shown in Fig. B.2. [But keep in mind that the solutions given above apply for sufficiently small deflections of the string such that the approximation in Eq. (B.1) is satisfied. Figure B.2 greatly exaggerates the relative size of the deflection for the sake of illustration.]

Consider what happens when a string is plucked at $t = 0$ at some specific point $x = P_0$ along its length, L. If the amplitude of the string at $t = 0$ at the plucking point is A, we see from Eq. (1) that

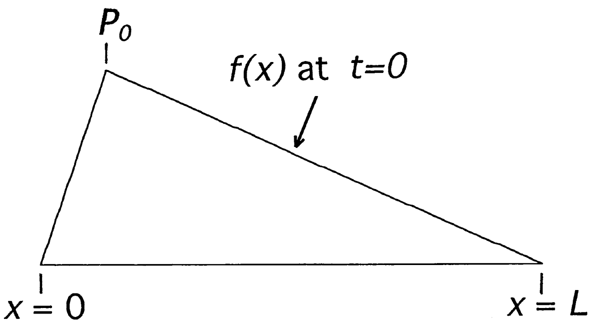

Fig. B.2 Shape of a plucked string at t = 0 (the amplitude is greatly exaggerated)

[2]The point in both cases is, of course, that $\cos(2\pi n F_0 t) = 1$ at $t = 0$, which leaves we with $y(x,0) = \sum_{n=1}^{\infty} A_n \sin(n\pi x/L)$.

$$y(x,0) = f(x) = \begin{cases} Ax/P0, & \text{for } 0 \le x \le P_0 \\ A(L-x)/(L-P_0), & \text{for } P_0 \le x \le L. \end{cases} \quad \text{(B.14)}$$

From Eq. (B.13) at t = 0,

$$f(x) = \sum_{n=1}^{\infty} A_n \sin(n\pi x/L). \quad \text{(B.15)}$$

Here, we can use the same orthogonality properties of the sine function summarized in Chap. 1 to obtain the values of the coefficients A_n, yielding

$$An = \frac{2}{L}\int_{x=0}^{L} f(x)\sin(n\pi x/L)dx. \quad \text{(B.16)}$$

The integral must be broken into two parts in accordance with the form of $f(x)$ given in Eq. (B.14). The spectral amplitudes are then determined from

$$A_n = \frac{2}{L}\int_{x=0}^{P_0}(A_x/P_0)\sin(n\pi x/L)dx + \frac{2}{L}\int_{P_0}^{L}[A(L-x)/(L-P_0)]\sin(n\pi x/L)dx. \quad \text{(B.17)}$$

Integrating by parts and collecting terms, one obtains

$$A_n = \frac{2AM^2}{(M-1)n^2\pi}\sin(n\pi/M) \quad \text{(B.18)}$$

for the spectral distribution, where $M = L/P_0$ is a measure of the plucking point and it is assumed that $n = 1, 2, 3, \ldots$ is an integer. (M does not have to be an integer.) Note that for $M = 2$ (plucking at the mid-point), one only gets odd harmonics and that $A_n = 0$ for n equal to integral multiples of M.

The time-dependent motion of the string is then obtained by substituting the amplitude coefficients A_n from Eq. (B.18) back into the original equation for $y(x,t)$ given at the left of Eq. (B.13). Examples of the motion are shown in Chap. 3.

B.4 The Struck String

Some instruments (especially, various forms of the piano and a few Hungarian instruments such as the Cembalom used by Kodaly) hit the string with a hammer. In this case, the right-hand solution in Eq. (B.13) is the appropriate form to start with because the boundary condition at $t = 0$ is one on velocity. Hence, we will start with a solution of the form,

$$y(x,t)\sum_{n=1}^{\infty} A_n \sin(n\pi x/L)\sin(2\pi n F_0 t). \tag{B.19}$$

The velocity distribution over the string is obtained by taking $\partial y/\partial t$, giving

$$v(x,t) = \frac{\partial y(x,t)}{\partial t} = 2\pi F_0 \sum_{n=1}^{\infty} n A_n \sin(n\pi x/L)\cos(2\pi n F_0 t). \tag{B.20}$$

In principle one could integrate the equation over some finite pulse duration during which the hammer was in contact with the string. However, we shall just assume here that a velocity distribution is suddenly imparted to the string by the hammer before the string has a chance to move. The approximation will be best for the low notes on the instrument where the vibrational periods are longest. In that approximation the velocity distribution at $t = 0$ is given by

$$v(x,0) = V(x) = 2\pi F_0 \sum_{n=1}^{\infty} n A_n \sin(n\pi x/L). \tag{B.21}$$

Then, in analogy with Eq. (B.16), the spectral coefficients are given by[3]

$$A_n = \frac{1}{n F_0 L}\int_0^L V(x)\sin(n\pi x/L)dx. \tag{B.22}$$

As an example, consider a hammer that imparts a rounded velocity distribution to the string of the type shown in Fig. B.3, for which the velocity distribution is given by

$$V(x) = V_0\left[1 - \left(\frac{P_0 - x}{R}\right)^2\right] \text{ for } P_0 - R \le x \le P_0 + R \tag{B.23}$$

and $V(x)$ is assumed to be zero everywhere else. $V(x)$ has a rounded maximum value of V_0 at $x = P_0$, with an effective width of $2R$. (Roughly speaking, R corresponds to the hammer radius at the tip.) Although the shape was arbitrarily assumed, it is not unlike that found at the top of felt hammers currently used in grand pianos.

For the assumption in Eq. (B.23), the spectral coefficients in Eq. (B.22) become

[3]i.e., noting that for m, n integers, $\int_0^L \sin(mx/L)\sin(nx/L)dx = \begin{cases} L/2, & \text{for } m = n. \\ 0, & \text{for } m \neq n. \end{cases}$

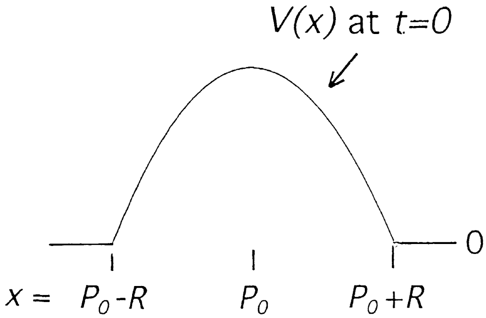

Fig. B.3 Shape of the velocity pulse given by Eq. (B.23)

$$A_n = V_0 \frac{2H^2}{n^4\pi^4 F_0} \left\{ -\cos n\pi \left(\frac{H+M}{MH}\right) + \cos n\pi \left(\frac{H-M}{MH}\right) \right.$$
$$\left. -\frac{n\pi}{H} \sin n\pi \left(\frac{H-M}{MH}\right) - \frac{n\pi}{H} \cos 2\pi \left(\frac{H+M}{MH}\right) \right\} \tag{B.24}$$

where n is the harmonic number, $H = L/R$ (the string length divided by the hammer radius) and $M = L/P_0$ (the ratio of the string length to the striking point, in analogy to the case of the plucked string). As in the case of the plucked string, Eq. (B.24) gives only odd harmonics when $M = 2$, or the string is struck in the middle. Also, $A_n = 0$ for $n = M$ (or the string is struck at a node for the M^{th} harmonic). In this approximation, voicing the hammer corresponds to adjusting the value of H.

The shape of the string as a function of time is obtained by putting the values of A_n from Eq. (B.24) back into the right-hand side of Eq. (B.13). Immediately after the hammer hits the string, a narrow pulse (of width 2τ at the left of Fig. B.5) pops up at the striking point ($x = P_0$, occurring at $t = 0$ in the figure). This narrow pulse consists of two equal-amplitude, oppositely-directed running waves. As time increases, the initial pulse broadens until the wave running to the left bounces off the support at $x = 0$, where it undergoes a "hard" reflection and changes sign. Now negative, it travels back in the $+x$ direction, canceling out its previous positive portion. Meanwhile, the running wave initially moving to the right has continued on its way. The result of adding these two running waves together is an isolated broader, positive pulse (at the right in Fig. B.4) that runs the length of the string.

The rise and fall times (τ) of this wider pulse are each equal to half of the initial narrow-pulse duration. However, the breadth of the wide pulse is determined by the time delay taken for that half of the initial pulse that bounces off the support at $x = 0$ to get back to the striking point at $x = P_0$. Hence, as indicated in the figure, the broad pulse time duration is $2P_0/c$, where c is the velocity of the wave. After reaching the point $x = L$, two "hard" reflections (in succession for each running wave) occur which send an inverted pulse back toward $x = 0$. Examples of these solutions, together with their spectral distribution, are shown in Chap. 4.

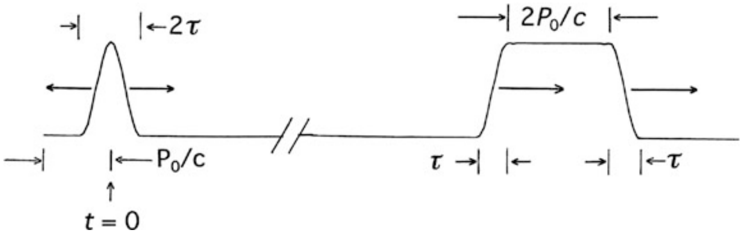

Fig. B.4 Pulses launched on the string by the striking process. Left: The initial pulse at the striking point. Right: The broader pulse running down the string after the first reflection

B.5 The Bowed String

As described in Chap. 5, the excitation of a violin string consists of a stick-slip process which is repeated at the fundamental round-trip frequency $(c/2L)$ and causes pulses to run back and forth on the string of length L. The problem is different from the plucked- and struck-string problems treated above in that the string at the contact point (which we will again take to be $x = P_0$) is forced to move at about the constant velocity of the bow until slipping occurs. When the string does slip, it returns rapidly to its initial point where it is again grabbed by the bow and the process repeats. The string displacement thus executes a sawtooth motion at the point P_0. Helmholtz (1885, pp.384–386) presented an approximate solution to the problem in which he assumed straight-line motion in the two halves of the stick-slip cycle. He then used Fourier analysis of this sawtooth motion and expressed the spectral amplitudes in the solution to the string equation in terms of those Fourier coefficients. The idealized motion is illustrated in Fig. B.5, where will assume the amplitude varies from -1 to $+1$ in the vertical direction and note that the vertical displacements are centered about the time axis.

As in the case of the struck string waveform, we will take the general solution for the shape of the string to be

$$y(x,t) = \sum_{n=1}^{\infty} A_n \sin(n\pi x/L)\sin(2\pi n F_0 t). \tag{B.25}$$

But here, the boundary condition that determines the expansion coefficients An is on the time-dependent saw-tooth motion at the bowing point $x = P_0$ shown in Fig. B.5. In Helmholtz's formulation of the problem, he expressed one cycle of the motion in a general Fourier series including both sine and cosine terms in the time. He then shifted the time axis to obtain a result involving a series of sine terms only. Although that approach is perfectly valid and straightforward, there is a lot tedious algebra required to keep track of all the terms. It is simpler to note at the start from symmetry that, if we choose the origin of the time axis to be centered in the slip cycle as shown in Fig. B.6, one only needs sine terms in the Fourier series. Thus, the

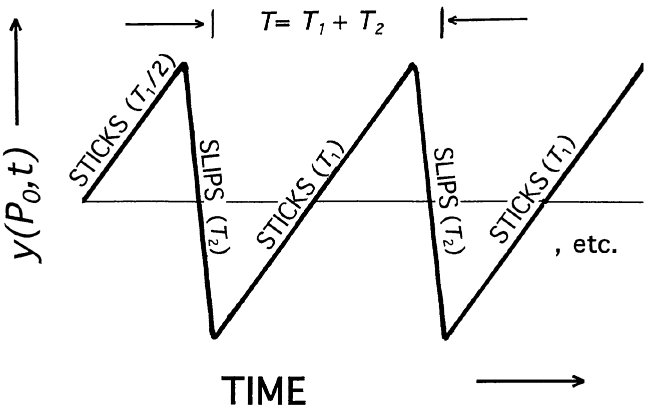

Fig. B.5 Slightly more than two idealized Stick-Slip cycles, corresponding to up-bowing. The total period is $T = T_1 + T_2$, where T_1 is the "Stick" time and T_2 is the "Slip" time

Fig. B.6 Choice of time origin to simplify the calculation of the Fourier series

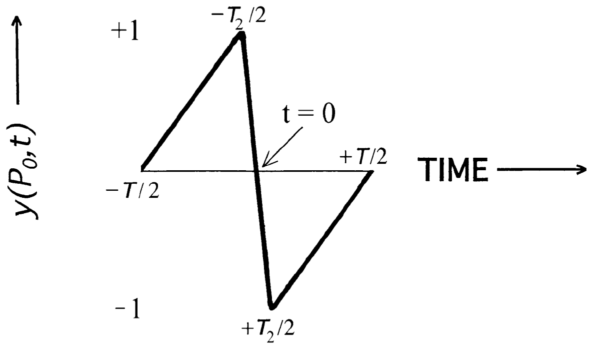

series for the motion at the bowing point may be written

$$y(P_0, t) = \sum_{n=1}^{\infty} C_n \sin(2\pi n F_0 t). \tag{B.26}$$

The Fourier coefficients are then given by

$$\begin{aligned} C_n &= \frac{2}{T} \int_{T/2}^{+T/2} \sin(2\pi n F_0 t) dt \\ &= \frac{2}{T} \int_{-T/2}^{-T_2/2} \left(t + \frac{T}{2} \right) \sin(2\pi n F_0 t) dt \\ &\quad + \frac{2}{T} \int_{-T_2/2}^{+T_2/2} \left[\frac{T_2}{2} - \left(t + \frac{T_2}{2} \right) \right] \frac{2}{T_2} \sin(2\pi n F_0 t) dt \end{aligned}$$

$$+\frac{2}{T}\int_{T_2/2}^{T/2}\left[-\frac{T_1}{2}+\left(t-\frac{T_2}{2}\right)\right]\frac{2}{T_1}\sin(2\pi nF_0t)dt,$$

which simplifies to

$$C_n = -\frac{2}{n^2\pi^2}\left(\frac{T}{T_1}\right)\left(\frac{T}{T_2}\right)\sin\left(n\pi\frac{T_2}{T}\right) \text{ where } T = T_1 + T_2. \tag{B.27}$$

One then substitutes Eq. (B.27) in Eq. (B.26) and compares the result with Eq. (B.25) for $x = P_0$. It is then seen that

$$y(x,t) = -A\sum_{n\neq L/P_0}^{\infty}\frac{2}{n^2\pi^2}\left(\frac{T}{T_1}\right)\left(\frac{T}{T_2}\right)\frac{\sin(n\pi T_2/T)}{\sin(n\pi P_0/L)}\sin(n\pi x/L)\sin(2\pi nF_0t), \tag{B.28}$$

where A has been introduced as an amplitude scaling factor and Eq. (B.28) was used to compute the figures illustrating the Helmholtz method in Chap. 5. The singularity that would occur if L/P_0 were an integer is avoided by setting the partial amplitude to zero for that harmonic. (That particular harmonic would not be excited because the bow would be at a node.) For more general behavior such as that reported by Pickering for real strings and discussed in Chap. 5, one must use the general form of the Fourier series including cosine terms in which the Fourier coefficients are computed numerically by methods equivalent to those discussed in Appendix C.

B.6 The Torsional Wave Equation[4]

As discussed in Chap. 5, the generation of torsional waves is important in the case of large diameter bowed strings under large bowing force. In this case, a form of the wave equation analogous to that in Eq. (B.5) also applies, but with very different wave velocity.

First, consider a hollow uniform cylinder of radius r and thickness dr stretched in the x-direction with the angular rotation at point x along the cylinder given by $\partial\varphi/\partial x$. The shear force on the cylinder material is given by $nr\partial\varphi/\partial x$ where n is defined as the "rigidity" given by

$$n \equiv \frac{Y}{2(\mu+1)} \text{ where } \frac{\text{Lateral Contraction}}{\text{Longitudinal Extension}}, \tag{B.29}$$

Y is Young's modulus, and by definition

[4]Nearly all treatises on mechanics ignore the torsional wave equation. The present derivation is based on one given by Lord Rayleigh (1877, pp. 243–254.)

$$\text{Longitudinal Extension} \equiv \frac{\text{Actual Length} - \text{Natural Length}}{\text{Natural Length}}. \tag{B.30}$$

The quantity n lies between $Y/2$ and $Y/3$ for different materials.
The moment of inertia dI for a hollow cylinder of length dx is given by

$$dI = \rho 2\pi r^3 dr dx$$

where ρ is the mass density. The net change in resisting torque from shear over that length is

$$\Delta\text{Torque} = n2\pi r^3 dr dx \frac{\partial^2\varphi}{\partial x^2} = n\frac{dI}{\rho}\frac{\partial^2\varphi}{\partial x^2}dx$$

where we have made use of a Taylor expansion to show that

$$\left(\frac{\partial\varphi}{\partial x}\right)_{x+dx} - \left(\frac{\partial\varphi}{\partial x}\right)_x = \frac{\partial^2\varphi}{\partial x^2}dx$$

Applying Newton's law relating torque and angular acceleration, we get the torsional wave equation,

$$n\frac{dI}{\rho}\frac{\partial^2\varphi}{\partial x^2}dx = dI\frac{\partial^2\varphi}{\partial t^2}dx \text{ or } \frac{\partial^2\varphi}{\partial x^2} = \frac{1}{n/\rho}\frac{\partial^2\varphi}{\partial t^2}. \tag{B.31}$$

Hence, the torsional waves have a velocity given by

$$c_T = \sqrt{\frac{n}{\rho}}. \tag{B.32}$$

Note that the radial dependence of the moment of inertia cancelled out in these equations. Therefore, the result for c_T is *independent of the radial mass distribution* as long as it has axial symmetry. One, of course, needs to know the values of the mass density ρ and of n from Eq. (B.30) for the string material in order to compute the velocity.

B.7 The Vibrating Membrane as a Two-Dimensional String

The extension of the wave equation to two-dimensional form follows in a straightforward manner from the derivation of the vibrating string equation given at the start of this appendix. Here, we will consider a thin membrane extending in the x and y directions with small vibrational amplitude in the z direction.

Fig. B.7 View looking down on the membrane

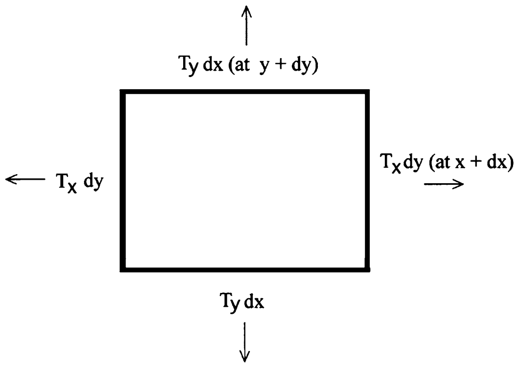

Here, we use a two-dimensional extension of the argument given in connection with Fig. B.1. (See Fig. B.7.) The constant tension T will now be per unit length along the x and y directions and we are concerned with the net restoring force in the z-direction acting on a differential mass element $\Delta m = \mu \Delta x \Delta y$, where σ is the mass density per unit area of the membrane. Applying Newton's Law to the motion in the z-direction for this differential membrane element, we get

$$F_z \approx T_x \Delta y \left[\left(\frac{\partial z}{\partial x} \right)_{x+\Delta x} - \left(\frac{\partial z}{\partial x} \right)_x \right] + T_y \Delta X \left[\left(\frac{\partial z}{\partial y} \right)_{y+\Delta y} - \left(\frac{\partial z}{\partial y} \right)_y \right] \Delta x$$
$$= \Delta m a_z = \sigma \Delta x \Delta y \frac{\partial^2 z}{\partial t^2}.$$

As with the one-dimensional case, we can get the component of force normal to the surface by expanding the functions dz/dx and dz/dy in a Taylor series about the point x, y noting that

$$\left(\frac{\partial z}{\partial x} \right)_{x+\Delta x} = \left(\frac{\partial z}{\partial x} \right)_x + \frac{\partial}{\partial x} \left(\frac{\partial z}{\partial x} \right)_x \Delta x^1 + \text{Order}(\Delta x^2) \text{ and } \left(\frac{\partial z}{\partial y} \right)_{y+\Delta y}$$
$$= \left(\frac{\partial z}{\partial y} \right)_y + \frac{\partial}{\partial y} \left(\frac{\partial z}{\partial y} \right)_y \Delta y^1 + \text{Order}(\Delta y^2)$$

Substituting in the force equation and neglecting quadratic terms in Δx, Δy, we get

$$F_z \approx T_y \frac{\partial}{\partial x} \left(\frac{\partial z}{\partial x} \right)_x \Delta x^1 + T_x \frac{\partial}{\partial y} \left(\frac{\partial z}{\partial y} \right)_y \Delta y^1 + \text{ Order}(\Delta x^2, \Delta y^2)$$

where we have assumed that T_x might not be equal to T_y for the sake of generality. (That permits having different wave velocities in the two orthogonal directions.) Substituting in the force equation and taking the limit as $\Delta x, \Delta y \to 0$, we get a non-isotropic form of the two-dimensional wave equation

$$\left(\frac{1}{T_y}\right)\frac{\partial^2 z}{\partial x^2} + \left(\frac{1}{T_x}\right)\frac{\partial^2 z}{\partial y^2} = \frac{\sigma}{T_x T_y}\frac{\partial^2 z}{\partial t^2}.$$

Of course, if $T_x = T_y$, this expression reduces to the more usual isotropic form of the two-dimensional wave equation,

$$\frac{\partial^2 z}{\partial x^2} + \frac{\partial^2 z}{\partial y^2} = \frac{1}{c^2}\frac{\partial^2 z}{\partial t^2} \tag{B.33}$$

for which the wave velocity, c, is the same in both directions. That is,

$$c = \sqrt{\frac{T}{\sigma}} \text{ for } T = T_x = T_y. \tag{B.34}$$

With the isotropic case, the variables are easily separable and we can write

$$Z(x, y, t) = X(x)Y(y)T(t) \tag{B.35}$$

which substituted in the wave equation yields

$$\frac{1}{X(x)}\frac{\partial^2 X(x)}{\partial x^2} + \frac{1}{Y(y)}\frac{\partial^2 Y(y)}{\partial y^2} = \frac{1}{c^2 T(t)}\frac{\partial^2 T(t)}{\partial t^2} \equiv -k^2 = \text{contant.} \tag{B.36}$$

The solutions must be valid for all values of x, y, and t and the only way that can happen is for the separate terms to equal constants. Here as in the one-dimensional case, we take a negative definite constant for the time-dependent part of the solution to insure stable oscillatory solutions. The first two terms on the left of the equation may be rewritten

$$\frac{1}{X(x)}\frac{\partial^2 X(x)}{\partial x^2} = -k_x^2, \quad \frac{1}{Y(y)}\frac{\partial^2 Y(y)}{\partial y^2} = -k_y^2, \text{ where } k_x^2 + k_y^2 = k^2 \tag{B.37}$$

where k_x and k_y are constants. This substitution gives rise to solutions of the form

$$\begin{aligned} X(x) &\propto \sin k_x x \text{ and / or } \cos k_x x \\ Y(y) &\propto \sin k_y y \text{ and / or } \sin k_y y \\ T(t) &\propto \cos \omega t \text{ and / or } \sin \omega t \end{aligned} \tag{B.38}$$

where $Z(x, y, t)$ is given by the product of the three.

Spatial boundary conditions determine the resonant frequencies. For example, if the membrane is clamped on all edges, the solutions must have zero amplitude there and the appropriate spatial functions are

$$X(x) \propto \sin k_x x \text{ and } Y(y) \propto \sin k_y y \tag{B.39}$$

with

$$k_x = n_x\pi/L_x \text{ and } k_y = n_y\pi/L_y \text{ where } n_x, n_y = 1, 2, 3, \ldots \tag{B.40}$$

The oscillation frequencies of these modes are then given by

$$\omega_n = c\sqrt{k_x^2 + k_y^2} = \pi c\sqrt{\left(\frac{n_x}{L_x}\right)^2 + \left(\frac{n_y}{L_y}\right)^2}. \tag{B.41}$$

The equations for the homogeneous membrane give rise to modes of the type illustrated in Fig. B.8.

Solutions for the nonisotropic membrane are of interest because of their relationship to those in thin soundboards (for example, in harpsichords and violins) in which the velocity of wave propagation is quite different in the two principal orthogonal directions. The solutions in that case may be obtained in exactly the same way using the principle of separability. However, it is easier to note that the solutions for the non-isotropic case may be obtained from those for the isotropic case by a simple coordinate transformation of the type

$$x' = T_y x \text{ and } y' = T_x y. \tag{B.42}$$

Hence, the case of nonequal velocities in the two orthogonal directions has solutions that are equivalent to the isotropic case with different relative dimensions of the rectangular membrane.

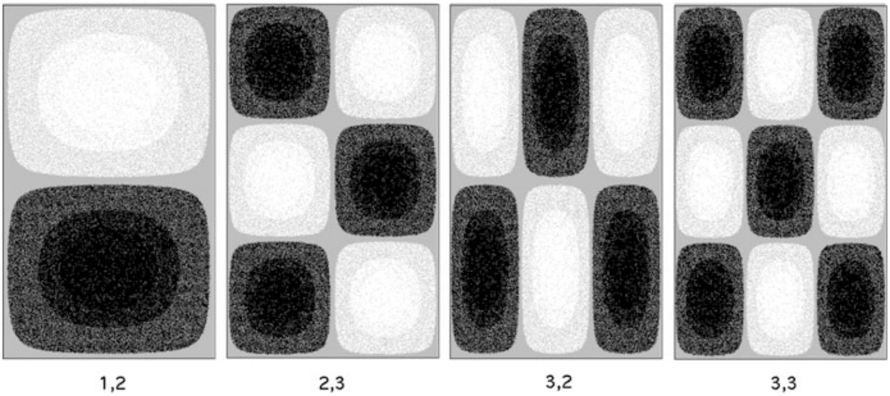

Fig. B.8 Modes for a rectangular membrane (or drumhead) in which the tensions (wave velocities) are equal in both coordinate directions and the sides are in the ratio of 2:3

As noted above, the equation of motion in this case is of the form

$$\left(\frac{1}{T_y}\right)\frac{\partial^2 z}{\partial x^2}+\left(\frac{1}{T_x}\right)\frac{\partial^2 z}{\partial y^2}=\left(\frac{\sigma}{T_x T_y}\right)\frac{\partial^2 z}{\partial t^2} \tag{B.43}$$

Again the equation is separable in the time and space variables by the substitution

$$Z(x, y, t) = X(x)Y(y)T(t). \tag{B.44}$$

Hence

$$\begin{aligned}\left(\frac{1}{T_y X(x)}\right)\frac{\partial^2 X(x)}{\partial x^2}+\left(\frac{1}{T_x Y(y)}\right)\frac{\partial^2 Y(y)}{\partial y^2} &= \frac{\sigma}{T_x T_y}\left(\frac{1}{T(t)}\right)\frac{\partial^2 T(t)}{\partial t^2}\\ &= -\omega^2 = \text{ constant}\end{aligned} \tag{B.45}$$

where a negative constant was again chosen to assure a stable oscillatory solution with angular frequency ω. For the two terms on the left of the equation to add up to a constant, each must separately be constant. Hence,

$$\frac{\partial^2 X(x)}{\partial x^2}+\omega_x^2 T_y X(x)=0 \text{ and } \frac{\partial^2 Y(y)}{\partial y^2}+\omega_y^2 T_x Y(y)=0 \tag{B.46}$$

with solutions

$$X(x) \propto \sin \omega_x \sqrt{T_y} x \text{ and } Y(y) \propto \sin \omega_y \sqrt{T_x} y, \tag{B.47}$$

where

$$\omega_x \sqrt{T_y} = n_x \pi / L_x \text{ and } \omega_y \sqrt{T_x} = n_y \pi / L_y \text{ where } n_x, n_y = 1, 2, 3, \ldots \tag{B.48}$$

That is, the modes are determined by the spatial boundary condition that the vibrational amplitudes are zero on the boundaries; that is, we assume the membrane is clamped on the edges. The oscillatory frequency for a given mode is then given by

$$\omega = \sqrt{\omega_x^2+\omega_y^2} = \pi\sqrt{n_x^2/L_x^2 T_y + n_y^2/L_y^2 T_x} \tag{B.49}$$

and they, in general, will not be harmonically related.

B.8 Circular Membranes

Drums utilize circular membranes in most cases. These are easiest to treat using circular (or cylindrical) coordinates. Consider a coordinate system where the radius vector r is in the xy plane at angle ϕ with respect to the x axis (Fig. B.9). (The new and old z-axes are identical.)

It may be shown that the two-dimensional wave-equation operator transforms as[5]

$$\frac{\partial^2 A(x,y)}{\partial x^2} + \frac{\partial^2 A(x,y)}{\partial y^2} = \frac{1}{r}\frac{\partial}{\partial r}\left(r\frac{\partial A(r,\varphi)}{\partial r}\right) + \frac{1}{r^2}\frac{\partial^2 A(r,\varphi)}{\partial \varphi^2}. \tag{B.50}$$

Hence, the wave equation in circular coordinates becomes

$$\frac{1}{r}\frac{\partial}{\partial r}\left(r\frac{\partial A}{\partial r}\right) + \frac{1}{r^2}\frac{\partial^2 A}{\partial \varphi^2} = \frac{1}{c^2}\frac{\partial^2 A}{\partial t^2} \text{ where } c = \sqrt{\frac{T}{\sigma}} \tag{B.51}$$

c is the running wave velocity (assumed to be the same in all directions), T is the constant tension per unit length around the circumference, and σ is the mass density per unit area.

Again, we can separate the variables in the form

$$A(r,\varphi,t) = R(r)\Phi(\varphi)T(t), \tag{B.52}$$

where $T(t)\cos(\omega t)$ or $T(t) = \sin(\omega t)$.

Fig. B.9 Relation of rectangular and cylindrical coordinates

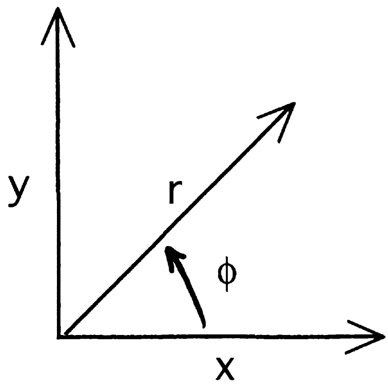

[5]See, e.g., Weatherburn (1951), pp. 15 and 16.

Then we get

$$\frac{\partial^2 \Phi}{\partial \varphi^2} + m^2 \Phi = 0 \text{ where } \Phi(\varphi) = \cos(m\varphi) \text{ or } \Phi(\varphi) = \sin(m\varphi). \tag{B.53}$$

Because $\Phi(\varphi)$ must be periodic in 2π so that the function closes on itself in one revolution about z-axis, we must have $m = 1, 2, 3, 4, \ldots$ This condition means that

$$\frac{\partial^2 R}{\partial r^2} + \frac{1}{r}\frac{\partial R}{\partial r} + \left(\frac{\omega^2}{c^2} - \frac{m^2}{r^2}\right) R = 0, \tag{B.54}$$

which is known as Bessel's Equation and has solutions of the form

$$J_m(x) = \sum_{p=0}^{\infty} (-1)^p \frac{(x/2)^{m+2p}}{p!(m+p)!}. \tag{B.55}$$

where $J_m(x)$ is a Bessel function of real argument of order m.[6] Hence, the radial solutions for the circular membrane are of the form

$$R(r) \propto J_m\left(\frac{\omega}{c} r\right) = J_m(kr). \tag{B.56}$$

A particular time-dependent solution is then

$$A(r, \varphi, t) \propto \cos(m\varphi) J_m(k_{m,n} r) \cos(2\pi f_{m,n} t). \tag{B.57}$$

The nodal diameter for a particular allowed solution is determined by the value of m and arises from the periodicity requirement on $\Phi(\varphi)$. The allowed values of the parameter k are then determined by the requirement that the rim of the circular drum corresponds to a root n of the Bessel function of that particular order, m. Thus, the resultant values of k depend on two integers, m and n. The frequency of the mode of vibration then is given by

$$f_{m,n} = \frac{k_{m,n} c}{2\pi} \tag{B.58}$$

To illustrate a particular mode for a circular kettle drum of radius, R_0, it is necessary to scale the argument of the Bessel function so that it goes through zero for a particular root when $r = R_0$. Thus, a given kettle drum mode distribution would be proportional to

[6]During the Great Depression, mathematicians were hired by the WPA to compute tables of Bessel Function up to order 600 or more and in high precision. These tables, which are now totally obsolete if any rudimentary computer is available, were stored in the basement of Low Library at Columbia University.

Table B.1 Values of $k_{m,n}$ (roots) for the Bessel function J_m

m, n	1	2	3	4	5
0	2.40483	5.52008	8.65373	11.7915	14.9309
1	3.83171	7.01559	10.1735	13.3237	16.4706
2	5.13562	8.41724	11.6198	14.796	17.9598
3	6.38016	9.76102	13.0152	16.2235	19.4090
4	7.58834	11.0647	14.3725	17.616	20.8269

Computed by the author

$$\cos(m\varphi) J_m\left(k_{m,n}\frac{r}{R_0}\right). \tag{B.59}$$

Approximate values for the first few roots of the Bessel function J_m are given in Table B.1. (Such modes are sometimes called "eigen functions" and the quantities $k_{m,n}$ are "eigen values.") Representative kettledrum mode shapes are shown in Fig. B.10 in 3-D.

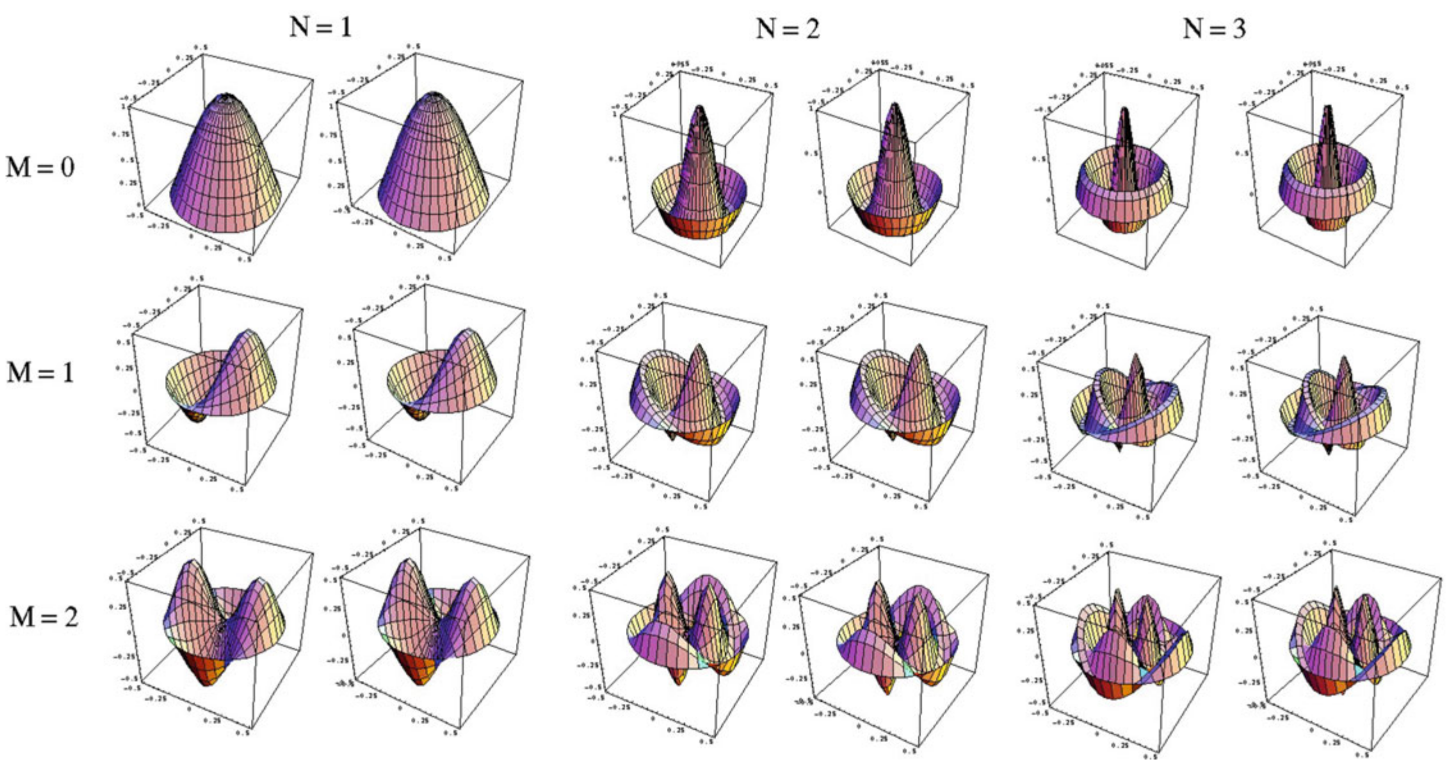

Fig. B.10 The first few kettledrum modes from Eq. (B.59) and Table B.1 are shown in stereoscopic pairs. Note that for M = 0, there are no nodal diameters; for M = 1, there is one nodal diameter; and for M = 2, there are two nodal diameters. Similarly, for N = 1 there is one circular node (at the rim of the drum); for N = 2 there are two circular nodes; and for N = 3 there are three such nodal circles. To see these figures stereoscopically, hold the paper as near to your eyes as permits comfortable focusing. For each pair, you should see four images—two with each eye. Make the two center images coincide in your brain. The amplitudes are exaggerated for clarity (The figures were computed by the author)

Appendix C
Fourier Analysis

We will include here some of the mathematical details dependent on calculus that were omitted in Chap. 2, together with a working program for discrete Fourier analysis. We will restrict the discussion to "well-behaved" periodic functions which obey

$$V(\theta + 2\pi) = V(\theta), \tag{C.1}$$

for which Fourier (1822) showed that the function $V(\theta)$ may be written

$$V(\theta) = C_0 + \sum_{n=1}^{\infty} A_n \sin n\theta + \sum_{n=1}^{\infty} B_n \cos n\theta. \tag{C.2}$$

We wish to evaluate the DC constant C_0 together with the harmonic coefficients A_n and B_n.

Determining the DC constant in Eq. (C.2) is particularly easy. Recalling the fact that the definite integral is just equal to the area under the curve,[1] it is apparent that the integrals of all the sine and cosine terms in Eq. (C.2) over one period will identically vanish; i.e., the sine and cosine functions have equal areas above and below the horizontal axis. Hence, in averaging Eq. (C.2) over one fundamental period, all of the $\sin n\theta$ and $\cos n\theta$ terms will drop out, leaving

$$C_0 = \frac{1}{2\pi} \int_0^{2\pi} V(\theta) d\theta \tag{C.3}$$

[1]The fact that the area under the curve in the integrand is given by the definite integral between two points on the horizontal axis is sometimes called "The Fundamental Theorem of Calculus."

© Springer Nature Switzerland AG 2018

W. R. Bennett, Jr., *The Science of Musical Sound*,
https://doi.org/10.1007/978-3-319-92796-1

where, as indicated using a notation invented by Fourier himself, the definite integral runs from 0 to 2π radians.

Determining the coefficients A_n and B_n for the waveform is a little harder. Here, we will make use of something known as the "orthogonality" of the sine and cosine functions over one period.[2] You can show from trigonometric identities that[3]

$$\int_0^{2\pi} \sin m\theta \cos n\theta d\theta = 0 \tag{C.4}$$

for all integral values of m and n.

Similarly, it can be shown that[4]

$$\int_0^{2\pi} \sin m\theta \sin n\theta d\theta = \int_0^{2\pi} \cos m\theta \cos n\theta d\theta = \begin{cases} \pi, & \text{for } m = n. \\ 0, & \text{for } m \neq n. \end{cases} \tag{C.5}$$

where m and n are integers.

To evaluate the general coefficient A_m, multiply both sides of Eq. (C.2) by $\sin m\theta$ and integrate from 0 to 2π. All the terms in the Fourier series then vanish except for

$$A_m = \frac{1}{\pi} \int_0^{2\pi} V(\theta) \sin m\theta d\theta. \tag{C.6}$$

Similarly to get B_m, multiply Eq. (C.2) by $\cos m\theta$ obtaining

$$B_m = \frac{1}{\pi} \int_0^{2\pi} V(\theta) \cos m\theta d\theta. \tag{C.7}$$

Then, as shown in Chap. 2, we may rewrite $V(\theta)$ as

$$V(\theta) C_0 + \sum_{n=1}^{\infty} C_n \sin(n\theta + \varphi_n), \tag{C.8}$$

---

[2]The term arises because the sines and cosines can be regarded as projections of orthogonal "vectors" in a multi-dimensional space in the sense that their generalized dot- (or scalar-) products vanish.

[3]Since

$2 \sin m\theta \cos n\theta = \sin(m+n)\theta + \sin(m-n)\theta$

and m and n are integers, the integrals of the sine functions on the right side of this identity over one period must vanish.

[4]E.g., consider the identity

$2 \sin m\theta \sin n\theta = \cos(m+n)\theta \cos(m-n)\theta$.

If $m \neq n$, integrals over one period on the right side both vanish. But if $m = n$, the second term on the right side of the trig identity is $\cos(0) = 1$. Hence, for $m = n$,

$\int_0^{2\pi} \sin m\theta \sin n\theta d\theta = \frac{1}{2} \int_0^{2\pi} d\theta = \pi$

where the constants are given by

$$C_n = \sqrt{A_n^2 + B_n^2} \text{ for } n \geq 1 \text{ and } \varphi_n = \arctan(B_n/A_n). \tag{C.9}$$

The procedure for determining the Fourier coefficients then consists of computing the integrals in Eqs. (C.3), (C.6), and (C.7), which generally must be done numerically from digital samples of the waveform over one period. Then one uses Eq. (C.9) to determine the net harmonic amplitude and phase. There is one pitfall to avoid in computing the phase from the arctangent relation in Eq. (C.9). Computer programming languages and pocket calculators do not always have provision for automatically putting the angle whose tangent is (B/A) in the correct quadrant. If the computer only deals with the numerical result from evaluating $x = B/A$, it cannot tell what the quadrant should be from the statement $\phi = \text{ATN}(x)$. If A is positive, the answer for ϕ will be correct and the angle will fall in either the first or fourth quadrant. However, if A is negative, the answer will be wrong and should fall in the second or third quadrant. The problem is solved in BASIC by including statements such as

$$\begin{aligned} &\text{ATN}(B/A) \\ &\text{IF } A < 0 \text{THEN } \phi = \phi + \pi. \end{aligned} \tag{C.10}$$

The FORTRAN programming language has a single arctangent statement of the type ATAN2(B/A) that takes care of the problem. If any phase angle were off by π, reconstruction of the waveform from the Fourier coefficients would give the wrong shape. Of course, the spectrum of harmonic amplitudes wouldn't be altered. Reconstruction of the original waveform is, of course, obtained by substituting the coefficients C_n and ϕ back into Eq. (C.8). If the reconstructed waveform does not match the original, you have either made a mistake or have not taken enough harmonics into account. (See Fig. 2.12.)

C.1 Energy Distribution in a Fourier Series

It is generally true in classical physics (i.e., non quantum-mechanical problems) that the energy in a vibrating system is proportional to the square of the amplitude of the disturbance. That fact is shown in detail for the harmonic oscillator in Appendix A. What we are interested in here is the average value of the square of the amplitude over the fundamental period of the Fourier series. The relative values are usually of main concern rather than the absolute values. Suppose we have a waveform of the type

$$y(t) = \sum_{n=1}^{\infty} C_n \sin(n\omega t + \varphi_n). \tag{C.11}$$

Then, the average energy over one cycle is[5]

$$Energy \propto \frac{1}{T} \int_0^{2\pi} y(t)^2 dt = \sum_{n=1}^{\infty} C_n^2 \tag{C.12}$$

where $T = 1/f = 2\pi/\omega$ is the fundamental period of the waveform. Hence, the relative energy in the n^{th} harmonic is simply proportional to C_n^2.

C.2 Program for Discrete Fourier Analysis[6]

The following program is written in BASIC, but could easily be rewritten in FORTRAN or another language. In what follows, REM means a remark that is ignored by the computer. Explanatory comments after the apostrophe (') are also ignored when the computer runs.

```
REM Dimension statements[7]

        DIM A(50), B(50), C(50), P(50)   ' For Fourier
coefficients
        DIM V(255)          ' To store the Data
        Pi = 4*ATN(1.0)     ' Pi = Greek \pi

REM Enter data for one period = P[8]
READ P
```

[5]To prove the statement, note that $y^2(t)$ could be written
$y(t)^2 = \sum_{n=1}^{\infty} C_n \sin(n\omega t + \varphi_n) \sum_{m=1}^{\infty} C_m \sin(m\omega t + \varphi_n)$.
Hence,
Energy $\propto \frac{1}{T} \sum_{n=1}^{\infty} \sum_{m=1}^{\infty} C_n C_m \int_0^T \sin(n\omega t + \varphi_n) \sin(m\omega t + \varphi_n) dt$
where the terms for $m \neq n$ vanish because of orthogonality of the sine functions.

[6]Note: In order to save running time, it really pays to compile the program.

[7]Arrays are just subscripted variables; e.g., A(N) is the same as the mathematical variable AN. Dimension(DIM) statements tell the computer to set aside the maximum number of elements that could appear in the array; e.g., DIM A(50) means that there could be 50 elements (harmonics) in array A(N).

[8]The READ statement assigns the next previously unread number within DATA statements in the program to a given variable. E.g., here P = 109, which is the total number of points in the following DATA statements and V(1) = 3. The loop structure, FOR I = 1 TO P permits using the same statement, READ V(I), within the loop over and over for P times. The loop is closed by the NEXT I statement. Note that the waveform is periodic. (The first and last points are both equal

```
FOR  I=1 TO P
READ V(I) NEXT I

REM Mode–Locked Garden Hose (normalized to ±1000)
REM P= Number of points in Period = the first datum
 DATA 109
DATA 3,20,43,68,111,176
DATA 273,426,634,861,1000,989
DATA 864,705,563,452,358,273
DATA 199,136,85,45,17,−14
DATA −40,−63,−85,−105,−125,−129
DATA −151,−162,−165,−165,−165,−165
DATA −170,−165,−170,−170,−170,−173
DATA −173,−170,−162,−159,−156,−153
DATA −151,−142,−139,−136,−131,−128
DATA −128,−128,−125,−119,−114,−108
DATA −102,−94,−91,−91,−91,−91
DATA −91,−91,−91,−91,−91,−91
DATA −85,−82,−82,−80,−74,−74
DATA −74,−80,−80,−80,−80,−80
DATA −82,−82,−82,−85,−88,−91
DATA −91,−91,−91,−91,−91,−85
DATA −82,−80,−74,−71,−68,−65
DATA −60,−57,−45,−37,−28,−14
DATA   3

REM Fundamental frequency in Hz
DATA  307.692     ' Not used in this program

REM Display of the Waveform[9]
Xmax=550          'Xmax and Ymax are the maximum number
Ymax=500          'of pixels available and vary with the
computer
REM Plot Horizontal Axis
        Pen=0
    X=0
        Y=Ymax/2
    GOSUBS PLOT
```

to 3.) The DATA were all taken with an A- to-D (Analog-to-Digital) converter with 1 part in 1000 resolution, hence are in the range 1000.

[9]Xmax and Ymax are the maximum number of points (“pixels”) used on the plotting device. Pen is a “Pen- Lift” variable. (Imagine plotting on an old-fashioned xy-recorder.) See Subroutine PLOT: for its meaning.

```
        Pen=1
    X=Xmax
    GOSUB PLOT
REM Plot Waveform
        Pen=0
        FOR I=1 TO P
                Y=0.5*Ymax*(1+V(I)/1000)
        X=(I-1)*Xmax/(P-1)
        GOSUB PLOT
                Pen=1
    NEXT I

REM Chosing the maximum number of harmonics[10]

PRINT ''Nmax''
INPUT Nmax
REM Harmonic Analysis[11]

A0=2*Pi/(P-1)     ' A0 is a constant used in the loop
 on N.
FOR N=0 TO Nmax   ' N=0 corresponds to the constant or
DC term
        A(N)=0
        B(N)=0
        FOR I=1 TO P
                A(N)=A(N)+V(I)*SIN(N*A0*(I-1))
                B(N)=B(N)+V(I)*COS(N*A0*(I-1))
    NEXT I
        A(N)=A(N)*2/(P-1)
        B(N)=B(N)*2/(P-1)
```

[10]Normally one could simply estimate the maximum number of harmonics (Nmax) from the number of wiggles in one period of the waveform and INPUT (enter) that number from the keyboard. The present case is tricky because the waveform is a sharp pulse without wiggles. One way is to make a guess (e.g., Nmax = 20) and see how closely the waveform reconstructed from the Fourier coefficients agrees with the original. Then increase (or decrease) Nmax as needed. See Fig. 2.12.

[11]This part of the program takes most of the running time. A(N) and B(N) correspond to the Fourier amplitudes given by the integrals in Eq. (C.6) and (C.7). They are done here numerically by a method equivalent to drawing straight lines between the successive points and adding up the areas (the "trapezoidal Rule"). Each variable A(N) and B(N) is initially set to zero and the increments repeatedly added within the loop FOR I = 1 TO P-1 in a series of the type$A(N)0.5(y_1 + y_2)\Delta x 0.5(y_2 + y_3)\Delta x + \ldots + 0.5(y_{P-1} + y_P)\Delta x = (y_1 + y_2 + y_3 + \ldots + y_{P-1})\Delta x + 0.5(y_P - y_1)\Delta x$which simplifies because $y_P = y_1$ (i.e., the series is periodic.) Here, e.g., $y_i = V(I) *$ SIN$(N * A0 * (I - 1))$ and $\Delta x = 1$. The net Fourier amplitude $C(N)$ and phase $P(N)$ are computed using Eqs. (C.6), (C.7), and (C.8).

```
    C(N)=SQR(A(N)*A(N)+B(N)*B(N))
        IF N>0 THEN P(N)=ATN(B(N)/A(N))  ' avoid DC term
        IF A(N)<0 THEN P(N)=P(N)+Pi      'arctangent
 problem
NEXT N
REM DC or constant term next
        C(0)=B(0)/2
REM Plot Histogram of the Coefficients
        REM Find Maximum Harmonic coefficient , Cmax
        Cmax=-1E30        'A negative number below the
smallest likely C(N)
    FOR N=1 TO Nmax
                IF C(N)>Cmax THEN Cmax=C(N)
    NEXT N
        FOR N=1 TO Nmax
                X=(N-1)*Xmax/Nmax
        Y=0
                Pen=0
        GOSUB PLOT
                Y=C(N)*Ymax/Cmax
        Pen=1
                GOSUB PLOT
    NEXT N
```

C.3 Additional Waveforms

Additional musical instrument waveforms are presented below in the same format as that given above for the garden hose for those who might like to study them and for use elsewhere in this book. These data were taken in Davies Auditorium at Yale, using a high-quality Sennheiser MKH104 omnidirectional microphone with uniform response (±1 dB) over the range from 50 Hz to 20 kHz and the Hewlett-Packard equipment shown in Fig. 2.9. The 10-bit A-to-D converter used had a dynamic range of about 60 dB. The instruments were played without vibrato by professional musicians to whom the author is greatly indebted. The brass instruments were played by James Undercoffler; the violins, by Syoko Aki; the oboe, heckelphone, krummhorn and rohr schalmei by James Ryan; and flute and piccolo by Leone Buyse. I am indebted to the late William Liddell for the use of his krummhorns, to Richard Rephann for the loan of the historic brass instruments from the Yale Instrument Collection, and to Robert Sheldon of the Smithsonian Collection in Washington, DC for playing the serpent. The heckelphone was loaned by the Yale Concert Band and the rohr schalmei was borrowed from the author's personal pipe organ.

F-Cornet

```
DATA 107
DATA −4,44,114,163,212,249
DATA 280,301,311,319,321,321
DATA 311,290,259,223,166,111
DATA 57,5,−47,−83,−106,−122
DATA −124,−119,−98,−83,−67,−52
DATA −41,−47,−62,−83,−109,−150
DATA −192,−231,−259,−285,−301,−303
DATA −293,−269,−228,−166,−96,−13
DATA 78,174,275,370,477,578
DATA 681,777,870,948,995,1000
DATA 974,886,764,617,433,244
DATA 67,−101,−238,−345,−412,−448
DATA −461,−448,−415,−383,−337,−301
DATA −272,−259,−251,−269,−301,−332
DATA −365,−399,−425,−446,−453,−456
DATA −446,−425,−399,−383,−368,−355
DATA −347,−337,−329,−301,−262,−241
DATA −210,−166,−117,−65,−4
REM Cornet Frequency in Hz
DATA 316.075
```

Piccolo Trumpet

```
DATA 168
DATA −5,97,195,280,367,450
DATA 530,610,680,755,807,857
DATA 898,935,967,982,997,1000
```

```
 Piccolo  Trumpet DATA −755,−720,−673,−623,−563,−500
DATA     168      DATA −433,−355,−272,−193,−110,−5
DATA     −5,97,195,280,367,450    REM Piccolo Trumpet
  Frequency in Hz
DATA     530,610,680,755,807,857 DATA    597.672
DATA     898,935,967,982,997,1000
DATA 995,987,965,940,910,875
DATA 835,797,742,695,637,585
DATA 527,475,417,357,302,247
DATA 187,130,85,37,−10,−50
DATA −80,−110,−140,−160,−180,−193
DATA −203,−200,−200,−193,−170,−155
DATA −130,−93,−55,−12,35,77
DATA 125,177,227,277,325,367
DATA 408,450,490,517,545,567
```

```
DATA 580,587,590,590,580,560
DATA 540,515,485,450,408,367
DATA 327,285,240,190,147,97
DATA 55,15,-35,-65,-100,-133
DATA -155,-180,-200,-215,-230,-233
DATA -245,-245,-242,-245,-242,-240
DATA -238,-235,-238,-235,-235,-242
DATA -253,-260,-265,-282,-300,-320
DATA -343,-363,-390,-413,-440,-463
DATA -490,-513,-535,-557,-583,-603
DATA -623,-643,-660,-680,-690,-715
DATA -733,-753,-773,-793,-810,-830
DATA -845,-857,-873,-875,-875,-882
DATA -873,-870,-857,-835,-810,-785
DATA -755,-720,-673,-623,-563,-500
DATA -433,-355,-272,-193,-110,-5
REM Piccolo Trumpet Frequency in Hz
DATA 597.672

REM Visual reconstruction from the Fourier
  coefficients[12]

Pen=0
FOR I=1 TO P
        V(I)=C(0)          ' constant or DC term
    FOR N=1 TO Nmax
                V(I)=V(I)+C(N)*SIN(N*A0*I+P(N))
        NEXT N
        Y=0.5*Ymax*(1+V(I)/1000)
    X=(I-1)*Xmax/(P-1)
    GOSUB PLOT
        Pen=1
NEXT I

REM Dummy Input to retain display
INPUT Q$
```

[12]Here, we reconstruct the Fourier Series to compare with the original waveform initially stored in V(I). (The contents of the array V(I) are changed when the program runs.) Note that without the constant or DC term, the reconstructed waveform may be offset vertically from the original waveform. An effective DC offset can sometimes arise from the presence of low-frequency background noise that is unrelated to the waveform of interest. Several languages also permit constructing the sound of the waveforms, in which case the fundamental frequencies contained in the last DATA statement is important.

```
END

SUBROUTINE[13]

PLOT

RETURN

REM Pen=0 plots points at (X,Ymax–Y), with origin
  at (0,Ymax)
REM Pen=1 Draws line from last point to coordinates
  (X, Ymax–Y)
IF Pen=0 THEN POINT (X, Ymax–Y)
IF Pen=1 THEN LINE (X, Ymax–Y)
```

Note: Some programming languages permit constructing the sound of the waveform. The fundamental frequencies for each waveform are included in Hz in the DATA statements for that purpose.

French Horn (Loud)

```
DATA  151
DATA  21,112,188,242,273,318
DATA  356,387,399,394,385,371
DATA  349,309,264,200,133,76
DATA  38,21,17,17,26,52
DATA  67,95,121,147,159,171
DATA  176,166,157,143,140,138
DATA  128,124,124,124,133,143
DATA  147,147,143,140,135,133
DATA  119,105,93,76,62,26
DATA −12,−52,−95,−138,−181,−214
DATA −252,−283,−299,−314,−309,−295
DATA −268,−249,−240,−233,−214,−195
DATA −166,−128,−76,−10,64,121
DATA  176,216,245,273,285,295
DATA  292,292,302,314,333,340
```

[13]The instructions POINT (X,Y) and LINE (X,Y) are intended to plot a point at coordinates X, Y whenPen = 0 and a line from the previously plotted point to coordinates X, Y if Pen = 1, respectively, assuming the origin is in the lower left-hand corner. Plotting commands of this type are contained in most languages, but with varying designations. Most languages now put the origin in the upper left hand corner of the plotting device, in which case one needs to replace Y by Ymax-Y as has been done in the subroutine here. One may also need scaling factors dependent on the maximum number of pixels available in the x and y directions. The convention on naming subroutines varies from one version of BASIC to another. In some versions the term PLOT has a different, specific meaning built into the operating system.

```
DATA  349,347,347,349,375,428
DATA  508,575,627,656,672,679
DATA  684,684,689,684,670,641
DATA  596,551,508,451,380,304
DATA  214,128,45,−43,−164,−314
DATA −461,−589,−670,−703,−717,−743
DATA −791,−846,−895,−931,−960,−988
DATA −1000,−971,−924,−886,−855,−838
DATA −836,−841,−838,−829,−774,−698
DATA −613,−527,−437,−335,−219,−95
DATA  21
REM French Horn Frequency in Hz DATA  222.488
```

French Horn (Soft)

```
DATA  151
DATA  4,46,87,121,154,183
DATA  212,231,262,272,291,297
DATA  306,297,297,291,283,268
DATA  264,247,237,229,216,206
DATA  200,191,179,166,158,141
DATA  131,116,121,112,106,104
DATA  100,98,96,83,87,79
DATA  73,71,62,56,48,40
DATA  40,42,46,54,58,62
DATA  64,71,67,73,71,71
DATA  75,81,96,104,114,133
DATA  156,166,183,212,225,247
DATA  272,297,322,349,372,399
DATA  422,441,462,484,499,516
DATA  528,541,555,563,563,572
DATA  570,563,555,545,528,511
DATA  486,464,424,391,356,308
DATA  262,218,164,116,56,−10
DATA −71,−135,−210,−279,−345,−407
DATA −482,−541,−607,−661,−719,−773
DATA −825,−867,−911,−940,−965,−979
DATA −996,−1000,−994,−983,−973,−950
DATA −925,−892,−857,−811,−767,−717
DATA −659,−603,−536,−468,−403,−343
DATA −285,−233,−175,−127,−71,−25
DATA  4
REM Soft Fr. Horn Frequency in Hz DATA  223.294
```

Ophicleide

```
DATA  196
```

```
DATA  −4,−117,−186,−235,−283,−324
DATA  −348,−393,−421,−421,−377,−324
DATA  −247,−170,−73,40,126,170
DATA   158,142,113,45,−32,−81
DATA  −138,−202,−259,−287,−312,−340
DATA  −360,−364,−364,−377,−364,−348
DATA  −316,−308,−287,−275,−291,−324
DATA  −348,−377,−393,−413,−405,−389
DATA  −364,−340,−328,−324,−324,−312
DATA  −291,−259,−259,−259,−267,−287
DATA  −291,−283,−279,−247,−170,−73
DATA   49,158,259,372,462,526
DATA   579,607,611,607,575,518
DATA   462,417,401,385,360,332
DATA   308,300,267,235,178,121
DATA   77,32,24,32,61,81
DATA   89,93,109,97,97,105
DATA   134,194,251,255,186,77
DATA  −24,−85,−101,−97,−85,−101
DATA  −101,−40,40,105,142,142
DATA   154,186,223,271,316,381
DATA   421,421,405,364,328,304
DATA   316,364,421,478,518,514
DATA   486,413,304,142,−89,−348
DATA  −632,−911,−1219,−1510,−1741
DATA  −1915,−1960,−1911,−1781,−
DATA   1603,−1381,−1154
DATA  −927,−700,−462,−219,28,235
DATA      429,595,749,879,955,996
DATA      1000,1000,972,964,935,866
DATA      777,688,599,514,437,364
DATA      304,255,211,170,158,142
DATA      126,121,130,126,130,142
DATA      142,126,89,−4
REM Ophicleide Frequency in Hz
DATA      85.103
```

Serpent

```
DATA 203
DATA −5,53,113,167,207,237
DATA 233,223,207,170,140,90
DATA 47,−7,−47,−87,−107,−113
DATA −107,−80,−43,10,73,133
DATA 187,223,250,263,263,250
DATA 223,200,157,130,73,20
```

```
DATA −40,−97,−147,−200,−240,−267
DATA −287,−280,−267,−240,−203,−180
DATA −163,−133,−123,−127,−120,−123
DATA −127,−123,−130,−133,−127,−133
DATA −133,−113,−107,−73,−30,37
DATA 103,160,210,237,240,250
DATA 237,207,170,127,90,73
DATA 60,50,40,23,20,−13
DATA −47,−80,−120,−150,−187,−193
DATA −193,−173,−150,−133,−107,−80
DATA −57,−50,−43,0,60,143
DATA 237,323,440,533,620,687
DATA 740,747,640,460,253,20
DATA −353,−737,−1053,−1333,−1497
DATA −1527,−1440,−1273,−993,−667
DATA −327,−20,210,340,340,260
DATA 160,80,−7,−20,50,147,277
DATA 420,553,667,773,853,943
DATA 997, 1000,970,927,810
DATA 673,500,273,40,−193
DATA −387,−507,−560
DATA −540,−447,−337,−217,−93,23
DATA 83,130,147,143,140,140
DATA 147,153,167,173,153,117
DATA 77,23,−40,−60,−100,−133
DATA −173,−203,−240,−267,−280,−280
DATA −300,−287,−273,−257,−257,−230
DATA −227,−213,−207,−213,−200,−193
DATA −163,−150,−110,−70,−5
REM Serpent Frequency in Hz
DATA 61.702
```

Andreas Amati Violin (G String)

```
DATA 171
DATA 14,−153,−330,−507,−641,−732,−
DATA 813,−900,−967,−1000
DATA −967,−880,−737,−603,−498,−450,−
DATA 426,−431,−440,−426
DATA −402,−354,−306,−330,−335,−306,−
DATA 273,−177,53,211,364
DATA 474,545,593,608,641,641,603
DATA 574,493,431,416,431
DATA 512,603,651,651,584,459,316,
DATA 187,86,0,−100,−177
DATA −234,−273,−239,−177,−100
```

```
DATA 33,134,201,220,249,278
DATA 335,392,469,507,469,383,297
DATA 191,124,72,91,124
DATA 148,225,354,550,775,895
DATA 880,689,397,144,−10,29
DATA 144,239,311,278,206,163
DATA 234,335,383,440,392
DATA 258,33,−62,−24,57,115
DATA 96,29,−124,−234,−249
DATA −182,−38,57,110,115,124
DATA 144,230,340,440,474
DATA 402,301,196,67,−62,−201
DATA −344,−445,−464,−388
DATA −273,−144,−38,129,244,392
DATA 507,531,512,435
DATA 378,354,344,378,435,536
DATA 646,737,766,699,627
DATA 545,512,478,474,459,402
DATA 378,354,335,340,344
DATA 340,301,249,167,77,14
REM Amati Violin Frequency in Hz
DATA 196.71
```

Ordinary Violin (G String)

```
DATA 130
DATA 76,389,686,854,945,980
DATA 872,600,290,27
DATA −75,7,168,325,456,566
DATA 662,748,796,761
DATA 644,491,336,226,137,111
DATA  157,254,332,403
DATA  496,606,690,690,597,440
DATA  254,77,−102,−215
DATA −296,−354,−407,−460,−513,−566
DATA −637,−746,−878,−976
DATA −1000,−912,−743,−584,−454
DATA −341,−186,49,270,440
DATA  531,518,458,389,350,305
DATA  237,166,115,53
DATA −18,−62,−82,−111,−146,−146
DATA −122,−58,−2,31
DATA  53,53,27,0,7,49
DATA  124,212,281,369
DATA 467,549,566,451,283,53
DATA −104,−170,−146,−86
```

```
DATA −53,−33,31,119,181,243
DATA 310,296,184,−31
DATA −283,−442,−515,−546,−540
DATA −558,−580,−617,−642,−666
DATA −639,−577,−584,−692,−808,−878
DATA −816,−569,−199,76
REM Violin Frequency in Hz
DATA 194.41
```

Oboe (Lauré)

```
DATA 194
DATA 2,−181,−397,−581,−717,−809
DATA −839,−829,−777,−697,−596,−486
DATA −370,−261,−159,−79,−10,45
DATA 82,107,127,149,161,174
DATA 179,179,174,169,156,149
DATA 134,124,104,84,55,15
DATA −35,−79,−112,−144,−159,−164
DATA −161,−159,−154,−151,−159,−161
DATA −164,−169,−159,−144,−114,−84
DATA −50,−10,37,84,127,179
DATA 218,246,261,253,223,176
DATA 127,69,10,−40,−77,−122
DATA −159,−189,−223,−251,−270,−283
DATA −288,−280,−273,−263,−258,−258
DATA −258,−258,−258,−258,−251,−243
DATA −241,−231,−218,−208,−191,−169
DATA −154,−139,−124,−122,−122,−129
DATA −141,−154,−159,−159,−156,−151
DATA −139,−129,−122,−124,−129,−134
DATA −151,−169,−179,−199,−208,−231
DATA −243,−253,−258,−258,−251,−238
DATA −213,−191,−161,−139,−104,−74
DATA −40,−5,27,55,77,89
DATA 97,97,94,87,74,60
DATA 37,15,−20,−60,−104,−156
DATA −213,−280,−347,−409,−474,−526
DATA −566,−588,−586,−558,−499,−422
DATA −330,−221,−109,15,136,256
DATA 377,501,620,739,831,913
DATA 960,993,1000,995,983,963
DATA 938,913,883,856,821,789
DATA 752,715,663,600,496,355
DATA 176,2
REM Oboe Frequency in Hz
```

```
DATA 259.581
```

Heckelphone

```
DATA 130
DATA −8,142,250,308,300,283
DATA 262,196,58,33,42,42
DATA 29,−8,−54,−104
DATA −225,−321,−417,−475,−488
DATA −417,−242,0
DATA 217,225,346,608,867,1000
DATA 942,642,25,−50,−108,−267
DATA −475,−650,−667,−471,−217,−204
DATA −167,−25,171,317,417,425
DATA 329,308,229,92,−50,−142
DATA −208,−267, −358,−425,−458,−454
DATA −425,−388,−304,−221,13,142
DATA 262,346,392,425,442,425
DATA 238,158,75,−33,−125,−242
DATA −367,−450, −388,−317,−233
DATA −142,−75,13,112,192,225
DATA 258,292,292,250,175,46,−104
DATA −254,−292,−321,−317,−292,−25
DATA −188,−121,50,196,396,612
DATA 746,725,608,479, 262,167
DATA 50,−117,−283,−400,−417,−350
DATA −67,108,258,367,442,475
DATA 500,458,−17,−321,−600,−817
DATA −892,−808,−671,−538,−192,−8
REM Heckelphone Frequency in Hz
DATA 129.777
```

Krummhorn

```
DATA 174
DATA −59,−91,−157,−216,−100,−78
DATA −162,−176,333,1000,623,−130
DATA −412,−355,−100,422,853,850
DATA 490,−100,−623,−760,−760,−603
DATA −150,255,157,−169,−277,−196
DATA −250,−309,−150,113,206,279
DATA 377,331,108,−74,−51,15
DATA 145,353,510,507,333,164
DATA 93,152,243,341,431,439
DATA 419,373,257,230,186,59
DATA 64,135,201,206,86,−78
DATA −194,−196,−142,−83,47,103
```

```
DATA 39,-32,-91,-167,-199,-120
DATA 0,34,27,54,83,118
DATA 125,137,196,230,174,115
DATA 83,20,-120,-316,-471,-412
DATA -277,-81,152,211,47,-137
DATA -267,-353,-319,-176,-69,-25
DATA 10,47,93,100,132,142
DATA 142,162,157,105,27,-44
DATA -78,-110,-118,-110,-78,-44
DATA -32,-51,-74,-98,-103,-137
DATA -137,-110,-78,-88,-113,-123
DATA -78,-34,-5,-20,-88,-196
DATA -353,-451,-453,-512,-534,-578
DATA -534,-446,-397,-324,-306,-358
DATA -306,-245,-140,-61,69,96
DATA 162,152,142,172,213,289
DATA 294,294,309,225,145,-59
REM Krummhorn Frequency in Hz DATA 192.52
```

Rohrschalmei (Laukuft)

```
DATA 129
DATA 4,-94,-132,-186,-172,-224
DATA -256,-202,-146,-116,-68,-20
DATA -36,-64,-64,-104,-168,-136
DATA -98,-16,82,126,212,158
DATA 158,152,20,-80,-188,-282
DATA -206,720,692,444,1000,648
DATA 694,230,68,-228,-938,-826
DATA -726,-830,-474,-168,126,322
DATA 376,562,408,280,316,206
DATA 40,16,-44,-96,-178,-168
DATA -170,-194,-242,-402,-568,-488
DATA -584,-754,-604,-410,-370,-32
DATA 144,476,542,678,848,816
DATA 638,272,146,-176,-320,-420
DATA -482,-450,-400,-202,-43,-132
DATA -40,56,-16,0,-36,88
DATA 172,246,414,404,366,430
DATA 364,276,88,-48,-124,-282
DATA -272, -238,-314,-306,-282,-306
DATA -266,-136,-124,12,52,128
DATA 212,166,262,220,192,164
DATA 152,78,4
REM Rohrschalmei Frequency in Hz
DATA 259.674
```

Flute

```
DATA 192
DATA 18,−54,−75,−101,−134,−165
DATA −178,−247,−281,−291,−335,−376
DATA −428,−425,−464,−438,−446,−425
DATA −402,−412,−330,−299,−250,−160
DATA −82,21,93,180,216,317
DATA 325,358,320,289,255,222
DATA 144,119,111,85,5,26
DATA 5,−34,−52,−57,−106,−67
DATA −64,−75,−34,−34,8,−5
DATA 36,59,101,111,90,119
DATA 119,98,39,57,15,−26
DATA 3,15,0,8,8,−41
DATA −62,−77,−106,−126,−183,−232
DATA −260,−240,−253,−247,−191,−157
DATA −103,−67,−26,28,108,131
DATA 250,340,430,503,595,634
DATA 660,698,675,619,526,448
DATA 369,340,206,124,88,−26
DATA −82,−178,−250,−291,−302,−371
DATA −407,−410,−436,−464,−521,−559
DATA −582,−652,−765,−881,−920,−972
DATA −912,−910,−838,−678,−577,−479
DATA −353,−247,−134,−21,62,121
DATA 155,216,204,193,222,201
DATA 204,216,237,291,376,428
DATA 585,799,840,892,959,1000
DATA 907,747,588,430,222,−46
DATA −289,−376,−518,−598,−655,−655
DATA −621,−526,−459,−327,−188,−26
DATA 90,170,268,361,454,454
DATA 443,485,495,423,407,348
DATA 291,227,144,77,62,18
REM Flute Frequency in Hz
DATA 262.05
```

Piccolo

```
DATA 170
DATA −11,34,101,100,218,276
DATA 333,391,451,508,556,590
DATA 631,643,679,695,706,707
DATA 706,695,667,652,631,604
DATA 590,542,525,487,460,422
```

```
DATA   388,362,341,326,307,295
DATA   276,269,247,240,247,237
DATA   225,218,192,189,168,151
DATA   134,106,91,74,53,36
DATA   36,14,−10,−29,−34,−62
DATA  −77,−86.−115,−115,−125,−129
DATA  −139,−146,−149,−146,−153,−146
DATA  −146,−137,−137,−127,−127,−118
DATA  −108,−89,−72,−55,−38,−10
DATA   24,48,94,125,170,206
DATA   247,285,317,353,388,408
DATA   436,458,460,484,494,477
DATA  482,468,458,451,429,412
DATA  388,369,345,331,321,293
DATA  266,249,216,199,173,161
DATA  115,86,46,22,−14,−70
DATA  −120,−182,−245,−317,−386,−480
DATA  −556,−616,−686,−751,−815,−859
DATA  −897,−935,−959,−981,−993,−990
DATA  −990,−1000,−993,−993,−964,−954
DATA  −959,−930,−914,−887,−887,−856
DATA  −811,−763,−731,−671,−631,−568
DATA  −499,−444,−367,−317,−261,−175
DATA  −118,  −62,−11
REM Piccolo Frequency in Hz
DATA  593.877
```

C.4 Program for Discrete Fourier Analysis

The following program is written in MATLAB using much of the same code from the original BASIC program by Bennett.

C.4.1 Contents

- Load waveform data for one period
- Variables
- Compute the Fourier Coefficients
- Plot the Waveform
- Plot Histogram of the Coefficients
- Reconstruct the Waveform from the Fourier Coefficients

- Plot the Waveform

```
clear all;
```

C.4.2 Load waveform data for one period

Call load_waveforms.m

```
load_waveforms;
```

C.4.3 Variables

```
% Choose the maximum number of harmonics
Nmax=20;

% Select which waveform to analyze
waveform = 'gardenhose';

switch waveform
    case 'gardenhose'
        V=gardenhose;
        strLegend=sprintf('Garden Hose\nf_{n=1}
         =307.692 Hz');
    case 'fcoronet'
        V=fcoronet;
        strLegend=sprintf('F-Cornet\nf_{n=1}
         =316.075 Hz');
    case 'piccolotrumpet'
        V=piccolotrumpet;
        strLegend=sprintf('Piccolo Trumpet\nf_{n=1}
         =597.672 Hz');
    case 'frenchhornloud'
        V=frenchhornloud;
        strLegend=sprintf('French Horn (Loud)\nf_{n=1}
         =222.488 Hz');
    case 'frenchhornsoft'
        V=frenchhornsoft;
        strLegend=sprintf('French Horn (Soft)\nf_{n=1}
         =223.294 Hz');
    case 'ophicleide'
        V=ophicleide;
```

```
        strLegend=sprintf('Ophicleide\nf_{n=1}
         =85.103 Hz');
    case 'serpent'
        V=serpent;
        strLegend=sprintf('Serpent\nf_{n=1}
         =61.702 Hz');
    case 'amativiolin'
        V=amativiolin;
        strLegend=sprintf('A.Amati Violin (G)\nf_{n=1}
         =196.71 Hz');
    case 'violin'
        V=violin;
        strLegend=sprintf('Ordinary Violin
        (G)\nf_{n=1}=194.41 Hz');
    case 'oboelaure'
        V=oboelaure;
        strLegend=sprintf('Oboe (Laure)\nf_{n=1}
         =259.581 Hz');
    case 'heckelphone'
        V=heckelphone;
        strLegend=sprintf('Heckelphone\nf_{n=1}
         =129.777 Hz');
    case 'kurmhorn'
        V=krummhorn;
        strLegend=sprintf('Krummhorn\nf_{n=1}
         =192.52 Hz');
    case 'rohrschalmei'
        V=rohrschalmei;
        strLegend=sprintf('Rohrschalmei (Laukuft)\
         nf_{n=1}
         =259.674 Hz');
    case 'flute'
        V=flute;
        strLegend=sprintf('Flute\nf_{n=1}=262.05 Hz');
    case 'piccolo'
        V=piccolo;
        strLegend=sprintf('Piccolo\nf_{n=1}
         =593.877 Hz');
end
```

C.4.4 Compute the Fourier Coefficients

Call fouriercoef_trapezoid.m

```
[A0 A B0 B C0 C PHI]=fouriercoef_trapezoid(V,Nmax);
```

C.4.5 Plot the Waveform

```
figure;
plot(V./max(abs(V)),'Color','k','LineWidth',3)
line([0 length(V)],[0 0],'Color','k','LineWidth',1)
set(gca,'LineWidth',2,'FontSize',14)
set(gca,'YLim',[-1.1 1.1],'YTick',[0]);
set(gca,'XLim',[0 length(V)],'XTick',[]);
xlabel('Time','FontSize',14);
ylabel('Microphone Signal','FontSize',14);
pbaspect([2 1 1])
```

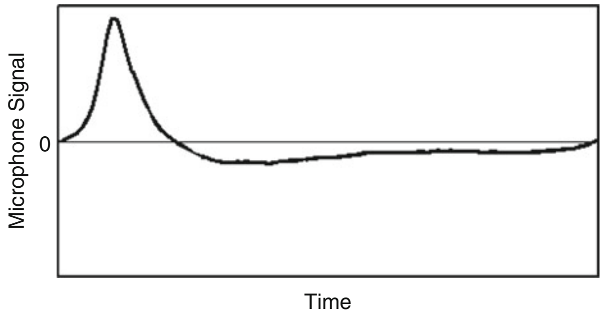

C.4.6 Plot Histogram of the Coefficients

```
figure;
stem([1:Nmax],C./max(C),'Color','k','LineWidth',3,
 'Marker','none')
set(gca,'YLim',[0 1],'YTickLabel',[]);
set(gca,'XLim',[0 Nmax],'XTick',[0:2:Nmax]);
set(gca,'LineWidth',2,'FontSize',14)
xlabel('Harmonic Number, (n)','FontSize',14);
```

```
ylabel('Fourier Coefficients, C(n)','FontSize',14);
pbaspect([2 1 1])
text(12,.8,strLegend,'FontSize',14,
 'HorizontalAlignment','left');
```

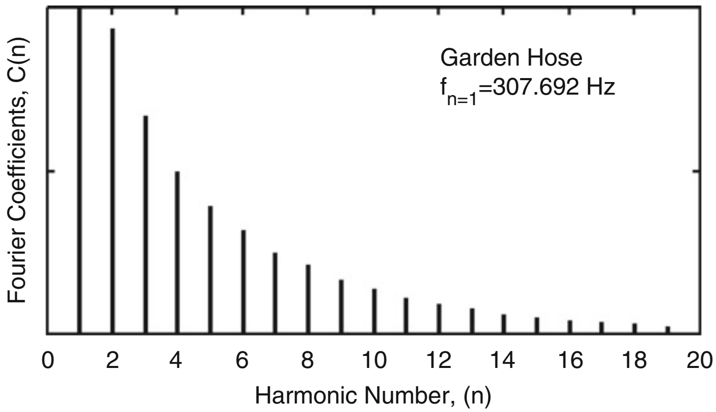

C.4.7 Reconstruct the Waveform from the Fourier Coefficients

```
P=length(V);
for I=1:P
    V2(I)=C0;
    for N=1:Nmax
        V2(I)=V2(I)+C(N)*sin(N*A0*(I-1)+PHI(N));
    end
end
```

C.4.8 Plot the Waveform

```
figure; hold on;
plot(V./max(abs(V)),'Color','k','LineWidth',3)
plot(V2./max(abs(V2)),'--','Color','b','LineWidth',3)
line([0 length(V)],[0 0],'Color','k','LineWidth',1)
set(gca,'LineWidth',2,'FontSize',14)
set(gca,'YLim',[-1.1 1.1],'YTick',[0]);
set(gca,'XLim',[0 length(V)],'XTick',[]);
```

```
xlabel('Time','FontSize',14);
ylabel('Microphone Signal','FontSize',14);
clear strLegend;
strLegend{1}='Recorded Waveform';
strLegend{2}=sprintf('Reconstructed Waveform,
 Nmax = %u', Nmax);
legend(strLegend);
pbaspect([2 1 1])
```

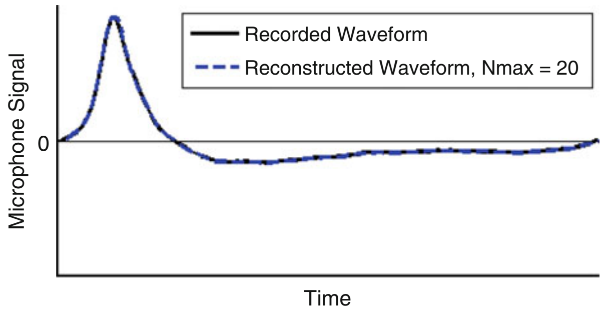

C.5 Additional Waveforms

Additional musical instrument waveforms are presented below in the same format as that given above for the garden hose for those who might like to study them and for use elsewhere in this book. These data were taken in Davies Auditorium at Yale, using a high-quality Sennheiser MKH104 omnidirectional microphone with uniform response (± 1 dB) over the range from 50 Hz to 20 kHz and the Hewlett-Packard equipment shown in Fig. 2.9. The 10-bit A-to-D converter used had a dynamic range of about 60 dB. The instruments were played without vibrato by professional musicians to whom the author is greatly indebted. The brass instruments were played by James Undercoffler; the violins, by Syoko Aki; the oboe, heckelphone, krummhorn and rohr schalmei by James Ryan; and flute and piccolo by Leone Buyse. I am indebted to the late William Liddell for the use of his krummhorns, to Richard Rephann for the loan of the historic brass instruments from the Yale Instrument Collection, and to Robert Sheldon of the Smithsonian Collection in Washington, DC for playing the serpent. The heckelphone was loaned by the Yale Concert Band and the rohr schalmei was borrowed from the author's personal pipe organ.

C.5.1 Contents

- Mode-Locked Garden Hose (normalized to +/- 1000)
- F-Cornet
- Piccolo Trumpet
- French Horn (Loud)
- French Horn (Soft)
- Ophicleide
- Serpent
- Andreas Amati Violin (G String)
- Ordinary Violin (G String)
- Oboe (Laure)
- Heckelphone
- Krummhorn
- Rohrschalmei (Laukuft)
- Flute
- Piccolo

C.5.2 Mode-Locked Garden Hose (normalized to +/- 1000)

```
%DATA 109 % P = Number of points in Period = the first
datum gardenhose=[...
3,20,43,68,111,176,...
273,426,634,861,1000,989,...
864,705,563,452,358,273,...
199,136,85,45,17,-14,...
-40,-63,-85,-105,-125,-129,...
-151,-162,-165,-165,-165,-165,...
-170,-165,-170,-170,-170,-173,...
-173,-170,-162,-159,-156,-153,...
-151,-142,-139,-136,-131,-128,...
-128,-128,-125,-119,-114,-108,...
-102,-94,-91,-91,-91,-91,...
-91,-91,-91,-91,-91,-91,...
-85,-82,-82,-80,-74,-74,...
-74,-80,-80,-80,-80,-80,...
-82,-82,-82,-85,-88,-91,...
-91,-91,-91,-91,-91,-85,...
-82,-80,-74,-71,-68,-65,...
-60,-57,-45,-37,-28,-14,...
3];
% Fundamental frequency in Hz
%DATA  307.692
```

C.5.3 F-Cornet

```
%DATA  107
fcoronet=[...
-4,44,114,163,212,249,...
280,301,311,319,321,321,...
311,290,259,223,166,111,...
57,5,-47,-83,-106,-122,...
-124,-119,-98,-83,-67,-52,...
-41,-47,-62,-83,-109,-150,...
-192,-231,-259,-285,-301,-303,...
-293,-269,-228,-166,-96,-13,...
78,174,275,370,477,578,...
681,777,870,948,995,1000,...
974,886,764,617,433,244,...
67,-101,-238,-345,-412,-448,...
-461,-448,-415,-383,-337,-301,...
-272,-259,-251,-269,-301,-332,...
-365,-399,-425,-446,-453,-456,...
-446,-425,-399,-383,-368,-355,...
-347,-337,-329,-301,-262,-241,...
-210,-166,-117,-65,-4];
% Cornet Frequency in Hz
%DATA  316.075
```

C.5.4 Piccolo Trumpet

```
%DATA  168
piccolotrumpet=[...
-5,97,195,280,367,450,...
530,610,680,755,807,857,...
898,935,967,982,997,1000,...
995,987,965,940,910,875,...
835,797,742,695,637,585,...
527,475,417,357,302,247,...
187,130,85,37,-10,-50,...
-80,-110,-140,-160,-180,-193,...
-203,-200,-200,-193,-170,-155,...
-130,-93,-55,-12,35,77,...
125,177,227,277,325,367,...
408,450,490,517,545,567,...
580,587,590,590,580,560,...
```

```
540,515,485,450,408,367,...
327,285,240,190,147,97,...
55,15,-35,-65,-100,-133,...
-155,-180,-200,-215,-230,-233,...
-245,-245,-242,-245,-242,-240,...
-238,-235,-238,-235,-235,-242,...
-253,-260,-265,-282,-300,-320,...
-343,-363,-390,-413,-440,-463,...
-490,-513,-535,-557,-583,-603,...
-623,-643,-660,-680,-690,-715,...
-733,-753,-773,-793,-810,-830,...
-845,-857,-873,-875,-875,-882,...
-873,-870,-857,-835,-810,-785,...
-755,-720,-673,-623,-563,-500,...
-433,-355,-272,-193,-110,-5];
% Piccolo Trumpet Frequency in Hz
%DATA   597.672
```

C.5.5 French Horn (Loud)

```
%DATA  151
frenchhornloud=[...
21,112,188,242,273,318,...
356,387,399,394,385,371,...
349,309,264,200,133,76,...
38,21,17,17,26,52,...
67,95,121,147,159,171,...
176,166,157,143,140,138,...
128,124,124,124,133,143,...
147,147,143,140,135,133,...
119,105,93,76,62,26,...
-12,-52,-95,-138,-181,-214,...
-252,-283,-299,-314,-309,-295,...
-268,-249,-240,-233,-214,-195,...
-166,-128,-76,-10,64,121,...
176,216,245,273,285,295,...
292,292,302,314,333,340,...
349,347,347,349,375,428,...
508,575,627,656,672,679,...
684,684,689,684,670,641,...
596,551,508,451,380,304,...
214,128,45,-43,-164,-314,...
-461,-589,-670,-703,-717,-743,...
```

```
-791,-846,-895,-931,-960,-988,...
-1000,-971,-924,-886,-855,-838,...
-836,-841,-838,-829,-774,-698,...
-613,-527,-437,-335,-219,-95,...
21];
% French Horn Frequency in Hz
%DATA  222.488
```

C.5.6 French Horn (Soft)

```
%DATA  151
frenchhornsoft=[...
4,46,87,121,154,183,...
212,231,262,272,291,297,...
306,297,297,291,283,268,...
264,247,237,229,216,206,...
200,191,179,166,158,141,...
131,116,121,112,106,104,...
100,98,96,83,87,79,...
73,71,62,56,48,40,...
40,42,46,54,58,62,...
64,71,67,73,71,71,...
75,81,96,104,114,133,...
156,166,183,212,225,247,...
272,297,322,349,372,399,...
422,441,462,484,499,516,...
528,541,555,563,563,572,...
570,563,555,545,528,511,...
486,464,424,391,356,308,...
262,218,164,116,56,-10,...
-71,-135,-210,-279,-345,-407,...
-482,-541,-607,-661,-719,-773,...
-825,-867,-911,-940,-965,-979,...
-996,-1000,-994,-983,-973,-950,...
-925,-892,-857,-811,-767,-717,...
-659,-603,-536,-468,-403,-343,...
-285,-233,-175,-127,-71,-25,...
4];
% Soft Fr. Horn Frequency in Hz
%DATA  223.294
```

C.5.7 Ophicleide

```
%DATA  196
ophicleide=[...
-4,-117,-186,-235,-283,-324,...
-348,-393,-421,-421,-377,-324,...
-247,-170,-73,40,126,170,...
158,142,113,45,-32,-81,...
-138,-202,-259,-287,-312,-340,...
-360,-364,-364,-377,-364,-348,...
-316,-308,-287,-275,-291,-324,...
-348,-377,-393,-413,-405,-389,...
-364,-340,-328,-324,-324,-312,...
-291,-259,-259,-259,-267,-287,...
-291,-283,-279,-247,-170,-73,...
49,158,259,372,462,526,...
579,607,611,607,575,518,...
462,417,401,385,360,332,...
308,300,267,235,178,121,...
77,32,24,32,61,81,...
89,93,109,97,97,105,...
134,194,251,255,186,77,...
-24,-85,-101,-97,-85,-101,...
-101,-40,40,105,142,142,...
154,186,223,271,316,381,...
421,421,405,364,328,304,...
316,364,421,478,518,514,...
486,413,304,142,-89,-348,...
-632,-911,-1219,-1510,-1741,...
-1915,-1960,-1911,-1781,-1603,-1381,-1154,...
-927,-700,-462,-219,28,235,...
429,595,749,879,955,996,...
1000,1000,972,964,935,866,...
777,688,599,514,437,364,...
304,255,211,170,158,142,...
126,121,130,126,130,142,...
142,126,89,-4];
% Ophicleide Frequency in Hz
%DATA  85.103
```

C.5.8 Serpent

```
%DATA  203
serpent=[...
-5,53,113,167,207,237,...
233,223,207,170,140,90,...
47,-7,-47,-87,-107,-113,...
-107,-80,-43,10,73,133,...
187,223,250,263,263,250,...
223,200,157,130,73,20,...
-40,-97,-147,-200,-240,-267,...
-287,-280,-267,-240,-203,-180,...
-163,-133,-123,-127,-120,-123,...
-127,-123,-130,-133,-127,-133,...
-133,-113,-107,-73,-30,37,...
103,160,210,237,240,250,...
237,207,170,127,90,73,...
60,50,40,23,20,-13,...
-47,-80,-120,-150,-187,-193,...
-193,-173,-150,-133,-107,-80,...
-57,-50,-43,0,60,143,...
237,323,440,533,620,687,...
740,747,640,460,253,20,...
-353,-737,-1053,-1333,-1497,...
-1527,-1440,-1273,-993,-667,...
-327,-20,210,340,340,260,...
160,80,-7,-20,50,147,277,...
420,553,667,773,853,943,...
997, 1000,970,927,810,...
673,500,273,40,-193,...
-387,-507,-560,...
-540,-447,-337,-217,-93,23,...
83,130,147,143,140,140,...
147,153,167,173,153,117,...
77,23,-40,-60,-100,-133,...
-173,-203,-240,-267,-280,-280,...
-300,-287,-273,-257,-257,-230,...
-227,-213,-207,-213,-200,-193,...
-163,-150,-110,-70,-5];
% Serpent Frequency in Hz
%DATA  61.702
```

C.5.9 Andreas Amati Violin (G String)

```
%DATA  171
amativioling=[...
14,-153,-330,-507,-641,-732,-813,-900,-967,-1000,...
-967,-880,-737,-603,-498,-450,-426,-431,-440,-426,...
-402,-354,-306,-330,-335,-306,-273,-177,53,211,364,...
474,545,593,608,641,641,603,...
574,493,431,416,431,...
512,603,651,651,584,459,316,...
187,86,0,-100,-177,...
-234,-273,-239,-177,-100,...
33,134,201,220,249,278,...
335,392,469,507,469,383,297,...
191,124,72,91,124,...
148,225,354,550,775,895,...
880,689,397,144,-10,29,...
144,239,311,278,206,163,...
234,335,383,440,392,...
258,33,-62,-24,57,115,...
96,29,-124,-234,-249,...
-182,-38,57,110,115,124,...
144,230,340,440,474,...
402,301,196,67,-62,-201,...
-344,-445,-464,-388,...
-273,-144,-38,129,244,392,...
507,531,512,435,...
378,354,344,378,435,536,...
646,737,766,699,627,...
545,512,478,474,459,402,...
378,354,335,340,344,...
340,301,249,167,77,14];
% Amati Violin Frequency in Hz
%DATA  196.71
```

C.5.10 Ordinary Violin (G String)

```
%DATA  130
violin=[...
76,389,686,854,945,980,...
872,600,290,27,...
-75,7,168,325,456,566,...
```

```
662,748,796,761,...
644,491,336,226,137,111,...
157,254,332,403,...
496,606,690,690,597,440,...
254,77,-102,-215,...
-296,-354,-407,-460,-513,-566,...
-637,-746,-878,-976,...
-1000,-912,-743,-584,-454,...
-341,-186,49,270,440,...
531,518,458,389,350,305,...
237,166,115,53,...
-18,-62,-82,-111,-146,-146,...
-122,-58,-2,31,...
53,53,27,0,7,49,...
124,212,281,369,...
467,549,566,451,283,53,...
-104,-170,-146,-86,...
-53,-33,31,119,181,243,...
310,296,184,-31,...
-283,-442,-515,-546,-540,...
-558,-580,-617,-642,-666,...
-639,-577,-584,-692,-808,-878,...
-816,-569,-199,76];
% Violin Frequency in Hz
%DATA 194.41
```

C.5.11 Oboe (Laure)

```
%DATA  194
oboelaure=[...
2,-181,-397,-581,-717,-809,...
-839,-829,-777,-697,-596,-486,...
-370,-261,-159,-79,-10,45,...
82,107,127,149,161,174,...
179,179,174,169,156,149,...
134,124,104,84,55,15,...
-35,-79,-112,-144,-159,-164,...
-161,-159,-154,-151,-159,-161,...
-164,-169,-159,-144,-114,-84,...
 -50,-10,37,84,127,179,...
 218,246,261,253,223,176,...
 127,69,10,-40,-77,-122,...
-159,-189,-223,-251,-270,-283,...
```

```
-288,-280,-273,-263,-258,-258,...
-258,-258,-258,-258,-251,-243,...
-241,-231,-218,-208,-191,-169,...
-154,-139,-124,-122,-122,-129,...
-141,-154,-159,-159,-156,-151,...
-139,-129,-122,-124,-129,-134,...
-151,-169,-179,-199,-208,-231,...
-243,-253,-258,-258,-251,-238,...
-213,-191,-161,-139,-104,-74,...
-40,-5,27,55,77,89,...
97,97,94,87,74,60,...
37,15,-20,-60,-104,-156,...
-213,-280,-347,-409,-474,-526,...
-566,-588,-586,-558,-499,-422,...
-330,-221,-109,15,136,256,...
377,501,620,739,831,913,...
960,993,1000,995,983,963,...
938,913,883,856,821,789,...
752,715,663,600,496,355,...
176,2];
% Oboe Frequency in Hz
%DATA 259.581
```

C.5.12 Heckelphone

```
%DATA  130 [JLR probably a typo, should be 138]
%[JLR] Note: There are two typos in the manuscript
which are fixed here heckelphone=[...
-8,142,250,308,300,283,...
262,196,58,33,42,42,...
29,-8,-54,-104,...
-225,-321,-417,-475,-488,...
-417,-242,0,...
217,225,346,608,867,1000,...
942,642,25,-50,-108,-267,...
-475,-650,-667,-471,-217,-204,...
-167,-25,171,317,417,425,...
329,308,229,92,-50,-142,...
-208,-267, -358,-425,-458,-454,...
-425,-388,-304,-221,13,142,...
262,346,392,425,442,425,...
238,158,75,-33,-125,-242,...
-367,-450,-388,-317,-233,...
```

```
-142,-75,13,112,192,225,...
258,292,292,250,175,46,-104,...
-254,-292,-321,-317,-292,-250,... %[JLR] last point
 changed to -250
-188,-121,50,196,396,612,...
746,725,608,479,262,167,...
50,-117,-283,-400,-417,-350,...
-67,108,258,367,442,475,...
500,458,-17,-321,-600,-817,...
-892,-808,-671,-538,-192,-8];
% Heckelphone Frequency in Hz
%DATA 129.777
```

C.5.13 Krummhorn

```
%DATA 174
krummhorn=[...
-59,-91,-157,-216,-100,-78,...
-162,-176,333,1000,623,-130,...
-412,-355,-100,422,853,850,...
490,-100,-623,-760,-760,-603,...
-150,255,157,-169,-277,-196,...
-250,-309,-150,113,206,279,...
377,331,108,-74,-51,15,...
145,353,510,507,333,164,...
93,152,243,341,431,439,...
419,373,257,230,186,59,...
64,135,201,206,86,-78,...
-194,-196,-142,-83,47,103,...
39,-32,-91,-167,-199,-120,...
0,34,27,54,83,118,...
125,137,196,230,174,115,...
83,20,-120,-316,-471,-412,...
-277,-81,152,211,47,-137,...
-267,-353,-319,-176,-69,-25,...
10,47,93,100,132,142,...
142,162,157,105,27,-44,...
-78,-110,-118,-110,-78,-44,...
-32,-51,-74,-98,-103,-137,...
-137,-110,-78,-88,-113,-123,...
-78,-34,-5,-20,-88,-196,...
-353,-451,-453,-512,-534,-578,...
-534,-446,-397,-324,-306,-358,...
```

```
-306,-245,-140,-61,69,96,...
162,152,142,172,213,289,...
294,294,309,225,145,-59];
% Krummhorn Frequency in Hz
%DATA 192.52
```

C.5.14 Rohrschalmei (Laukuft)

```
%DATA  129
rohrschalmei=[...
4,-94,-132,-186,-172,-224,...
-256,-202,-146,-116,-68,-20,...
-36,-64,-64,-104,-168,-136,...
-98,-16,82,126,212,158,...
158,152,20,-80,-188,-282,...
-206,720,692,444,1000,648,...
694,230,68,-228,-938,-826,...
-726,-830,-474,-168,126,322,...
376,562,408,280,316,206,...
40,16,-44,-96,-178,-168,...
-170,-194,-242,-402,-568,-488,...
-584,-754,-604,-410,-370,-32,...
144,476,542,678,848,816,...
638,272,146,-176,-320,-420,...
-482,-450,-400,-202,-43,-132,...
-40,56,-16,0,-36,88,...
172,246,414,404,366,430,...
364,276,88,-48,-124,-282,...
-272, -238,-314,-306,-282,-306,...
-266,-136,-124,12,52,128,...
212,166,262,220,192,164,...
152,78,4];
% Rohrschalmei Frequency in Hz
%DATA 259.674
```

C.5.15 Flute

```
%DATA 192
flute=[...
18,-54,-75,-101,-134,-165,...
-178,-247,-281,-291,-335,-376,...
```

```
-428,-425,-464,-438,-446,-425,...
-402,-412,-330,-299,-250,-160,...
-82,21,93,180,216,317,...
325,358,320,289,255,222,...
144,119,111,85,5,26,...
5,-34,-52,-57,-106,-67,...
-64,-75,-34,-34,8,-5,...
36,59,101,111,90,119,...
119,98,39,57,15,-26,...
3,15,0,8,8,-41,...
-62,-77,-106,-126,-183,-232,...
-260,-240,-253,-247,-191,-157,...
-103,-67,-26,28,108,131,...
250,340,430,503,595,634,...
660,698,675,619,526,448,...
369,340,206,124,88,-26,...
-82,-178,-250,-291,-302,-371,...
-407,-410,-436,-464,-521,-559,...
-582,-652,-765,-881,-920,-972,...
-912,-910,-838,-678,-577,-479,...
-353,-247,-134,-21,62,121,...
155,216,204,193,222,201,...
204,216,237,291,376,428,...
585,799,840,892,959,1000,...
907,747,588,430,222,-46,...
-289,-376,-518,-598,-655,-655,...
-621,-526,-459,-327,-188,-26,...
90,170,268,361,454,454,...
443,485,495,423,407,348,...
291,227,144,77,62,18];
% Flute Frequency in Hz
%DATA 262.05
```

C.5.16 Piccolo

```
%DATA  170
piccolo=[...
-11,34,101,100,218,276,...
333,391,451,508,556,590,...
631,643,679,695,706,707,...
706,695,667,652,631,604,...
590,542,525,487,460,422,...
388,362,341,326,307,295,...
```

```
276,269,247,240,247,237,...
225,218,192,189,168,151,...
134,106,91,74,53,36,...
36,14,-10,-29,-34,-62,...
-77,-86.-115,-115,-125,-129,...
-139,-146,-149,-146,-153,-146,...
-146,-137,-137,-127,-127,-118,...
-108,-89,-72,-55,-38,-10,...
24,48,94,125,170,206,...
247,285,317,353,388,408,...
436,458,460,484,494,477,...
482,468,458,451,429,412,...
388,369,345,331,321,293,...
266,249,216,199,173,161,...
115,86,46,22,-14,-70,...
-120,-182,-245,-317,-386,-480,...
-556,-616,-686,-751,-815,-859,...
-897,-935,-959,-981,-993,-990,...
-990,-1000,-993,-993,-964,-954,...
-959,-930,-914,-887,-887,-856,...
-811,-763,-731,-671,-631,-568,...
-499,-444,-367,-317,-261,-175,...
-118, -62,-11];
% Piccolo Frequency in Hz
%DATA 593.877
```

C.6 Harmonic Analysis

This part of the program takes most of the running time. A(N) and B(N) correspond to the Fourier amplitudes given by the integrals in Eqs. (C.6) and (C.7). They are done here numerically by a method equivalent to drawing straight lines between the successive points and adding up the areas (the "trapezoidal Rule").

```
function [A0 A B0 B C0 C PHI]
 =fouriercoef_trapezoid(V,Nmax)

% The net Fourier amplitude C(N) and phase PHI(N)
 are computed using
% Eqs (C.6), (C.7), and (C.8).

% Check for input errors
error(nargchk(1, 2, nargin));
if (nargin < 2); Nmax = 20; end;
```

```
P=length(V);

A0=2*pi/(P-1); % A0 is a constant used in the loop on N.

for N=1:Nmax % FOR N=0 TO Nmax
% N=0 corresponds to the  constant or DC term,
 we will calculate it later

    A(N)=0;
    B(N)=0;

    for I=1:P % FOR I=1 TO P
        A(N)=A(N)+V(I)*sin(N*A0*(I-1));
        B(N)=B(N)+V(I)*cos(N*A0*(I-1));
    end; % NEXT I

    A(N)=A(N)*2/(P-1);
    B(N)=B(N)*2/(P-1);
    C(N)=sqrt(A(N)*A(N)+B(N)*B(N));

    %IF N>0 THEN P(N)=ATN(B(N)/A(N)) % avoid DC term
    PHI(N)=atan(B(N)/A(N));
    %IF A(N)<0 THEN P(N)=P(N)+Pi 'arctangent problem
    if (A(N) < 0); PHI(N)=PHI(N)+pi; end;

end; %NEXT N

% DC or constant term (A0 calculation above)
B0=sum(V)*2/(P-1);
C0=B0/2;
```

Published with MATLAB®7.12

Appendix D
The Well-Tempered Scale

The numbers here were computed to 0.06 ppm and rounded off to the nearest 0.01 Hz assuming the 1936 international convention that $A_4 = 440.0000$ Hz, using $2^{1/12} = 1.05946310$. Note as a check: $1.05946310^{12} = 2.00000012$

Frequency in Hz

A	27.50	55.00	110.00	220.00	440.00	880.00	1760.00	3520.00	7040.00	14080.00
A♯	29.14	58.27	116.54	233.08	466.16	932.33	1864.66	3729.31	7458.62	14917.25
B	30.87	61.74	123.47	246.94	493.88	987.77	1975.53	3951.07	7902.13	15804.27
C	32.70	65.41	130.81	261.63	523.25	1046.50	2093.00	4186.01	8372.02	16744.04
C♯	34.65	69.30	138.59	277.18	554.37	1108.73	2217.46	4434.92	8869.85	17739.69
D	36.71	73.42	146.83	293.66	587.33	1174.66	2349.32	4698.64	9397.28	18794.55
D♯	38.89	77.78	155.56	311.13	622.25	1244.51	2489.02	4978.03	9956.07	19912.13
E	41.20	82.41	164.81	329.63	659.26	1318.51	2637.02	5274.04	10548.08	21096.17
F	43.65	87.31	174.61	349.23	698.46	1396.91	2793.83	5587.65	11175.31	22350.61
F♯	46.25	92.50	185.00	369.99	739.99	1479.98	2959.96	5919.91	11839.83	23679.65
G	49.00	98.00	196.00	392.00	783.99	1567.98	3135.96	6271.93	12543.86	25087.72
G♯	51.91	103.83	207.65	415.30	830.61	1661.22	3322.44	6644.88	13289.75	26579.51

© Springer Nature Switzerland AG 2018

W. R. Bennett, Jr., *The Science of Musical Sound*,
https://doi.org/10.1007/978-3-319-92796-1

Solutions

Problems of Chap. 1

1.1 The oil would spread out very rapidly over the water, reducing its surface tension and thereby preventing wave motion at the short wavelengths characterized by the ripples.

1.2 (a) 3.11 m. (b) 615 THz.

1.3 Answers: The frequency is $233.08/(1.441 \times 10^{17}) = 1.62 \times 10^{-15}$ Hz. The period is 6.183×10^{14} s = 19.59 million years.

1.4 (a) 633 nm. (b) 43.6 ft.

1.5 (a) 3.8. (b) 2.7

1.6

From the original length of the string, one expects frequencies at $nc/2L$ where n = 1,2,3,.... But because of reflections from the kink you also get odd harmonics of $3c/8L$ and of $3c/4L$. Note that the string is free to move up and down at the kink, so that the frequencies on either side of the kink are determined by only one "hard" phase shift per round trip, and the resonances have the same form as those for a closed pipe.

1.7 (a) Multiples of 110 Hz. (Neglecting phase shift and time delays in the amplifier, the running wave phase shift would be $2\pi f_L/c$ per trip around the loop.) (b) It would oscillate at some other frequency if there were significant phase shift in the amplifier (e.g., from tone controls or a large gain variation with frequency.)

1.8 Answer: The pipe is closed at the top, initially by the flap valve, and then by the water flowing down the pipe. The fundamental frequency of the pipe starts out at $c/4L = 46$ Hz, with odd harmonics at 138, 230,... Hz. As the water goes down the pipe, the acoustic length shortens and the pitch for each harmonic goes up.

© Springer Nature Switzerland AG 2018

W. R. Bennett, Jr., *The Science of Musical Sound*,
https://doi.org/10.1007/978-3-319-92796-1

1.9 The main frequencies are 523 Hz, 622 Hz, 740 Hz, 932 Hz, 1570 Hz, 1865 Hz, 2217 Hz, and 2797 Hz. Starting at C above A=440 Hz, the notes are C, E♭, G♭, B♭, G, B♭, D♭, and F. (See figure for musical notation.) The first two intervals are minor thirds, giving the whistle its characteristic, mournful sound. The bottom half might be regarded as a half-diminished seventh. The second half is just the first chord raised by a twelfth. (The lower chord would resolve on a diminished seventh and then on a B♭ minor chord) (Fig. S.1).

1.10 Answers: Hard phase shifts occur at both the ceiling and the floor, hence one might expect the main resonances to be given approximately by $f_n = nc/2L$. Resonances do occur at those frequencies (multiples of 55 Hz.) But because the floor is in the focal plane of the concave ceiling, resonances also occur at $f_n = nc/8L$. (The running wave from a point source on the floor makes eight transits to the ceiling and back before it closes on itself.) Assuming the radius of curvature of the ceiling is 20 ft and twice the ceiling height, the main resonances would occur every 13.75 Hz throughout the audio band. (Speech is totally unintelligible, but the mumbling sound is impressive.)

1.11 One reason is that the open end of a closed pipe radiates as a monopole source (equally in all directions), whereas an open pipe acts like a dipole with the maximum radiated intensity going in the vertical direction (unless the pipe is turned 90°).

1.12 By listening to the full Doppler shift on the bells at grade crossings, he or she could determine the median pitch and the total fractional change in frequency on the Well Tempered Scale. From that, one could calculate the speed.

1.13 Answers: (a) 38.2 mph. (b) About one whole step.

1.14 The Doppler effect from sound reflected by the rotating blades creates a warbling effect.

1.15 (a) 676 Hz. (b) 786 Hz. (c) 738 Hz.

1.16 +715 Hz. (Note that the velocity of the image of the radar gun is twice the speed of the car.)

1.17 Answer: $c/4L = 1040/(4 \times 6.9) = 37.7$ Hz.

1.18 Answer: Since $f = 65.4$ Hz, $\lambda = c/f = 1087/65.4 = 16.6$ ft.

Fig. S.1 The steam engine whistle

Problems of Chap. 2

2.1 $\Delta F \approx 2\pi \Delta t \approx 0.032$ Hz.

2.2 (a) To go through 50 Hz would require at least
$\Delta t \approx \frac{1}{2\pi \Delta F} = \frac{1}{2\pi 50} = 318$ ms.
Therefore, to go through 10,000 Hz, it would take a minimum of about 64 s, or (b) a scanning rate of 156 Hz/s.

2.3 See Eqs. (2.7) and (2.8)

2.4 10 dB

2.5 $20Log_{10}(80 \times 5280/10) + 60 = 152$ dB

2.6 Serber was about 15.4 miles away. Los Alamos was about 250 miles from the test site. The blast would have been about 24 dB louder at Serber's position.

2.7 $20Log_{10}[3000/1] + 60 \approx 129$ dB (or about as loud as a rock band in a typical concert setting).

2.8 About 60 dB ($\approx 20Log_{10}1024$.)

2.9 About 96 dB ($\approx 20Log_{10}2^{16} = 320Log102$). But as shown by Bennett (1948), one gets an extra 3 dB by averaging the quantization errors in most systems.

2.10 Answer: The sound intensity per unit area would be attenuated by a factor of 36, which corresponds to a decrease of 16 dB. Hence, the sound level at the neighbor's house should be about 64 dB (something between normal conversation and shouting at 4 ft).

2.11 Answer: (a) $20Log_{10}(4) \approx 12$ dB. (b) $10Log_{10}(4) \approx 6$ dB.

2.12

Frequency (Hz)	31.5	63	125	250	500	1000	2000
Signal (dB)	65	78	88	80	70	67	50
Amplitudes ($\div$1000) $\approx$	1.8	7.9	25	10	3.2	2.2	0.3

2.13

Frequency (Hz)	31.5	63	125	250	500	1000	2000	4000	8000
Signal (dB)	50	52.5	52.5	55	60	67.5	60	57.5	52.5
Amplitudes ($\div$100) $\approx$	3.2	4.2	4.2	5.6	10	23	10	7.5	4.2

2.14

n =	1	3	5	7	9	11
dB	0	−9.5	−14	−17	−19	−21

2.15 A closed organ pipe.

2.16 The spectral components would have side bands at ±6 Hz.

Problems of Chap. 3

3.1 If only one coil located at x_0 were used, nulls in the spectrum would occur at $\frac{n\pi x_0}{L} = m\pi$ where $m = 1, 2, 3, \ldots$ hence, at the harmonics $n = L/x_0 \approx 9, 18, 27, \ldots$

3.2 If the output voltages from the two coils in Fig. 3.10 were added, the result would be

$V(t) \propto \sum_{n=1}^{\infty} A_n \{\sin[n\pi(x_0 + a)/L] + \sin[n\pi(x_0 - a)/L)]\} f_n(t)$
$= 2\sum_{n=1}^{\infty} A_n \sin\left(\frac{n\pi x_0}{L}\right) \cos\left(\frac{n\pi a}{L}\right) f_n(t)$ and the spectrum would have minima at $n = m\frac{L}{x_0}$ and $n = (2m-1)\frac{L}{2a}$ where $m = 1, 2, 3 \ldots$ which for the dimensions given in the text would occur at $n \approx 9, 18, 26, 27, 36, 43,$ etc.

3.3 The separation between the negative and positive peaks for the 56.8 Hz resonance should correspond to half the wavelength of the surface wave along the grain direction. Hence, for the long dimension assumed above, $\lambda/2 \approx 28.1$ inches and the surface wave velocity would be about

$c_{\text{Surface}} = \lambda f \approx (56.2)(56.8) = 3192\,\text{in./s} \approx 266\,\text{ft/s},$ or about 1/4 of that for the velocity of sound in air.

3.4 The frequency is F = 261.6 Hz. The tension = 6.64 106 dynes = 14.9 lbs.

3.5 We want the density per unit length to be the same. Hence, the cross-sectional area of the wire should be $1.4/7.83 = 0.1788$ times that of the gut string, or the diameter of the steel wire should be $0.423 \times 0.029\,\text{in.} = 0.012\,\text{in.}$

Problems of Chap. 4

4.1 Answer: About 9.4 times for the Stein prellmechanik action, 9.2 times for the Broadwood action, and 9.5 times for the Streicher action.

4.2 Answer: Remove all the dampers for notes on that chord before dropping it. (Don't try that with a good piano!!! If the cast iron frame breaks, it is virtually impossible to repair it.)

4.3 Answer: The highest loss (symmetric) mode occurs when all three strings are in phase. Intermediate loss modes occur when one string is 180° out of phase with the other two. The lowest loss (odd-symmetric) mode occurs when the outer strings are 180° out of phase and the middle string is not vibrating.

4.4 Answer. The strength of the wire increases with its cross-sectional area, but so does its density per unit length. Hence, the ratio of the breaking tension to the density per unit length is about constant and that ratio determines the wave velocity, hence the pitch, at the breaking point.

4.5 The wavelength is $\lambda \approx 2 \times 72 = 144$ in.; hence, the wave velocity $c = \lambda f = 144 \times 87.3 = 12{,}571$ in./s ≈ 1048 ft/s.

4.6 The tension is about 9×10^7 dynes ≈ 202 pounds of force.

4.7 About 29 lbs, or about 6 lbs more than to bring the string up to normal pitch. (It takes about $1.26 \times 202 \approx 255$ lbs of force to break the string. The mechanical advantage of the tuning hammer is $10/0.1125 \approx 8.9$)

4.8 About 388 ft/s. (The maximum and minimum are separated by half a wavelength.)

4.9 For F2, about 3.001; for C9, about 6.8.

Problems of Chap. 5

5.1 Answer: E= $3 \times 440/2 = 660$ Hz, D= $2 \times 440/3 = 293.33$ Hz, G = $2 \times 293.33/3 = 195.55$ Hz. On the WTS, E = 659.25 Hz, D = 293.66 Hz, and G = 196.00 Hz.

5.2 For the A string, c $= 2 \times 33 \times 440 = 29{,}040$ cm/s; for the G string, c = 12,906 cm/s.

5.3 $\mu = T/c^2 = 2.838 \times 10^{-5}$ g/cm^3.

5.4 195.55 Hz.

5.5 $391.1 - 330 = 61.1$ Hz, or B two octaves below middle C.

5.6 The difference frequency is an octave below the D, so the "Tartini Tone" doesn't stand out the way it would for a double third or fourth.

5.7 $1490/8 = 186$ strokes per second.

Problems of Chap. 6

6.1 $c/4L \approx 43$ Hz.

6.2 Open pipe resonances would occur at about 92 Hz, 184 Hz, 276 Hz, and so on.

6.3 (a) The voice frequency is proportional to $1/\sqrt{M}$, where M is the effective molecular weight of the gas in the lungs. Therefore our SCUBA diver wants M to be about $29 \times (120/77.8)^2 \approx 69$.

(b) Let X = the fraction of oxygen in the tank and Y = the fraction of krypton in the tank. Then $X + Y = 1$ $32X + 84Y = 69$

Solving these two equations yields $X \approx 0.288$ for the fraction of oxygen, and $Y \approx 0.712$ for the fraction of krypton.

6.4 No. He'll only be able to reach 2725 Hz (about halfway between E and F.)

Problems of Chap. 7

7.1 Answer: The total pressure from a 2-inch difference in the height of water per unit area in a U-tube manometer is 5.08 g/cm^2. The air-pressure regulator area is 6 ft^2 = 864 in.^{2} = 5574 cm^2. Hence the total weight needed is about 28.3 kg $\approx$ 62 lbs.

7.2 As a first approximation, the air velocity producing the edge tone in Fig. 7.13 is simply proportional to the air pressure. Hence the cut-up (L in the figure) should be reduced by 2/5 = 0.4 on each pipe.

7.3 Up to some point, the pressure in the toe of the pipe would increase proportionally to the area of the toe-hole after the pipe has been turned on.

7.4 From Appendix D, the fundamental pitch should be 261.6 Hz. Since the Rohr Schalmei is an open pipe, the overall length should be $L = 1100/(2261.6) = 2.10$ ft = 25.2 in. Since the large cavity is tuned to the second harmonic of the pipe, both it and the copper tube should be $25.2/2 = 12.6$ in. long.

7.5 Answer: The orchestral oboe is made from a narrow-scale conical piece of wood. (Of course, the reed is placed at the vertex where the pressure is a maximum.)

7.6 Use two pipes for each note, chosen to produce successive harmonics of a 16-ft open pipe. The ear will then interpret the combination as having 16-ft pitch. An 8-ft closed pipe would provide the fundamental pitch and its odd harmonics. Adding an open 8-ft pipe would provide the needed even harmonics. If the two are on the same note channel, they will also tend to lock in phase.

7.7 The total length of the large diameter semi-closed pipe should be $L = 1100/(4440) = 0.625$ ft $= 7.5$ in. The length of the short open pipe at the end should be tuned to the fifth harmonic of 440 Hz = 2200 Hz. Hence, the short length should be about $1100/(2 \times 2200) = 0.25$ ft $= 3$ in.

7.8 From Eq. (7.3),
$\frac{8.20}{5.80} = 12k$ or $k = 0.346/12 = 0.0289$ We want N such that $\log_e(2) = 0.0289N$ or $N = 24$ steps.

7.9 Answer: The 32-ft diapason is an open pipe with harmonics at 32-, 16-, and 8-ft pitch (the second, fourth, sixth, and eighth harmonic of the non-existent 64-ft pipe). The bordon is a closed pipe with a fundamental that is a fifth higher (i.e., third harmonic) than its nominal 64 foot pitch. Hence, the combination has frequencies at the second, third, fourth, sixth, and eighth harmonic of the phantom 64-ft pipe and the human ear will conclude that it actually has 64-ft pitch, even though the fundamental is completely missing. Assuming the velocity of sound is 1100 ft/sec, the frequencies would be:

64-ft open 8.59, 17.18, 25.7, 34.4, 42.9, 51.5, 60.1, 68.7, 77.3 Hz 32-ft Diapason—— 17.18, ——, 34.4, ——, 51.5, —-, 68.7, —- Hz 32-ft Bordon Quint ——, 25.7, —-, —-, —-, —-, —-, 77.3 Hz Effective harmonic 2 3 4 6 8 9

References

Abele H (1905) The violin and its story. John Leng & Co, New York
Allen EL, Holien H (1973) A laminagraphic study of pulse (vocal fry) register phonationİ. Folia Phoniatr 25:241–250
Apel W (1972) Harvard dictionary of music. Harvard University Press, Cambridge
Appelman DR (1967) The science of vocal pedagogy. Indiana University Press, Bloomington
Arms WT (1959) History of leyden Massachusetts. The Enterprise and Journal, Orange; Colrain, MA Library, call number 9744 A73
Arnold GE (1973) Physiology of speech. The new encyclopedia Britannica, vol 17. Encyclopedia Britannica, London, pp 477–492
Atkins H, Newman A (1978) Beecham stories. Futura Publications, London
Attenborough D (1998) The life of birds. BBC Video Co, London
Atwood W (1997) A bridge collection examined. Catgut Acoust Soc J 3(4):38–43
Audsley GA (1905) The art of organ building. Dodd, Mead, and Co, New York; Reprinted by Dover, New York in 1965 in two volumes. Emphasizes the history of organ building, vol 1 and Emphasizes the constructional details, vol 2
Backus J (1969) The acoustical foundations of music. WW Norton, New York
Baken RJ (1998) An overview of laryngeal functions for voice production. In: Sataloff RT (ed) Vocal health and pedagogy. Singular Publishing Group, San Diego, pp 27–45
Ballot B (1845) Akustische Versuche auf der Niederländischen Eisenbahn, nebst gelentlichen Bemerkungen zur Theorie des Hrn. Prof. Dopperİ. Poggendorff's Ann (also known as Ann Phys Chem, Leipzig) 66(11):321–351
Bartoli C (2002) Interview on "All things considered". National Public Radio, Washington, D.C.; Wednesday, September 25
Beare C (1980a) Dominique Peccatte. In: Sadie S (ed) The new groves dictionary of music and musicians, vol 14. MacMillan, London, p 323
Beare, C (1980b) Eugène Sartory.İ In: Sadie S (ed) The new groves dictionary of music and musicians, vol 16. MacMillan, London, p 512
Benade AH (1975) The Wolf tone on violin family instruments. Catgut Acoust Soc Newslett 24:21–23; Reprinted in Hutchins and Benade (1997) 1:117–120. This material was also reproduced in Benade, 1976, pp 567–575
Benade, AH (1976) Fundamentals of musical acoustics. Oxford University Press, New York
Bennett WR (1948) Spectra of quantized signals. Bell Syst Tech J 27:446–472
Bennett WR (1983) Secret telephony as a historical example of spread-spectrum communication. IEEE Trans Commun COM-31:98–104

© Springer Nature Switzerland AG 2018

W. R. Bennett, Jr., *The Science of Musical Sound*,
https://doi.org/10.1007/978-3-319-92796-1

Bennett WR Jr (1962) Gaseous optical masers. In: Heavens OS Applied optics supplement no.1 on optical masers. Optical Society of America, Washington, D.C.
Bennett WR Jr (1976) Scientific and engineering problem-solving with the computer. Prentice Hall, Englewood Cliffs
Bennett WR Jr (1977) The physics of gas lasers. Gordon and Breach, New York
Bennett WR Jr (1990) Heart sounds and murmurs. Lecture with digitally recorded illustrations in compact disc format. MCG International Inc., New Haven; CD No. DIDX 009454 (December)
Bennett WR Jr, Bennett J (1990) Dynamic spectral phonocardiograph. U.S. Patent No. 4,967,760 (November 6)
Berlyn GP, Richardson AD (2001) Wood: its properties in relation to its use in turning. In: Wood turning in North America since 1930. Amilcare Pizzi, Milan, pp 152–160
Blot E (2001) Liuteria Italiana IV (1800–1950), Eric Bloc editioni, Cremona
Boalch D (1974) Makers of harpsichords and clavichords. Oxford University Press, London
Bouase H (1929) Tuyaux et Resonators - Introduction a l'Etude des Instruments da Vent. Libraire Delagrave, Paris
Bouasse H, Fouché M (1929) Instruments à vent, par H. Bouasse avec la collaboration expérimentale de M. Fouché. Delagrave, Paris
Boyden DD, Schwarz B (1980) Sadie S (ed) Violin in the new groves dictionary of music and musicians, vol 20. MacMillan, London, pp 819–855
Braunwald E (1984) Editor of heart disease. W.B. Saunders Company, Philadelphia
Brigham EO, Murrow RE (1967) The fast Fourier transform. IEEE Spectr 4:63–70
Brookes K (2002) Craft masters, Tempo (Oct/Nov/Dec), vol 6. Temple University Radio, Philadelphia, pp 4–11
Broos B (1995) Un celebre Peijntre nommé Verme[e]rİ. In: Johannes V National Gallery of Art, Washington, DC, pp 47–65
Browne, MW (1996) Computer recreates call of dinosaur sound organ. The New York times, New York, p C7; Tuesday, March 12
Bucur V (1988) Wood structural, anistropy estimated by acoustic invariants.İ IAWA Bull 9(1):67–74; Also, see reproduction in Hutchins and Benade (1997) 2:795–802
Bucur V (2006) Acoustics of wood. Springer, Berlin
Campbell GA (1911) Cisoidal oscillations. Trans Am Inst Electr Eng 30:873–909
Campbell GA, Foster RM (1920) Maximum output networks for telephone substations and repeater circuits. Trans Am Inst Electr Eng 39:231–280
Cazden J (1993) Vocal acoustics in electronic musician (February) pp 97–100
Cencié ME (1990) Boy soprano, in Schubert, Der Hirt auf dem Felsen, with Roman Ortner (piano), and Erwin Monschein (clarinet), in Wiener Sängerknabe Philips CD Recording No. 426307-2; Band 7
Chladni EFF (1809) Traite d'Acoustique. Courcier, Paris
Conan-Doyle SA (1981) The adventure of the cardboard box. In: The original illustrated Sherlock Holmes; Reprinted from The Strand Magazine of 1892 to 1893. Castle Books, Seacaucus, p 207
Cooke P (1980) Pygmy music. In: Sadie S (ed) The new groves dictionary of music and musicians, 92 vol 15. MacMillan, London, pp 482–483 and "Yodel", In: Sadie S (ed) The new groves dictionary of music and musicians, 92, vol 20, MacMillan, London, p 574
Cooley JW, Tukey JW (1965) An algorithm for the machine calculation of complex Fourier series, vol 19. Math Comput, pp 297–301
Crandall IB (1926) Theory of vibrating systems. Van Nostrand, New York
Cremer L (1981) Physik der Geige. S. Hirzel Verlag, Stuttgart; Translated into English by John S. Allen as The physics of the violin. MIT Press, Cambridge
Cuesta C, Valette C (1988) Evolution temporelle de la Vibration des Cordes de Clavecin. Acustica 66:37–45
Davis PJ, Fletcher NH (eds) (1996) Vocal fold physiology. Singular Publishing Group, San Diego
Dick Heinrich Company (2003–2005) Quality products for musical instruments. Dick GMBH, Germany

Diegert CF, Williamson TE (1998) A digital acoustic model of the lambeosaurine hadrosaur Parasaurolophus tubicen. J Vertebr Paleontol 18:38A
Dolge A (1911) Pianos and their makers: a comprehensive history of the development of the piano, new edn, 1972. Dover, New York
Dom Bédos de Celles F (1766–1768) L'art du facteur d'orgues, vol I text, vol II plates. Delatour, Paris
Donnington R (1980) Vibrato. In: Sadie S (ed) The new groves dictionary of music and musicians, vol 19. MacMillan, London, pp 697–698
Drower MS (1974) Thebes (Egypt).İ In: The new encyclopedia Britannica, vol 18. Encyclopedia Britannica, London, p 264
Dudley H (1939) Remaking speech. J Acoust Soc Am 11:169–177
Dudley H (1940) The carrier nature of speech. Bell Syst Tech J 19:495–515
Dudely H (1955) Fundamentals of speech synthesis. J Audio Eng Soc 3:170–185
Dudley H, Tarnoczy TH (1950) The speaking machine of Wolfgang von Kempelen. J Acoust Soc Am 22:151–166
Dudley H, Riesz RR, Watkins SSA (1939) A synthetic speaker. J Franklin Inst 227:739–764
Elder D (1982) Pianists at play—interviews, master lessons, and technical regimes. The Instrumentalist Company Evanston, Illinois
Eulenstein K (1892) Eulensteins musikalische Laufbahn (edited by his daughter, Fanny Roodenfels, Stuttgart). Stadtarchiv, Heilbronn
Faber T (2005) Stradivari's genius. Random House, New York
Farga F (1950) Violins & violinists, translated by Egon Larsen and Bruno Raikin. Barrie & Rockliff, The Cresset Press, London
Farinelli (1994) Film biography of Carlo Broschi, directed by Gerard Corbiau (collaboratively produced in France, Belgium and Italy for Sony Pictures Classics)
Farnsworth BW (1940) High speed motion pictures of the human vocal tract. Bell Lab Rec 18(7):203–208
Feynman RP, Robert BL, Matthew LS (1963) The Feynman lectures on physics. Addison-Wesley, Reading, MA
Firth I (1976/77a) The nature of the tap tone in stringed instruments. Acustica 36(1):36–41
Firth I (1976/77b) A method for adjusting the pitch of top and back plates of the cello. Acustica 36(4):307–312
Flanagan JL (1972) Speech analysis synthesis and perception. Springer, Heidelberg
Forte M (2002) Chopin played by Madeleine Forte on the Erard Piano Paris, 1881—Yale collection of musical instruments, Roméo Records No. 7214
Fostle DW (1993) Henry Zeigler Steinway, a grand traditionİ, interview in audio magazine (January), pp 52–58
Fourier BJv (1822) La Theorie analytique de la chaleur (Paris). See Freeman's translation. Cambridge University Press, Cambridge, 1878
Friedlander FG (1953) On the oscillations of the bowed string. Proc Camb Philos Soc 49(3):516
Gaillard F (1939) Bach six suites for Violoncello Solo.İ Schirmer's library of musical classics, vol 1565; Preface
Gill D (ed) (1981) The book of the piano. Phaidon, Oxford
Giordano N (1998a) Mechanical impedance of a piano soundboard. J Acoust Soc Am 103:2128–2133
Giordano N (1998b) Sound production by a vibrating piano soundboard: experiment. J Acoust Soc Am 104:1648–1653
Giordano A, Dilworth J (2004) A fitting conclusion (Paganini's" Cannon" violin). STRAD 115, no. 1374: 1046-+
Giordano N, Winans JP II (1999) Plucked strings and the harpsichord. J Sound Vib 224:456–473
Giordano N, Winans II JP (2000) Piano hammers and their force compression characteristics: does a power law make sense? J Acoust Soc Am 107:2248–2255
Giordano N, Millis JP (2001) Hysteretic behavior of piano hammers. In: Proceedings of the international symposium on musical acoustics, Perugia

Gleason JB (1997) The development of language. Allyn and Bacon, Boston

Gold J (1995) Paganini: virtuoso, collector and dealer. J Violin Soc Am XIV(1):67–87

Gough CE (1981) The theory of string resonances on musical instruments. Acustica 49:124–141

Gray H (1918) Anatomy of the human body. Lea and Febiger, Philadelphia

Gray H, Warwick R, Williams PL (1980) Gray's anatomy. Saunders, Philadelphia

Grissino-Mayer H, Burckle L (2003) Stradivari violins, tree rings and the maunder minimum: a hypothesis. Dendrochronologia 21(1):41–45

Grissino-Mayer HD, Sheppard PR, Cleaveland MK (2004) A Dendroarchaeological re-examination of the 'Messiah' violin and other instruments attributed to Antonio Stradivari. J Archaeol Sci 31:167–174

Gruberova E (1988) Soprano, in Opera collection. Mozart, Die Zauber Flöte, Querschnite, Nikolaus Harnoncourt, CD 063-13810-9, Teldec Classics

Guettler K (2002) On playing 'harmonics' (flageolet tones). Catgut Acoust Soc J 4(5):5–7

Guhr K (1831) Uber Paganinis Kunst die Violin zu Spielen (Main, 1831). Translated from the original German by Sabilla Novello in 1915, revised by C. Egerton Lowe. Novello & Co., London; Also see the translation by Gold J (1982) Paganini's art of violin playing. Teresa Parker Associates, San Francisco

Gyütö M (1986) The Gyütö monks: Tibetan tantric choir WD-2001. 360Publishing, ASCAP and Windham Hill Records, Stanford

Hannings L, Chin Y (2006) J Violin Soc XX:146–162

Hanon CL (1900) The virtuoso pianist in sixty exercises for the piano translated from the French by Dr. Theodore Baker. G. Schirmer, Milwaukee

Hansell KK (1980) Sadie S (ed) Manzuoli, Giovanniİ in the new groves dictionary of music and musicians, vol 11. MacMillan, London, p 638

Hanson RJ, Schneider AJ, Hagedahl FW (1994) Anomalous low-pitched tones from a bowed violin string. Catgut Acoust Soc 2(6):1–7

Harrison JM, Thompson-Allen N (1996) Loudness level survey of the Newberry Memorial Organ, Yale University. J Acoust Soc Am 100:3909–3916

Hartley RVL (1939) Oscillations in systems with non-linear reactance. Bell Syst Tech J 15:424–440

Hawkshaw M, Sataloff RT, Bhatia R (2001) Chaos in voice research. In: The professional voice—the science and art of clinical care. Singular Publishing Group, San Diego, pp 185–190; Chapter 9

Hayes C (1951) The ape in our house. Harper, New York

Hayes JW (1982) String behavior and scale design. In: Travis JW (ed) A guide to restringing. JohnTravis, Takoma Park, pp 31–64

Hedley A, Brown M (1980) Chopin, Fryderyk Franciszek. In: Sadie S (ed) The new groves dictionary of music and musicians, vol 4. Oxford University Press, Oxford, pp 292–312

Helmholtz HLF (1885), Die Lehre von den Tonempfindungen. Longmans & Co, Harlow; Translated into English by Ellis (1885) and republished as "On the sensations of tone". Dover, New York, 1954

Heriot A (1975) The Castrati in Opera. Da Capo Press, Cambridge

Herken G (2002) Brotherhood of the bomb. Henry Holt & Co, New York

Heron-Allen E (1885) Violin-making: as it was and is. Ward Lock & Co., London; Reprinted in 2000 by Algrove, Ottawa

Hill A, Hill A, Hill WH (1902) Antonion Stradivari his life & work. William E. Hill & Sons, London, pp 1644–1737; Reprinted by Dover Publications, New York in 1963

Hill WH, Arthur F, Ebsworth A (1931) The violin-makers of the Guarneri family. William F. Hill & Sons, London, pp 1626–1762; Reprinted by Dover Publications, New York in 1989

Hirano M (1970) Regulation of register, pitch and intensity of the voice. Folia Phoniatr 22:1–20; Also see, "The regulatory mechanisms of the voice in singing"İ, instructional video tape produced by The Voice Foundation, Philadelphia, p 19103

Hubbard F (1965) Three centuries of harpsichord making. Harvard University Press, Cambridge

Hussey LW, Wrathall LR (1936) Oscillations in an electromechanical system. Bell Syst Tech J 15:441–445
Hutchins CM (1962) The physics of violins. Sci Am 207(5):78–93
Hutchins CM (1981) The acoustics of violin plates. Sci Am 245(4):170–187
Hutchins CM (1983) A history of violin research. J Acoust Soc Am 73:1421–1440
Hutchins CM (2004) The catgut acoustical society story. Catgut Acoust Soc J 5:16–30
Hutchins C, Schelleng JC (1967) A new concert violin. J Audio Eng 15(4)
Hutchins C, Benade V (eds) (1997) Research papers in violin acoustics, vols 1, 2. Acoustical Society of America, Woodbury, pp 1975–1993
Jansson E (1973) On higher air modes in the violin. Catgut Acoust Soc NL 19:13–15
Jansson E, Molin NE, Sundin H (1970) Resonances of a violin body studied by hologram interferometry and acoustical methods. Phys Scr 2:243–256
Jansson EV, Niewczyk BK, Fryden L (1997) On body resonance C3 and violin construction. Catgut Acoust Soc J 3(3):9–14
Javan A, Bennett WR Jr, Herriott DR (1961) Population inversion and continuous optical maser oscillation in a gas discharge containing a He-Ne mixtureİ. Phys Rev Lett 6:106–110
Jeans SJ (1937) Science & music. Cambridge University Press, Cambridge
Jonas F (1968) Translation of selected essays on music by Vladimir Vasilevich Stasov. Praeger, New York
Kaplan HM (1971) Anatomy and physiology of speech. McGraw Hill, New York
Katz M (2005) Capturing sound: how technology has changed music. University of California Press, Berkeley
Kempelen WRv (1791) Mechanismus der menschlicken Sprache nebst der Beschreibung seiner sprechenden Maschine. Available in the Yale University Beinecke Library. Also see, Dudley and Tarnoczy, 1950
Kent RD (1997) The speech sciences. Singular Publishing Group, San Diego
Kimura M (2001) The world below G—subharmonics extend the violin's range. STRINGS (August/ September), pp 24–29
Kindel J (1989) Modal analysis and finite element analysis of a piano soundboardİ. M.S. thesis, University of Cincinnati
Kindlmann PJ (1966) Measurement of excited state lifetimes. Ph.D. dissertation in Engineering and Applied Science, Yale University
Kolbert E (2005) The climate of man. The New Yorker, New York; April 25, pp 56–71; May 2, pp 64–73; and May 9, pp 52–63
Kottick EL, Marshall KD, Hendrickson TJ (1991) The acoustics of the harpsichord. Sci Am 110–115
Kroodsma D (2005) The singing life of birds. Houghton Mifflin, New York
Kuperman WA, Lynch JF (2004) Shallow-water acoustics. Phys Today 57(10) 55–61
Lebrecht N (2001) The maestro myth. Citadel Press, New York
Leipp E (1963a) Un 'Vocoder' Mécanique: La Guimbarde.İ Ann Télécommun 18(5–6):82–87
Leipp E (1963b) Étude Acoutsique de la Guimbarde. Acustica 13(6):382–396
Leipp E (1967) La Guimbarde. Bulletin du Groupe d'Acoustique Musicale, No. 25. Laboratoire d'Acoustique Faculté des Sciences, Paris
Lenehan M (1982) Building steinway grand piano K2521—the quality of the instrument. Atl Mon 1–27
Levin TC, Edgerton ME (1999) The throat singers of Tuva. Sci Am 281:70–77
Litten A (1963) Soprano, in Schubert, Der Hirt auf dem Felsen with Stanley Udy (piano), and William R. Bennett, Jr. (clarinet), recorded at Yale, December 1963
Loen JS (2001) Thickness graduation mapping: methods and goals. Catgut Acoust Soc J 4(4):5–6
Loen JS (2002) Fingerprints under the varnish: comparing thickness graduations of the 'Messiah' violin to golden age strads. Catgut Acoust Soc J 4(6):14–16
Loen J (2003) Thickness graduation mapping: surprises and discoveries. J Violin Soc Am XIX(2):41–66; Proceedings of the thirty-first annual convention

Loen JS (2004) Thickness graduation maps of classic violins, violas, and cellos, 1st edn. Jeffery S Loen, Kenmore
Luke JC (1971) Measurement and analysis of body vibrations of a violin. J Acoust Soc Am 49(4)(part 2):1264–1274
Mackay J (1997) Alexander Graham Bell—a life. Wiley, New York
Marshall KD (1985) Modal analysis of a violin. J Acoust Soc Am 77(2):695–709
Martin WH (1924) The transmission unit and telephone reference systems. Bell Syst Tech J 3:400–408
Martin DW, Ward WD (1961) Subjective evaluation of musical scale temperament in pianos. J Am Acoust Soc 33:582–585
McIntyre ME, Schumacher RT, Woodhouse J (1982) Aperiodicity in bowed-string motion. Acoustica 50:294–295
Mersmann H (1972) Editor of letters of Wolfgang Amadeus Mozart. Dover, New York; Reprinted from an original edition by J.M.Dent & Sons, London, 1928
Michelson AA (1903) Light waves and their uses. University of Chicago Press, Chicago
Millant R (1972) J. B. Vuillaume. W. E. Hill & Sons, London; This book is in English, French and German
Milstein N, Solomon V (1990) From Russia to the west—musical reminiscences of Nathan Milstein, translated by Antonina W. Bouis. Limelight Editions, New York
Moreschi A (1902, 1904) Vatican cylinder recordings reproduced on LP disc by opal records circa 1984; Record no. 823
Morrison M (1983) Video highlights from the voice clinic, vol 1. The Voice Foundation, Philadelphia, pp 19103
Neumayr A (1994) Music and medicine—Haydn, Mozart, Beethoven, Schubert—notes on their lives, works, and medical histories, translated by Bruce Cooper Clarke. Medi-Ed Press, Bloomington
Neuwirth R (1994) From sciarrino to subharmonics. STRINGS, September/October, pp 60–63
Nilsson B (1984) Master class, vol 60.İ The New Yorker, New York, pp 44–45
Nyquist H (1924) Certain factors affecting telegraph speed. Bell Syst Tech J 3:324–346
Odiaga L (1974) Johann Sebastian Bachİ, Editión del Patronato Popular y Porvenir Pro Música Clásica; CBS Discos del Perù; Recorded in New Haven by William R. Bennett; P.E.002-A and P.E.002-B
Olson HF (1952) Musical engineering. McGraw-Hill, New York; Republished as music, physics and engineering. Dover, New York, 1967
Pedersen PO (1934) Subharmonics in forced oscillations in dissipative systemsİ, Part I [Theoretical]. J Acoust Soc Am VI:227–238; Part II [Experimental], J Acoust Soc Am VII:64–70
Pepperberg IM (1991) Referential communication with an African grey parrot. Harvard Graduate Society News Letter (Spring), pp. 1–4. Also see, "Brain Parrot Dies…"İ by Benedict Carey, N.Y. Times, Tuesday, September 11, 2007, p A23 and "Alex Wanted a Cracker…"İ by George Johnson, N.Y. Times, September 16, 2007, pp 1,4 wk
Perrins CM, Middleton ALA (1985) The encyclopedia of birds. Facts on file, New York
Peschel ER, Peschel RE (1987) Medical insights into the Castrati in opera. Am Sci 75:578–583
Peterson (1999) Skubic M (ed) AutoStrobe 490-ST strobe tuner instruction manual. Peterson Electro-Musical Products, Alsip
Pickering, NC (1991) The bowed string. Amereon Ltd, Mattituck
Pickering NC (1993) Problems in string making. Catgut Acoust Soc J 2(3):1–4
Pierce JR, alias, Coupling JJ (1983) The science of musical sound. Scientific American Books, New York
Pleasants H (1981) The great singers from the dawn of opera to Caruso, Callas, and Pavarotti. Simon and Schuster, New York
Potter RK, George AK, Green HC (1947) Visible speech. D. Van Nostrand Company, New York
Railsback OL (1938) J Acoust Soc Am 9:274
Raman CV (1918) On the mechanical theory of vibrations of bowed strings. Bull Indian Assoc Cultiv Sci (Calcutta) 15:1–158

Raman CV (1988) Ramaseshan S (ed) Scientific papers of C. V. Raman volume II acoustics. Indian Academy of Sciences, Bangalore

Ramanujan S (1914) Modular equations and approximations to p. Q J Pure Appl Math 45:350–373

Rayleigh L, alias, Strutt JW (1877) Theory of sound, vols I and II. Macmillan Co. Reprinted by Dover, New York, 1945

Riesz RR (1932) The relationship between loudness and the minimum perceptible increment of intensity. J Am Acoust Soc 4:211–216

Ripin EM (1980) Groves dictionary of music, vol 14. Macmillan, London, pp 682–714

Ripin EM, Schott H, Barnes J, O'brien G (1980) Groves dictionary of music, vol 8. Macmillan, London, pp 216–246

Rioul O, Vetterli M (1991) Wavelets and signal processing. IEEE Signal Process Mag 8:14–38

Robbins WW, Weier TE (1950) Botany: an introduction to plant science. Wiley, New York

Rosen C (2002) Piano notes—the world of the pianist. The Free Press, New York

Rossing T (1990) The science of sound. Addison-Wesley, Reading

Rossing T, Fletcher N (1991) The physics of musical instruments. Springer, New York

Rothstein E (1994) A violinist tests music of her time. New York Times, New York, p C21; April 21

Rothstein E (1995) Emblems of mind—the inner life of music and mathematics. Avon Books, New York

Runge C (1903) Z Math Phys 48:443

Rymer R (2004) Saving the music tree. Smithsonian 35(1):52–63

Sacconi SF (2000) The "secrets"İ of Stradivari, translated by Andrew Dipper and Cristina Rivaroli with corrections to the first English edition of 1975 by Andrew Dipper. Eric Blot Edizioni, Cremona

Sadie S (1980) Mozart (3), Wolfgang Amadeus. In: Sadie S (ed) New groves dictionary of music and musicians, vol 12. MacMillan, London, pp 680–752

Salgo S (2000) Thomas Jefferson, musician and violinist. Thomas Jefferson Foundation, Moticello

Sataloff RT (1992) The human voice. Sci Am 267:108–115

Sataloff RT, Hawkshaw M, Bhatia R (1998) Medical applications of chaos theory,İ in: Davis PJ, Fletcher NH (eds) Vocal fold physiology. Singular Publishing Group, San Diego, pp 369–387

Saunders FA (1962) Violins old and new – an experimental study. Sound: Its Uses Control 1(4):7–15 (1962)

Savart F (1819) Rapport sur un mémoire relatif a la construction des instruments àă cordes et àă archet. Ann Chim Phys 2:225

Schawlow AL (1996) Charles townes as i have known him. In: Chiao RY (ed) Amazing light, a volume dedicated to Charles Hard Townes on his 80th birthday. Springer, New York, pp 1–6

Schelleng JC (1963) The violin as a circuit. J Accoust Soc Am 35:326–338; Especially, see Section VI

Schleske M (1998) On the acoustical properties of violin varnish. Catgut Acoust Soc J 3(6):27–43

Schneider D (2004) Living in sunny times. Am Sci 93:22, 23

Schonberg HC (1984) History's last castrato is heard again. The New York Times, New York, p H25; September 16

Schonberg HC (1985) The glorious ones: classical music's legendary perfomers. Times Books, New York, p 3

Schroeder MR (1999) Computer speech. Springer, Berlin

Schuck OH, Young RW (1943) Observations on the vibrations of piano strings. J Am Acoust Soc 15:1–11

Schwartz D (1996) Snatching scientific secrets from the Hippo's gaping jaws. Smithsonian 26(12):90–102

Segré G (2002) A matter of degrees—what temperature reveals about the past and future of our species. In: Planet and universe. Viking, New York

Serber R, Crease RP (1998) Peace & war. Columbia University Press, New York

Shakespeare W, Craig WJ (1966) Shakespeare: complete works. Oxford University Press, London. Print

Shanks D, Wrench JW (1962) Calculation of PTO 100,000 decimals. Math Comput 16:76; poccupies a 20-page table
Shorto R (2004) The island at the center of the world. Doubleday, New York
Silverman WA (1957) The violin hunter. Paganiniana, Neptune City
Sitwell S (1967) Liszt. Dover Publications, New York
Solomon M (1995) Mozart—a life. Harper Collins, New York
Sonnaillon B (1985) King of the instruments—a history of the organ. Rizzoli, New York
Stasov, V. V. Selected essays on music. London: Cresset P, 1968. Print
Steadman P (2001) Vermeer's camera. Oxford University Press, Oxford
Steinhardt A (1998) Indivisible by four—a string quartet in pursuit of harmony. Farrar Straus Giroux, New York
Steinhardt A (2006) Violin dreams. Houghton Mifflin, New York
Stetson KA, Powell RI (1965) Interferometric vibration analysis by wave front reconstruction. J Opt Soc Am 55:1593–1598
Stetson KA, Powell RI (1966) Hologram interferometry.İ J Opt Soc Am 56:1161–1166
Stevens KN (1998) Acoustic phonemes. The MIT Press, Cambridge
Sundberg J (1987) The science of the singing voice. Northern Illinois University Press, DeKalb
Synge JL, Griffith BA (1949) Principles of mechanics. McGraw-Hill Book Co., New York
Tammet D (2007) Born on a blue day. Free Press, New York
Taub R (2002) Playing the Beethoven piano sonatas. Amadeus Press, Portland
Taylor DA (1965) Paderewski's piano, Smithsonian, Maryland, pp 30–34
Thayer AW, Forbes E (eds) (1973) Thayer's life of Beethoven. Princeton University Press, Princeton
Travis JW (1982) A guide to restringing. John W. Travis, Takoma Park
Trent HM, Stone DE (1957) Elastic constants, hardness, strength, and elastic limits of solids.İ In: American institute of physics handbook. McGraw Hill, New York; Chapter 2f
TUVA (1990), Voices from the center of Asia, Smithsonian Fokways CD 40017
Valente B (1960) Schubert, Der Hirt auf dem Felsen, in Recital No. 2 by Harold Wright (clarinet), Rudolf Serkin (piano), Boston Records BR1024CD; Band 10
Van Dyke M (1982) An album of fluid motion. The Parabolic Press, Stanford
Walker T (1980) Castratoİ. In: Sadie S (ed) The new grove dictionary of music and musicians, vol 3. Macmillan, London, pp 875–876
Wang LM (1999) Radiation mechanisms from bowed violinsİ. Doctoral Thesis in Acoustics, Pennsylvania State University, State College, Pennsylvania
Wang LM, Burroughs CB (2001) Acoustic radiation from bowed violins. J Acoust Soc Am 110:543–555
Weatherburn CE (1951) Advanced vector analysis. Bell and Sons, London
Weinreich G (1977) Coupled piano strings. J Acoust Soc Am 62:1474–1484
Weinreich G (1997) Directional tone color. J Acoust Soc Am 101:2338–2346
Weinreich G (2002) Sound radiation from the violin—as we know it today. J Acoust Soc Am 5:37–42
West MJ, King AP (1990) Mozart's starling. Am Sci 78:106–114
Wheatstone C (1828) Erkläring der vermittels des Brummeisens hervorgebrachten Töne. Allg Musik Z (Leipzig) 30:626
Wheatstone C (1879) The scientific papers of Sir Charles wheatstone. Physical Society of London, London, pp 348–367
Whittaker E, Watson G (1902) Modern analysis, Chapter 12. Cambridge University Press, Cambridge
Whittaker ET, Watson GN (1920) A course of modern analysis, 3rd edn. Cambridge University Press, Cambridge
Winchester S (2003) Krakatoa—the day the world exploded: August 27, 1883. HarperCollins, New York
Wood AB (1955) A textbook of sound. Bell, London

Woodhouse J (2002) Body vibrations of the violin—what can a maker expect to control? J Acoust Soc Am 5:43–49
Wright J (1980) Jew's Harp.İ In: Sadie S (ed) The new grove dictionary of music and musicians, vol 9. MacMillan Publishers, London, pp 645–646
Yoshikawa S (1997, in Japanese) Bowing positions to play cello tones on the violin. J Acoust Soc Jpn (Nihon Onk yo Gak kai-shi) 53(12):955–963
Young RW (1957) Frequencies of simple vibrators. Musical scales. American institute of physics handbook. McGraw-Hill, New York, pp 3-100–3-107
Yung BN (1980) Chin23 part IV. Theoryİ. In: Sadie S (ed) The new grove dictionary of music and musicians, vol 4. MacMillan Publishers, London, pp 260–283
Zemansky MW (1951) Heat and thermodynamics. McGraw-Hill, New York

Index

© Springer Nature Switzerland AG 2018
W. R. Bennett, Jr., *The Science of Musical Sound*,
https://doi.org/10.1007/978-3-319-92796-1